

Understanding the complexities of  
Proterozoic redox using carbon,  
nitrogen and trace metal composition  
of organic rich shales

Thesis submitted in accordance with the requirements of the University of  
Adelaide for an Honours Degree in Geology

April Valerie Shannon  
October 2018



## **UNDERSTANDING THE COMPLEXITIES OF PROTEROZOIC REDOX USING CARBON, NITROGEN AND TRACE METAL COMPOSITION OF ORGANIC RICH SHALES**

### **RUNNING TITLE**

Understanding complexities of Proterozoic redox.

### **ABSTRACT**

The Great Oxidation Event (GOE, Paleoproterozoic ca. 2.34 Ga) marked a time of substantial increase in oxidation. However, since this discovery the evidence for a Neoproterozoic Oxygenation Event (NOE, ca. 800 Ma–580 Ma) has flourished. More controversial and most recently, the suggestion of a potential Mesoproterozoic Oxygenation Event has been put forward. The aim of this thesis is to obtain a coupled data set using carbon and nitrogen isotopes in conjunction with molybdenum and vanadium trace metals, as proxies for oceanic redox conditions throughout the Proterozoic. Collectively, samples involved span the late Paleoproterozoic through to late Neoproterozoic (ca. 1.74 Ga – 0.635 Ga), with a keen focus on the Mesoproterozoic. Carbon isotopes range from -32.99‰ (Barney Creek Formation) to -26.33‰ (Tent Hill Formation), suggesting a change in fraction of organic carbon burial from 0.12 and 0.40. This is almost a three-fold increase in organic carbon burial, which would predict an overall increase in production of O<sub>2</sub>. This is supported by an increase in V/Mo ratios coupled with decreasing Mo abundances through the Paleoproterozoic to Neoproterozoic, again a likely result of increasing of ocean oxygenation. With this in mind, a trend to lighter nitrogen isotopes followed by an increase to heavier δ<sup>15</sup>N can be analysed effectively. This trend in nitrogen isotopes is thought to be associated with an increase in Mo-based nitrogen fixation efficiency, followed by increased availability of aerobic nitrogen cycling (i.e. an abundance of NO<sub>3</sub><sup>-</sup> and NO<sub>2</sub><sup>-</sup>) to support the dominance of denitrification and anammox processes. Previous models that call for no significant growth in atmospheric oxygen post GOE or a singular Mesoproterozoic Oxygenation Event is not supported by this coupled data set. Carbon, nitrogen and trace metals present convincing evidence of an overall increase in ocean redox, and by proxy, atmospheric oxygen throughout the Mesoproterozoic and Neoproterozoic.

### **KEYWORDS**

Proterozoic, atmospheric oxygen, nitrogen, carbon, isotopes, trace metal, redox, Greater McArthur basin, Amadeus Basin, Adelaide Rift Complex, Borden Rift Basin, organic shales.

## TABLE OF CONTENTS

Understanding the complexities of proterozoic redox using carbon, nitrogen and trace metal composition of organic rich shales .....	i
Running title .....	i
Abstract.....	i
Keywords.....	i
List of Figures and Tables .....	4
Introduction .....	8
Background to redox proxies.....	11
Marine carbon cycle .....	11
Marine nitrogen cycle.....	13
Fixation.....	13
Nitrification .....	14
Assimilation.....	14
Heterotrophic denitrification .....	15
Anammox .....	15
Redox sensitive trace metals.....	17
Molybdenum and vanadium .....	17
Geological Background .....	18
Overview .....	18
Greater McArthur Basin, Northern Territory .....	19
Amadeus Basin, Northern Territory .....	19
Adelaide Rift Complex, South Australia.....	20
Borden Rift Basin, Arctic Canada .....	22
Methods .....	23
Sample Collection.....	23
Crushing.....	23
Source Rock Analyser (SRA).....	23
Acidification .....	24
Isotope Ratio Mass Spectrometry (IRMS) .....	24
Major and Trace Elemental Analysis .....	25
Results .....	26
ca. 1.74 Ga .....	26
Wollogorang Formation .....	26
ca. 1.64 Ga .....	26

Fraynes Formation .....	26
Barney Creek Formation .....	26
ca. 1.5 Ga to ca. 1.4 Ga.....	27
Mainoru Formation.....	27
Crawford Formation .....	27
Jalboi Formation.....	28
ca. 1.38 Ga .....	28
Velkerri Formation .....	28
ca. 1.33 Ga .....	28
Kyalla Formation .....	28
ca. 1.1 Ga .....	29
Arctic Bay Formation .....	29
ca. 0.80 Ga .....	29
Gillen Formation.....	29
ca. 0.66 Ga .....	30
Tapley Hill Formation .....	30
ca. 0.635 Ga .....	30
Tent Hill Formation .....	30
Discussion.....	31
Assessment of alteration in carbon and nitrogen isotopes.....	31
Organic carbon isotope record ( $\delta^{13}\text{C}$ ).....	36
Redox sensitive trace metal record.....	38
Organic nitrogen isotope record ( $\delta^{15}\text{N}$ ) .....	42
What can cause more positive $\delta^{15}\text{N}$ values?.....	43
Denitrification and anammox as dominant processes .....	44
$\text{N}_2$ fixation vs. denitrification – what makes one dominant over the other?.....	45
Trends in $\delta^{15}\text{N}$ .....	46
Interpretation 1 .....	46
Interpretation 2 .....	48
Conclusion .....	50
Acknowledgments .....	51
References .....	52
Appendix A: Extended Methods .....	56
Bootstrapping.....	56
Carbon and Nitrogen IRMS.....	56

Appendix B: Full organic and inorganic geochemical characterisations .....	57
Carbon and Nitrogen Isotope Data .....	57
.....	57
Trace metal data.....	70
Source Rock Analyser data.....	86

## LIST OF FIGURES AND TABLES

Figure 1. Simplified cartoon of the marine carbon cycle. Atmospheric carbon in the form of CO <sub>2</sub> diffuses into the ocean and exists in equilibrium with bioavailable carbon (HCO <sub>3</sub> <sup>-</sup> ), otherwise known as DIC. Organic matter preferentially takes up light carbon, therefore leaving the residual DIC isotopically heavy. This organic matter can be remineralized, returning the light isotopes back to the DIC. However, organic matter may go on to be buried, i.e. f <sub>org</sub> . This is represented as a black shale in the above diagram. This burial process creates a large fractionation between C <sub>org</sub> and DIC. The remaining carbon in the DIC goes on to make inorganic carbon (C <sub>carb</sub> ). Therefore, C <sub>carb</sub> reflects the isotopic signature of DIC pool. The long-term average fractionation factor is ~30‰, therefore, measuring isotopic signals of either C <sub>carb</sub> or C <sub>org</sub> , using equation 2, f <sub>org</sub> can be solved for.....	12
Figure 2. Simplified cartoon of the marine nitrogen cycle. N <sub>2</sub> enters the oceans and is 'fixed' via diazotrophs into bioavailable nitrogen as NH <sub>4</sub> <sup>+</sup> . This process is usually expressed with minimal fractionation, ~2‰. From here, assimilation or nitrification can occur. Nitrification* is the bacterial mediated process where ammonium is nitrified via oxidation. It is believed that this step (*) goes to completion, resulting in little fractionation. Organisms take nitrogen from the bioavailable pool of nitrogen (either NH <sub>4</sub> <sup>+</sup> or NO <sub>3</sub> <sup>-</sup> , as some can take up both), which is the process of assimilation. Again, it is believed that Assimilation* reactions go to completion, resulting in little fractionation occurs. N <sub>2</sub> leaves the ocean via 2 processes: Denitrification and Anammox. The red parts of these reactions are to indicate the different starting factors between the two. Denitrification and anammox are partial processes, and therefore fractionate, leaving the bioavailable nitrogen pool heavy, preferentially returning light isotopes to the atmosphere. These two processes occur at oxic-anoxic boundaries (oxygen minimum zones – indicated by the purple wedge in the above figure) as they require both environments to complete the reaction. Therefore, the organic matter that go on to eventually form shales are controlled by the dominance of either the fixation process, or the denitrification/anammox processes, which is ultimately what δ <sup>15</sup> N measures.....	16
Figure 3. Map of Australia showing the locations of the Australian formations used in this study. The outlines of the greater McArthur Basin (shown in red), the Amadeus Basin (shown in green), and the Adelaide Rift Complex (shown in blue), show the regional extent of each basin. The following formations are shown on the map: McArthur Basin formations: Wollogorang (dark green), Barney Creek (yellow), Fraynes (purple), Mainoru (dark red), Crawford (red), Jalboi (light-red), Velkerri (blue), Kyalla (orange), Jamison (dark-pink) and Hayfield (olive-green). Amadeus Basin: Gillen Formation (light-pink). The Adelaide Rift Complex: Tapley Hill Formation (dark-brown) and Tent Hill Formation (light-brown). Where there are multiple of the same coloured circles, there are multiple well locations used for that particular formation. Multiple formations obtained from the same well are depicted by different sized circles.	21
Figure 4. Blow up of the Borden Rift Basin of Arctic Canada, of location with respect to North America. The green circle represents the location of the Arctic Bay Formation.	22
Figure 5. C% vs. N% of Tent Hill (light brown), Tapley Hill (dark brown), Gillen (pink), Arctic Bay (light green), Kyalla (orange), Velkerri (blue), Lower Roper Group (red), Fraynes (purple), Barney Creek (yellow) and Wollogorang formations (dark green).	31

Figure 6a $\delta^{13}\text{C}$ vs. C% of formations Tent Hill (light brown), Tapley Hill (dark brown), Gillen (pink), Arctic Bay (light green), Kyalla (orange), Velkerri (blue colour), Lower Roper Group (red colour), Fraynes (purple), Barney Creek (yellow) and Wollogorang (dark green). Figure 6b $\delta^{15}\text{N}$ vs. N% of formations Tent Hill (light brown), Tapley Hill (dark brown), Gillen (pink), Arctic Bay (light green), Kyalla (orange), Velkerri (blue colour), Lower Roper Group (red colour), Fraynes (purple), Barney Creek (yellow) and Wollogorang (dark green). ....	32
Figure 7. Carbon isotope alteration plots, shown by $\delta^{13}\text{C}$ (‰), with formations; Tent Hill (light brown), Tapley Hill (dark brown), Gillen (pink), Kyalla (orange), Velkerri (blue), Lower Roper Group (red), Fraynes (purple), Barney Creek (yellow) and Wollogorang (dark green) formations. Figure 7a $\delta^{13}\text{C}$ (‰) vs. Hydrogen Index (HI).	
Figure 7b $\delta^{13}\text{C}$ (‰) vs. Thermal maximum ( $T_{\max}$ ). Figure 7c $\delta^{13}\text{C}$ (‰) vs. hydrocarbon Production Index (PI). Figure 7d $\delta^{13}\text{C}$ (‰) vs. free hydrocarbons (S1). For further explanations see Table 2.....	34
Figure 8. Nitrogen isotope alteration plots, shown by $\delta^{15}\text{N}$ , all showing formations; Tent Hill (light brown), Tapley Hill (dark brown), Gillen (pink), Kyalla (orange), Velkerri (blue), Lower Roper Group (red), Fraynes (purple), Barney Creek (yellow) and Wollogorang (dark green) formations. Figure 8a $\delta^{15}\text{N}$ vs. Hydrogen Index (HI). Figure 8b $\delta^{15}\text{N}$ vs. Thermal maximum, Tmax. Figure 8c $\delta^{15}\text{N}$ vs. hydrocarbon Production Index (PI). Figure 8d $\delta^{15}\text{N}$ vs. free hydrocarbons, S1. For further explanations see Table 2.....	35
Figure 9. $\delta^{13}\text{C}_{\text{org}}$ (‰) of Tent Hill (light brown), Tapley Hill (dark brown), Gillen (pink), Arctic Bay (light green), Kyalla (orange), Velkerri (blue), Lower Roper Group (red), Fraynes (purple), Barney Creek (yellow) and Wollogorang (dark green) formations, plotted against their estimated ages. The larger circles for each formation represent the bootstrapped average of each formation. Confidence intervals of 95% can be seen as error bars on these bootstrapped points. Where confidence intervals cannot be seen, the error bars are smaller than the size of the point. It is important to note that where each formation plots, may not be to their exact formation ages. This was done to ensure formations would be able to be seen, rather than overlapping. The larger of the blue lines represents the time of the Sturtian glaciation, and the smaller represents the Marinoan glaciation.....	37
Figure 10. Without comparing V/Mo ratios to Mo abundances, it is unclear which side of the curve a potential gradient represents as either oxic to sub-oxic or anoxic to euxinic trends could be argued for. Knowing the trend in Mo abundances gives an accurate interpretation of the V/Mo proxy.....	39
Figure 11a V/Mo bootstrapped average values for the Tent Hill (light brown), Tapley Hill (dark brown), Gillen (light pink), Hayfield (olive green), Jamison (dark pink), Kyalla (orange), Upper Velkerri (dark blue), Middle Velkerri (medium blue), Lower Velkerri (light blue), Lower Roper Group (red), Fraynes (purple), Barney Creek (yellow) and Wollogorang (dark green) formations plotted with respect to their depositional ages. Confidence intervals of 95% can be seen as error bars on these bootstrapped points. Where confidence intervals cannot be seen, the error bars are smaller than the size of the point. The larger of the blue lines represents the time of the Sturtian glaciation, and the smaller represents the Marinoan glaciation. Figure 11b V/Mo vs. Mo (ppm), bootstrapped data of said formations. Confidence intervals of 95%	

can be seen as error bars on these bootstrapped points. Where confidence intervals cannot be seen, the error bars are smaller than the size of the point. ....	40
Figure 12. $\delta^{15}\text{N}$ of Tent Hill (light brown), Tapley Hill (dark brown), Gillen (pink), Arctic Bay (light green), Kyalla (orange), Velkerri (blue), Lower Roper Group (red), Fraynes (purple) and Barney Creek (yellow), plot against their ages. The larger circles seen represent the bootstrapped average of all the points with 95% confidence intervals. Where confidence intervals cannot be seen is due to error bars being smaller than the size of the point. It is important to note that where each formation plots, may not be to their exact formation ages. This was done to ensure formations would be able to be seen, rather than overlapping data. The dashed line at $\delta^{15}\text{N} = 2\text{\textperthousand}$ represents fractionation believed to be associated with nitrogen fixation. The larger of the blue lines represents the time of the Sturtian glaciation, and the smaller represents the Marinoan glaciation. ....	43
Figure 13. $\delta^{15}\text{N}$ vs age plot as seen before in Figure 12. The black arrow here represents the potential overall trend of ‘Interpretation 1’. ....	47
Figure 14. $\delta^{15}\text{N}$ vs age plot as seen before in Figure 12. The black arrow here represents the potential overall trend of ‘Interpretation 2’. ....	49

Table 1. Geological formations used in study from McArthur Basin: Wollogorang Formation ca. 1.73 Ga (Kendall, Creaser, Gordon, & Anbar, 2009). Fraynes Formation ca. 1.64 Ga (Bullen, 2017). Barney Creek Formation ca. 1.64 Ga (Page & Sweet, 1998). Mainoru, Crawford and Jalboi Formations are constrained by an older tuff layer of age ca. 1.49 Ga and the younger above lying Velkerri formation of age ca. 1.38 Ga (Kendall et al., 2009; Yang et al., 2018). Velkerri Formation ca. 1.38 Ga (Kendall et al., 2009; Yang et al., 2018). Kyalla Formation ca. 1.33 Ga (Yang et al., 2018). Jamison Formation has a maximum depositional age of ca. 1.092 Ga (Yang et al., 2018), therefore, the Jamison Formation must be younger than 1.092 Ga. Similarly, the Hayfield Formation has a maximum depositional age of ca. 1.057 Ga (Yang et al., 2018) therefore, the Hayfield Formation must be younger than 1.057 Ga. Borden Rift Basin: Arctic Bay Formation ca. 1.05 Ga (Gibson et al., 2017). Amadeus Basin: Gillen Formation ca. 0.80 Ga (Macdonald et al., 2010; Swanson-Hysell et al., 2010). Adelaide Rift Complex: Tapley Hill Formation ca. 0.66 Ga (Kendall, Creaser, & Selby, 2006). Tent Hill Formation is stratigraphically correlated with GSSP, therefore, has an age younger than ca. 0.635 Ga(Knoll, Walter, Narbonne, & Christie-Blick, 2006). ....	18
Table 2. Definitions reproduced from Jarrett et al. (2018b). ....	24
Table 3. Carbon and Nitrogen isotope data of the Tent Hill Formation. ....	57
Table 4. Carbon and Nitrogen isotope data of the Tapley Hill Formation. ....	58
Table 5. Carbon and Nitrogen isotope data of the Gillen Formation. ....	59
Table 6. Carbon and Nitrogen isotope data of the Arctic Bay Formation. ....	60
Table 7. Carbon and Nitrogen isotope data of the Arctic Bay Formation continued. ....	61
Table 8. Carbon and Nitrogen isotope data of the Kyalla Formation. ....	62
Table 9. Carbon and Nitrogen isotope data of the Velkerri Formation. ....	63
Table 10. Carbon and Nitrogen isotope data of the Velkerri Formation continued. ....	64
Table 11. Carbon and Nitrogen isotope data of the Lower Roper Group: Jalboi and Crawford formations. ....	65
Table 12. Carbon and Nitrogen isotope data of the Lower Roper Group: Mainoru Formation. ....	66

Table 13. Carbon and Nitrogen isotope data of the Fraynes Formation.....	67
Table 14. Carbon and Nitrogen isotope data of the Barney Creek Formation. ....	68
Table 15. Carbon isotope data of the Wollogorang Formation. ....	69
Table 16. Carbon and Nitrogen isotope data of the standards used for the IRMS. ....	70
Table 17. Trace metal data of the Tent Hill Formation .....	71
Table 18. Trace metal data of the Tent Hill Formation continued. ....	72
Table 19. Trace metal data of the Tapley Hill Formation. ....	73
Table 20. Trace metal data of the Tapley Hill Formation continued. ....	74
Table 21. Trace metal data of the Gillen Formation.....	75
Table 22. Trace metal data of the Arctic Bay Formation. ....	76
Table 23. Trace metal data of the Arctic Bay Formation continued. ....	77
Table 24. Trace metal data of the Hayfield Formation.....	78
Table 25. Trace metal data of the Jamison Formation. ....	78
Table 26. Trace metal data of the Kyalla Formation. ....	79
Table 27. Trace metal data of the Velkerri Formation. ....	80
Table 28. Trace metal data of the Velkerri Formation continued. ....	81
Table 29. Trace metal data of the Lower Roper Group: Jalboi, Crawford and Mainoru formations.....	82
Table 30. Trace metal data of the Fraynes Formation. ....	83
Table 31. Trace metal data of the Barney Creek Formation. ....	84
Table 32. Trace metal data of the Wollogorang Formation. ....	85
Table 33. Trace metal data of the Barney Creek Formation continued. ....	85
Table 34. ‘Rock Eval’ data of the Tent Hill Formation.....	86
Table 35. ‘Rock Eval’ data of the Tapley Hill Formation.....	87
Table 36. ‘Rock Eval’ data of the Gillen Formation. ....	88
Table 37. ‘Rock Eval’ data of the Kyalla Formation. ....	89
Table 38. ‘Rock Eval’ data of the Velkerri Formation.....	90
Table 39. ‘Rock Eval’ data of the Velkerri Formation continued. ....	91
Table 40. ‘Rock Eval’ data of the Lower Roper Group: Jalboi, Crawford and Mainoru formations.....	92
Table 41. ‘Rock Eval’ data of the Mainoru Formation continued.....	93
Table 42. ‘Rock Eval’ data of the Fraynes Formation. ....	94
Table 43. ‘Rock Eval’ data of the Barney Creek Formation. ....	95
Table 44. ‘Rock Eval’ data of the Barney Creek Formation continued. ....	96
Table 45. ‘Rock Eval’ data of the Wollogorang Formation. ....	97
Table 46. ‘Rock Eval’ data of the standards used: Green River Shale, the SRA standard and an Adelaide standard.....	98

## INTRODUCTION

In contrast to present day, the early Earth was characterised by the absence of atmospheric oxygen. The motivation for this thesis is to better understand oxygenation of the Earth during the Proterozoic. Prior to the Proterozoic, the Archean was essentially devoid of oxygen, such that  $pO_2$  levels were <0.001% of present atmospheric levels (PAL) (Bekker et al., 2004; Blaustein, 2016), compared to present day values of ~21%  $pO_2$ , i.e. oxic environment (Lyons, Reinhard, & Planavsky, 2014). Geochemical data suggest that the oxygenation of the Earth's Precambrian atmosphere occurred in two main events; the Great Oxidation Event (GOE, ca. 2.35 Ga) (Blaustein, 2016) and the Neoproterozoic Oxidation Event, where the timing of the NOE is debated, with estimates ranging between ca. 800 Ma (Cole et al., 2016) and ca. 580 Ma (Scott et al., 2008). The emergence and evolution of oxygenic photosynthesis is accepted to have been the definitive explanation for the first rise in atmospheric oxygen.

The onset of the GOE is marked by the disappearance of mass independent fractionation (MIF) of sulphur isotopes (Bekker et al., 2004; Lyons et al., 2014). Preservation of large MIF signals recorded prior to the GOE is related to the lack of an ozone layer (Bekker et al., 2004), which is associated with a pervasively anoxic atmosphere. Therefore, the disappearance of MIF post GOE indicates an increase in oxygen (Bekker et al., 2004). Further evidence of the GOE includes the disappearance of detrital pyrite from the sedimentary record. The preservation of detrital pyrite in sedimentary rocks older than ca. 2.4 Ga is evidence of low O<sub>2</sub> concentrations and its disappearance from the record afterwards is indicative of a rise in oxygen (Anbar et al., 2007). The NOE remains highly debated, while most geochemical proxies support a significant rise in  $pO_2$  during the Neoproterozoic, the exact timing and nature of the oxygenation event is still

disputed (Och & Shields-Zhou, 2012). Some papers propose a constant atmospheric oxygen level since ca. 3.8 Ga (Och & Shields-Zhou, 2012) where others have suggested a more stepwise evolution in oxygenation (Gilleaudeau et al., 2016; Planavsky et al., 2014). How ever the oxygenation occurred, it is mostly agreed upon that the NOE marks a time whereby deep oceans contained sufficient levels of dissolved oxygen to sustain diverse eukaryotic ecosystems.

More controversially, recent studies have indicated the possibility of one or more significant Mesoproterozoic oxygenation events (MOE) (Gilleaudeau et al., 2016), with oxygen levels sufficiently high enough to support large metazoan life (Zhang et al., 2016). However, this remains controversial, with other studies suggesting a continuing low Mesoproterozoic atmospheric  $p\text{O}_2$  (Planavsky et al., 2014). Research into the MOE has produced conflicting interpretations, which may be due to either; limited knowledge of the oxygen thresholds required to trigger responses in redox proxies, redox variability within basins, or a more complex and dynamic redox behaviour with both high and low  $p\text{O}_2$  throughout the Mesoproterozoic.

Carbon and nitrogen are abundant elements in organic matter and a crucial component of the biogeochemical cycle within the biosphere and atmosphere, and therefore useful in the study of redox sensitive paleo-environments. Changes in the marine redox structure would therefore directly correlate to both carbon and nitrogen cycling within the global ocean, which should be expressed in the carbon and nitrogen isotopic signature of organic-rich sedimentary rocks—reflecting the redox transition. Carbon ( $\delta^{13}\text{C}$ ) and nitrogen ( $\delta^{15}\text{N}$ ) isotopes, in conjunction with redox sensitive trace metals, molybdenum (Mo) and vanadium (V), can be used as proxies for ocean redox structure,

and thereby atmospheric redox, to further unravel the oxygenation of the Earth during the Paleoproterozoic to Neoproterozoic.

Proterozoic basins such as the McArthur basin, Amadeus basin, Borden Rift Basin (Arctic Canada) and the Adelaide Rift Complex, represent a preserved record throughout the Paleoproterozoic to Neoproterozoic. Here we present carbon, nitrogen and trace metal data from these basins to establish a chemo-stratigraphic record and provide insights into oxygenation during the Proterozoic; a time where a comprehensive coupled dataset is lacking.

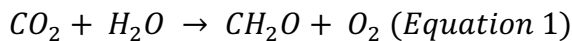
These data sets will be fundamental to further understanding the origins of early complex, eukaryotic life and the rise of atmospheric oxygen, specifically, to better understand the nature of atmospheric oxygenation during the Paleoproterozoic to Neoproterozoic and its relationship and interaction with evolving complex life (Blaustein, 2016).

## Background to redox proxies

### MARINE CARBON CYCLE

Atmospheric carbon, CO<sub>2</sub>, enters the ocean via diffusion and exists in equilibrium with the bioavailable form HCO<sub>3</sub><sup>-</sup> (Worden et al., 2015), also referred to as the dissolved inorganic carbon (DIC) pool. Organic carbon (C<sub>org</sub>) preferentially takes up light carbon (<sup>12</sup>C), leaving the DIC pool isotopically heavy (Schrag, Higgins, Macdonald, & Johnston, 2013). However, C<sub>org</sub> can be re-mineralised back into the water column, returning light carbon back to the DIC pool. Large fractionation occurs between DIC and C<sub>org</sub> (~30‰, Hayes, Strauss, & Kaufman, 1999) when C<sub>org</sub> is buried and removed from the water column (*f<sub>org</sub>*).

This process of net carbon burial leads to net oxygen production, due to the following simplified equation for primary productivity:



Consequently, an increase in *f<sub>org</sub>* reflects an increase in O<sub>2</sub> production. Carbonates (C<sub>carb</sub>) that precipitate from the DIC pool, with little fractionation of carbon isotopes, broadly record the isotopic signature of the DIC pool (Schrag et al., 2013). Therefore, changes in the isotopic composition of the DIC pool are dominated by the burial of organic matter (*f<sub>org</sub>*). Knowing either the δ<sup>13</sup>C of carbonates (C<sub>carb</sub>) or of buried organic matter (C<sub>org</sub>) can be used to estimate *f<sub>org</sub>*, using the following equation (assuming long term average of fractionation between the two is ~30 per mil) (Hayes et al., 1999);

$$\delta^{13}C_{in} = \delta^{13}C_{org}f_{org} + \delta^{13}C_{carb}(1 - f_{org}) \text{ (Equation 2)}$$

Changes in the isotopic composition of C<sub>carb</sub> throughout the geological record have been interpreted to reflect changes in *f<sub>org</sub>* (Schrag et al., 2013). This isotopic mass

balance, therefore, involves a link between the carbon cycle, net oxygen production and thus atmospheric oxygen content of the Earth (Lyons et al., 2014; Schrag et al., 2013).

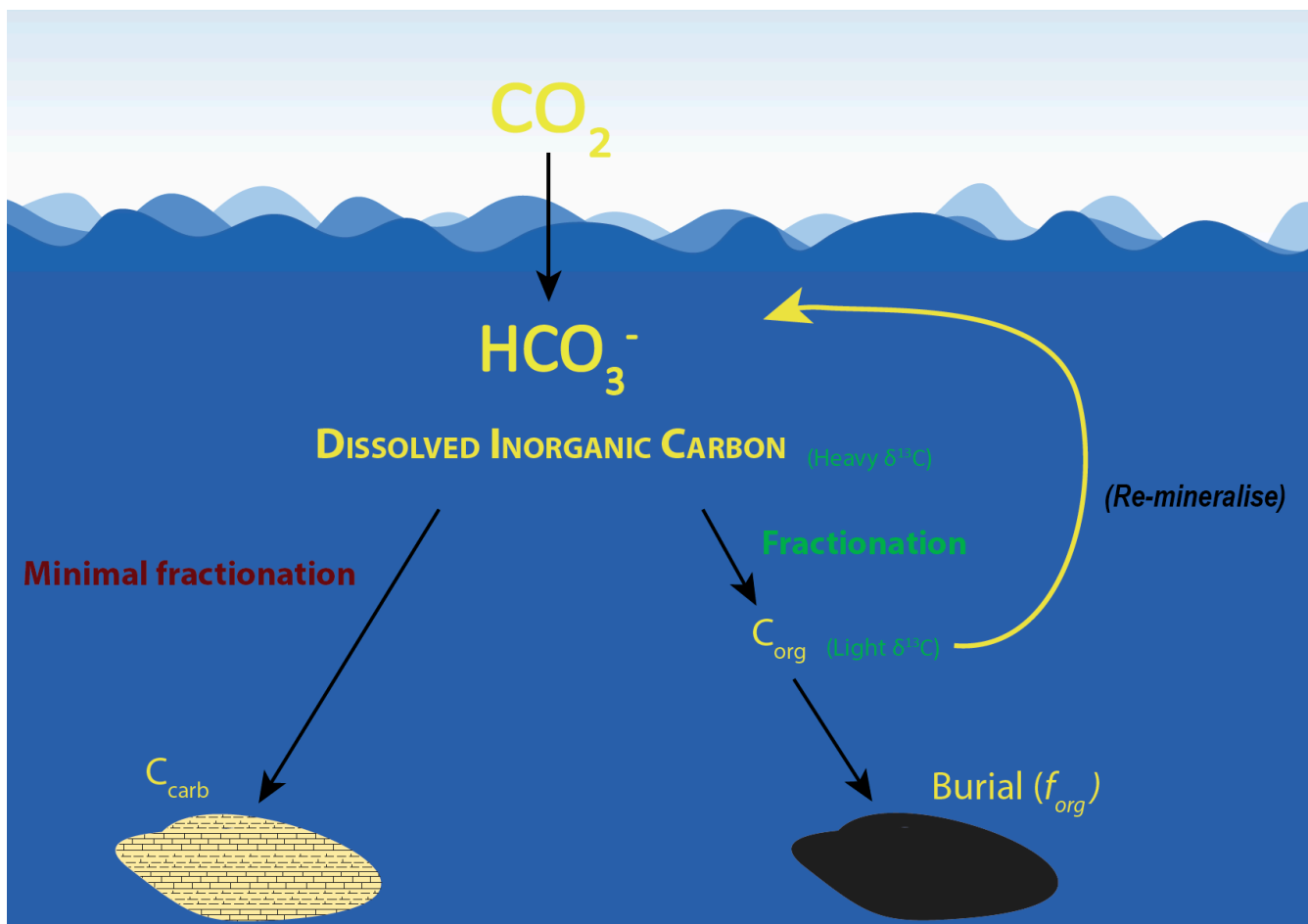


**Figure 1.** Simplified cartoon of the marine carbon cycle. Atmospheric carbon in the form of  $\text{CO}_2$  diffuses into the ocean and exists in equilibrium with bioavailable carbon ( $\text{HCO}_3^-$ ), otherwise known as DIC. Organic matter preferentially takes up light carbon, therefore leaving the residual DIC isotopically heavy. This organic matter can be re-mineralized, returning the light isotopes back to the DIC. However, organic matter may go on to be buried, i.e.  $f_{\text{org}}$ . This is represented as a black shale in the above diagram. This burial process creates a large fractionation between  $\text{C}_{\text{org}}$  and DIC. The remaining carbon in the DIC goes on to make inorganic carbon ( $\text{C}_{\text{carb}}$ ). Therefore,  $\text{C}_{\text{carb}}$  reflects the isotopic signature of DIC pool. The long-term average fractionation factor is  $\sim 30\%$ , therefore, measuring isotopic signals of either  $\text{C}_{\text{carb}}$  or  $\text{C}_{\text{org}}$ , using equation 2,  $f_{\text{org}}$  can be solved for.

## MARINE NITROGEN CYCLE

### FIXATION

The primary source of nitrogen in open oceans is formed from the mixing of deep nitrate-rich water, surface runoff and diffusion of atmospheric nitrogen, N<sub>2</sub> (Zehr & Kudela, 2011). N<sub>2</sub> is the most abundant form of nitrogen in seawater. However, it is only biologically available to particular cyanobacteria (i.e. diazotrophs, Zehr & Kudela, 2011). Diazotrophs use the enzyme nitrogenase to fix N<sub>2</sub> into bioavailable nitrogen (i.e. ammonium, NH<sub>4</sub><sup>+</sup>) (Hutchins, Mulholland, & Fu, 2009). This process results in minimal isotopic fractionation of δ<sup>15</sup>N (approximately +2‰). However, the isotopic fractionation expressed can change depending on the isozyme makeup of nitrogenase. Molybdenum (Mo) based nitrogenase has been recognised as the most efficient and common nitrogenase, with only limited fractionation of nitrogen isotopes (i.e. -2.94 ± 0.44‰ to -1.74 ± 0.22‰) (Zhang, Sigman, François, Morel, & Kraepiel, 2014). Vanadium (V) based nitrogenase, a less efficient nitrogenase (typically expressed under Mo-deficient conditions), has significantly larger isotopic fractionations (-6.84 ± 0.34‰ to -6.33 ± 0.26‰) (Zhang et al., 2014) and iron based nitrogenase, gives approximately -7.99 ± 0.25‰ to -6.87 ± 0.52‰ (Zhang et al., 2014) isotopic fractionation. Regardless of the type of nitrogenase used, diazotrophs are most efficient under nitrogen limited conditions, where considerable amounts of nitrogen can be fixed. However, due to the requirement of either Mo, V or Fe, N<sub>2</sub>-fixation can be limited by the availability of these trace elements, which is strongly controlled by water column redox (Zehr & Kudela, 2011).

## NITRIFICATION

Nitrification is considered to be a two-step process, the first being the rate-limiting process, involving ammonium oxidation (ammonification) and nitrite oxidation, an aerobic process with each step carried out by different bacteria (Capone, 2008; Shiozaki et al., 2016; Zehr & Kudela, 2011). Where ammonium is released into the ocean via the breakdown of organic matter, it is nitrified via oxidation to nitrite ( $\text{NO}_2^-$ ) and nitrate ( $\text{NO}_3^-$ ) under oxic conditions (Ader et al., 2016). Ammonium oxidation of nitrogen is not inhibited by light availability, consequently, nitrification occurs throughout the water column (Zehr & Kudela, 2011). However, rates of nitrification are limited by organic matter and oxygen concentrations, suggesting that nitrification is enhanced under oxic conditions and reduced under anoxic conditions (Ward, 1996). Nitrification neither adds nor removes nitrogen from the marine nitrogen cycle, however, it is a significant step as it oxidises ammonium to nitrate in deep ocean reservoirs (Ward, 1996).

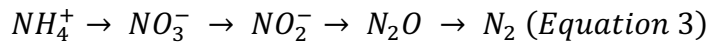
Nitrification generally goes to completion, as seen by the 1:1 ratio between  $\delta^{15}\text{N}$ -sediments and  $\delta^{15}\text{N}$ -nitrate (Galbraith, Sigman, Robinson, & Pedersen, 2008), consequently, the large isotopic fractionation associated with nitrification is generally not expressed.

## ASSIMILATION

Most heterotrophic bacteria are able to ingest and use nitrogen in its inorganic form, ammonium, where it can then be converted to nitrate and nitrite. Similar to nitrification, assimilation reactions go to completion and consequently the isotopic fractionation associated with assimilation is not expressed.

## HETEROTROPHIC DENITRIFICATION

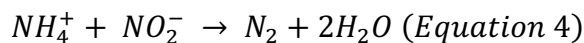
Denitrification is the major biotic pathway for the loss of fixed nitrogen in the environment (Ward, 1996), where nitrogen is converted to atmospheric N<sub>2</sub> via reduction reactions (Hutchins et al., 2009):



Heterotrophic denitrification creates a large fractionation, preferentially returning light δ<sup>15</sup>N to the atmosphere. Denitrification occurs where both nitrate (oxidised nitrogen) and ammonium coexist, consequently this process occurs at the oxic-anoxic interface of benthic sediments, and at sub-oxic to anoxic areas within Oxygen Minimum Zones (OMZ's) (Zehr & Kudela, 2011).

## ANAMMOX

Anammox (anaerobic ammonium oxidation) is a bacterial mediated process in which nitrite and ammonium are converted directly into N<sub>2</sub> and water, returning nitrogen to the atmosphere (Hutchins et al., 2009). Again, this process occurs at the interface between oxic and anoxic zones as anammox requires both oxidised and reduced forms of N (Zehr & Kudela, 2011), fuelled by diffusion of ammonium from below and of oxygen from above (Zehr & Kudela, 2011). Anammox bacteria acquire energy from ammonia oxidation, and release N<sub>2</sub> as an oxidation product, rather than nitrite (Zehr & Kudela, 2011) creating a large fractionation of nitrogen, where the residual pool is δ<sup>15</sup>N heavy;



In summary, as assimilation and nitrification processes go to completion, the δ<sup>15</sup>N of bioavailable nitrogen is controlled by the relative rates of N<sub>2</sub> fixation, heterotrophic denitrification and anammox. The magnitude of N<sub>2</sub> fixation is limited under nitrogen-

rich conditions, however, more significantly, it is inhibited under reducing conditions due to both Mo and V limitation—both elements used in the nitrogenase process. Furthermore, the extent of denitrification and anammox is controlled by the size and abundance of OMZs, the availability of nitrate and nitrite, and the supply of organic matter. Therefore, the  $\delta^{15}\text{N}$  of marine waters is controlled by the relative balance between  $\text{N}_2$  fixation, heterotrophic denitrification and anammox, all of which are influenced by the redox state of the ocean and atmosphere.

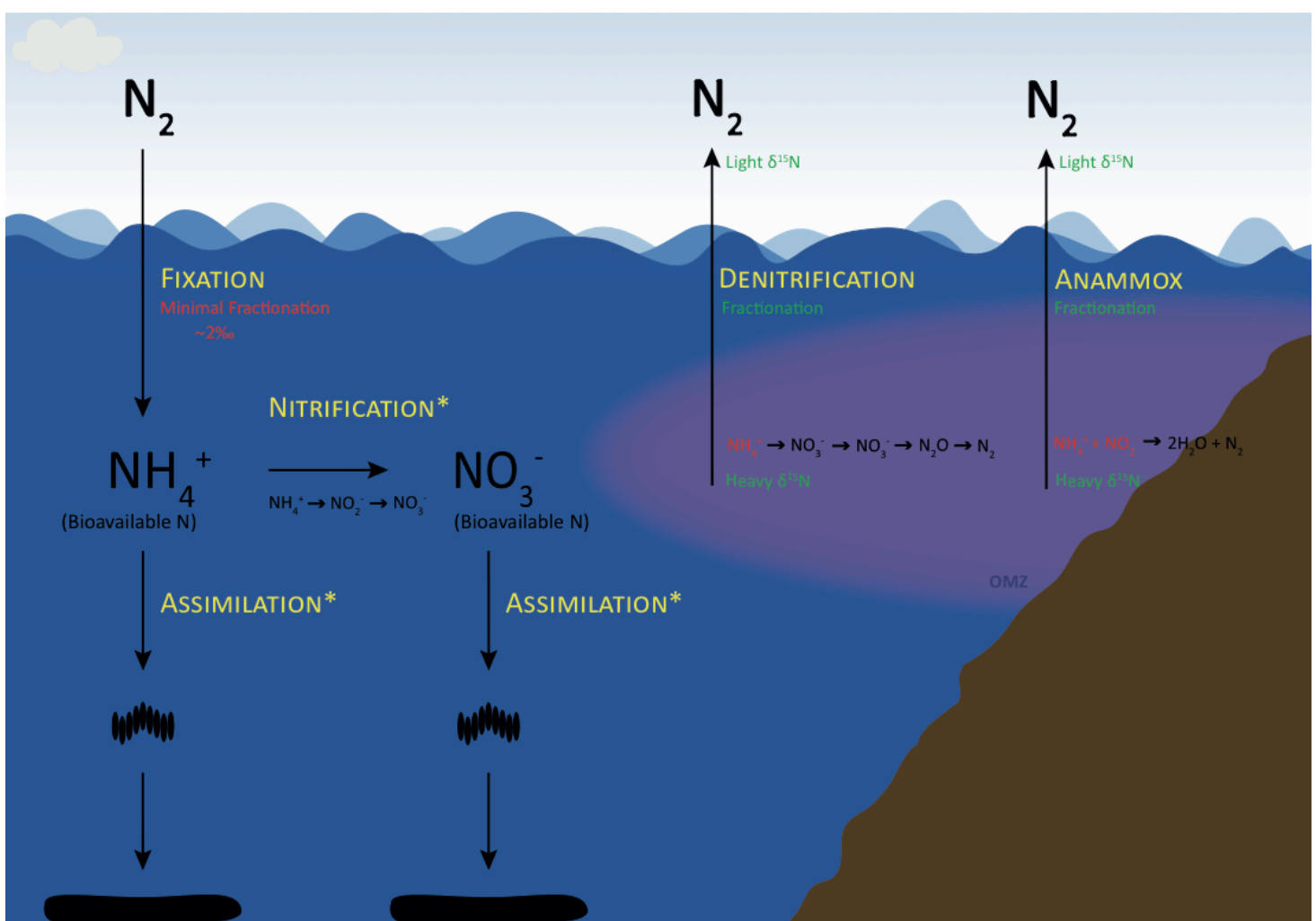


**Figure 2. Simplified cartoon of the marine nitrogen cycle.**  $\text{N}_2$  enters the oceans and is ‘fixed’ via diazotrophs into bioavailable nitrogen as  $\text{NH}_4^+$ . This process is usually expressed with minimal fractionation, ~2‰. From here, assimilation or nitrification can occur. Nitrification\* is the bacterial mediated process where ammonium is nitrified via oxidation. It is believed that this step (\*) goes to completion, resulting in little fractionation. Organisms take nitrogen from the bioavailable pool of nitrogen (either  $\text{NH}_4^+$  or  $\text{NO}_3^-$ , as some can take up both), which is the process of assimilation. Again, it is believed that Assimilation\* reactions go to completion, resulting in little fractionation occurs.  $\text{N}_2$  leaves the ocean via 2 processes: Denitrification and Anammox. The red parts of these reactions are to indicate the different starting factors between the two. Denitrification and anammox are partial processes, and therefore fractionate, leaving the bioavailable nitrogen pool heavy, preferentially returning light isotopes to the atmosphere. These two processes occur at oxic-anoxic boundaries (oxygen minimum zones – indicated by the purple wedge in the above figure) as they require both environments to complete the reaction. Therefore, the organic matter that go on to eventually form shales are controlled by the dominance of either the fixation process, or the denitrification/anammox processes, which is ultimately what  $\delta^{15}\text{N}$  measures.

## REDOX SENSITIVE TRACE METALS

### MOLYBDENUM AND VANADIUM

Mo and V are common proxies used for ocean redox as they are enriched in sediments under reducing conditions and depleted under oxic conditions, displaying distinct changes through oxic, sub-oxic, anoxic and euxinic conditions (Piper & Calvert, 2009). Both elements occur as oxidised species in seawater where under mildly reducing, sub-oxic conditions, V reduces first due to its higher redox potential, thus the V/Mo ratio increases under sub-oxic conditions (Algeo & Maynard, 2004; Tribouillard, Algeo, Lyons, & Riboulleau, 2006). Under sub-oxic to anoxic conditions, Mo begins to reduce, along with V where the V/Mo ratio will decrease. Under euxinic (sulphidic) conditions, Mo reacts strongly with hydrogen sulphide such that it is essentially removed from seawater and porewaters. V usually cannot be further reduced, and is only further enriched in sediments when sulphide levels are high enough to allow further reduction of  $V^{4+}$  to  $V^{3+}$  (Breit & Wanty, 1991; Lewan & Maynard, 1982; Wanty & Goldhaber, 1992). Consequently, Mo undergoes greater enrichment than V under euxinic conditions. Thus, the anoxic to euxinic transition is characterised by decreasing V/Mo ratios and increasing Mo values within sediments (Breit & Wanty, 1991).

## GEOLOGICAL BACKGROUND

### Overview

The organic-rich shale samples investigated in this project come from multiple basins, principally within the greater McArthur Basin, Northern Territory. Further samples have been obtained from the Amadeus Basin, Northern Territory, the Adelaide Rift Complex, South Australia, and the Borden Rift Basin, Arctic Canada (Table 1).

**Table 1. Geological formations used in study from McArthur Basin: Wollogorang Formation ca. 1.73 Ga (Kendall, Creaser, Gordon, & Anbar, 2009). Fraynes Formation ca. 1.64 Ga (Bullen, 2017). Barney Creek Formation ca. 1.64 Ga (Page & Sweet, 1998). Mainoru, Crawford and Jalboi Formations are constrained by an older tuff layer of age ca. 1.49 Ga and the younger above lying Velkerri formation of age ca. 1.38 Ga (Kendall et al., 2009; Yang et al., 2018). Velkerri Formation ca. 1.38 Ga (Kendall et al., 2009; Yang et al., 2018). Kyalla Formation ca. 1.33 Ga (Yang et al., 2018). Jamison Formation has a maximum depositional age of ca. 1.092 Ga (Yang et al., 2018), therefore, the Jamison Formation must be younger than 1.092 Ga. Similarly, the Hayfield Formation has a maximum depositional age of ca. 1.057 Ga (Yang et al., 2018) therefore, the Hayfield Formation must be younger than 1.057 Ga. Borden Rift Basin: Arctic Bay Formation ca. 1.05 Ga (Gibson et al., 2017). Amadeus Basin: Gillen Formation ca. 0.80 Ga (Macdonald et al., 2010; Swanson-Hysell et al., 2010). Adelaide Rift Complex: Tapley Hill Formation ca. 0.66 Ga (Kendall, Creaser, & Selby, 2006). Tent Hill Formation is stratigraphically correlated with GSSP, therefore, has an age younger than ca. 0.635 Ga (Knoll, Walter, Narbonne, & Christie-Blick, 2006).**

Formation	Group	Basin	Dating method	Age constraint
Wollogorang	Tawallah	McArthur	Re-Os shale	ca. 1.73 Ga
Fraynes	Limbunya	McArthur/Birrindudu Sub-basin	Stratigraphic correlation with Barney Creek Fm.	ca. 1.64 Ga
Barney Creek	McArthur	McArthur	Zircon/U-Pb	ca. 1.64 Ga
Mainoru	Roper	McArthur	Constrained by an older tuff age and the younger Velkerri Formation	ca. 1.49 – 1.38 Ga
Crawford	Roper	McArthur	Constrained by an older tuff age and the younger Velkerri Formation	ca. 1.49 – 1.38 Ga
Jalboi	Roper	McArthur	Constrained by an older tuff age and the younger Velkerri Formation	ca. 1.49 – 1.38 Ga
Velkerri	Roper	McArthur	Detrital zircon/U-Pb and Re-Os shale	ca. 1.38 Ga
Kyalla	Roper	McArthur/Beetaloo Sub-basin	Detrital zircon/U-Pb	ca. 1.33 Ga
Jamison	Balmain	McArthur	Detrital zircon/U-Pb	< ca. 1.092 Ga
Hayfield	Balmain	McArthur	Detrital zircon/U-Pb	< ca. 1.057 Ga
Arctic Bay	Equalulik	Borden Rift	Re-Os	ca. 1.05 Ga
Gillen	Bitter Springs	Amadeus	Correlation via $\delta^{13}\text{C}$ chemo-stratigraphy	ca. 0.80 Ga
Tapley Hill	Umberatana	Adelaide Rift Complex	Re-Os	ca. 0.66 Ga
Tent Hill	Wilpena	Adelaide Rift Complex	Stratigraphic correlation with GSSP.	< ca. 0.635 Ga

This sample collection comes from distributed basins throughout Australia (North Australia and Gawler Cratons) with further samples from Northern Canada (Laurentia), which together span multiple cratons and time periods to present a more global rather than regional record.

### **Greater McArthur Basin, Northern Territory**

The McArthur Basin is a laterally extensive, intracontinental, Proterozoic (ca. 1.85-1.3Ga), sedimentary basin covering a large area of the North Australian Craton ( $\sim 180,000 \text{ km}^2$ ), located in the north-east of the Northern Territory (Sheridan, Johns, Johnson, & Menpes, 2018; Spinks, Schmid, & Pagès, 2016). The basin is made up of a series of prominent sedimentary packages including the Birrindudu Basin, McArthur Basin and the Tomkinson Province, which together make up the greater McArthur Basin (Munson, 2016). These sedimentary successions consist of marine, shallow marine to fluvial sediments, and several major regressive-transgressive cycles have been identified (Sheridan et al., 2018; Spinks et al., 2016).

### **Amadeus Basin, Northern Territory**

The Amadeus Basin is an intra-cratonic, Neoproterozoic to early Cambrian, basin (Normington & Edgoose, 2018; Wells, Forman, Ranford, & Cook, 1970). Located in central Australia, predominantly within the southern part of the Northern Territory and extending into Western Australia, covering  $\sim 170,000 \text{ km}^2$ . The basin comprises a succession of clastic, carbonate and evaporite sediments (Normington & Edgoose, 2018). Three principal tectonic events formed the basin: initial extension in the Mesoproterozoic, with late Neoproterozoic compression (Petermann Orogeny), and episodic compression from the Silurian to Devonian (Alice Springs Orogeny) (Buick,

Storkey, & Williams, 2008; Plummer, 2018; Roberts & Houseman, 2018; Wells et al., 1970) Epeirogenic movement and subsidence was followed by widespread evaporites that were deposited in a shallow, restrictive sea (Wells et al., 1970). The sediments of this evaporite cycle were named the Bitter Springs Formation, where most of the gypsum in the Amadeus basin is found. Thick beds of evaporites are present in the Gillen Member of the Bitter Springs Formation (Wells et al., 1970), which are now referred to as the Gillen Formation of the Bitter Springs Group (Normington & Edgoose, 2018).

### **Adelaide Rift Complex, South Australia**

The Adelaide Rift Complex, formerly referred to as the Adelaide Geosyncline, is a Neoproterozoic to early Cambrian basin complex located in South Australia (Haines, Turner, Kelley, Wartho, & Sherlock, 2004; Preiss, 2000). Sediments were deposited originally in an intracontinental rift complex within Rodinia before super-continental breakup which ultimately developed the rift basin (Mahan, Wernicke, & Jercinovic, 2010). Deposition ceased during the early Cambrian due to the Delamerian Orogeny which now controls the present distribution of rock units (Haines et al., 2004; Preiss, 2000). The Heysen Supergroup—one of the three supergroups that encompass sediments of the Adelaide Rift Complex—comprises glacial, interglacial and post glacial sediments of the Umberatana and Wilpena Groups (Mahan et al., 2010), where the Tapley Hill and Tent Hill formations used in this study come from.

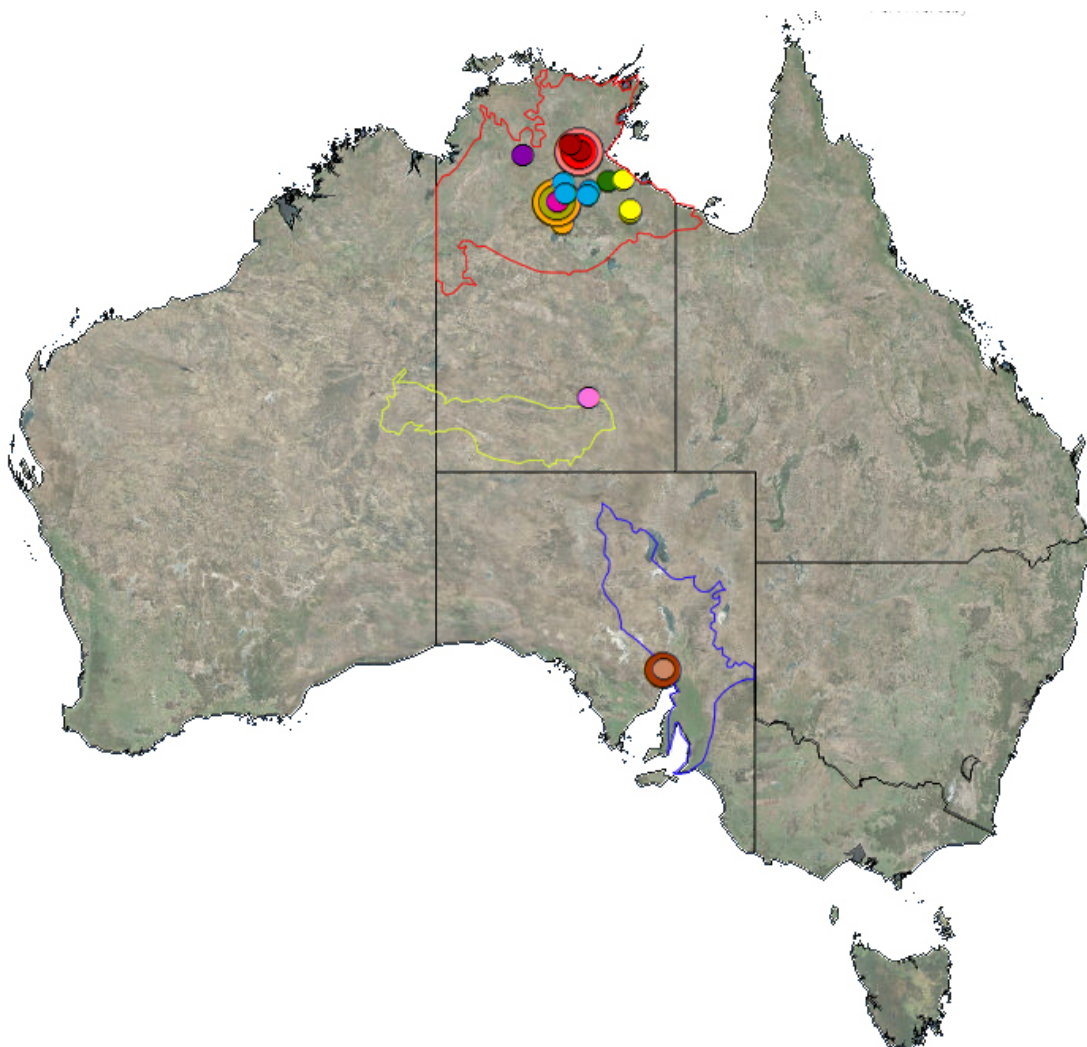


**Figure 3. Map of Australia showing the locations of the Australian formations used in this study. The outlines of the greater McArthur Basin (shown in red), the Amadeus Basin (shown in green), and the Adelaide Rift Complex (shown in blue), show the regional extent of each basin. The following formations are shown on the map: McArthur Basin formations: Wollogorang (dark green), Barney Creek (yellow), Fraynes (purple), Mainoru (dark red), Crawford (red), Jalboi (light-red), Velkerri (blue), Kyalla (orange), Jamison (dark-pink) and Hayfield (olive-green). Amadeus Basin: Gillen Formation (light-pink). The Adelaide Rift Complex: Tapley Hill Formation (dark-brown) and Tent Hill Formation (light-brown). Where there are multiple of the same coloured circles, there are multiple well locations used for that particular formation. Multiple formations obtained from the same well are depicted by different sized circles.**

## Borden Rift Basin, Arctic Canada

The Borden Rift Basin, also referred to as the Bylot Supergroup, is a thick succession of Mesoproterozoic – Neoproterozoic sediments, exposed within the fault-bounded Borden Rift Basin of the northernmost Baffin and Bylot Islands (North-eastern Canada, (Gibson et al., 2017; Kah, Sherman, Narbonne, Knoll, & Kaufman, 1999). The supergroup is comprised of three main lithostratigraphic groups, Nunatsiaq Group, Uluksan Group and the Eqalulik Group, separated via regional unconformities (Kah et al., 1999). Black shales deposited during marine transgressions formed the Arctic Bay Formation of the Eqalulik group (Gibson et al., 2017).

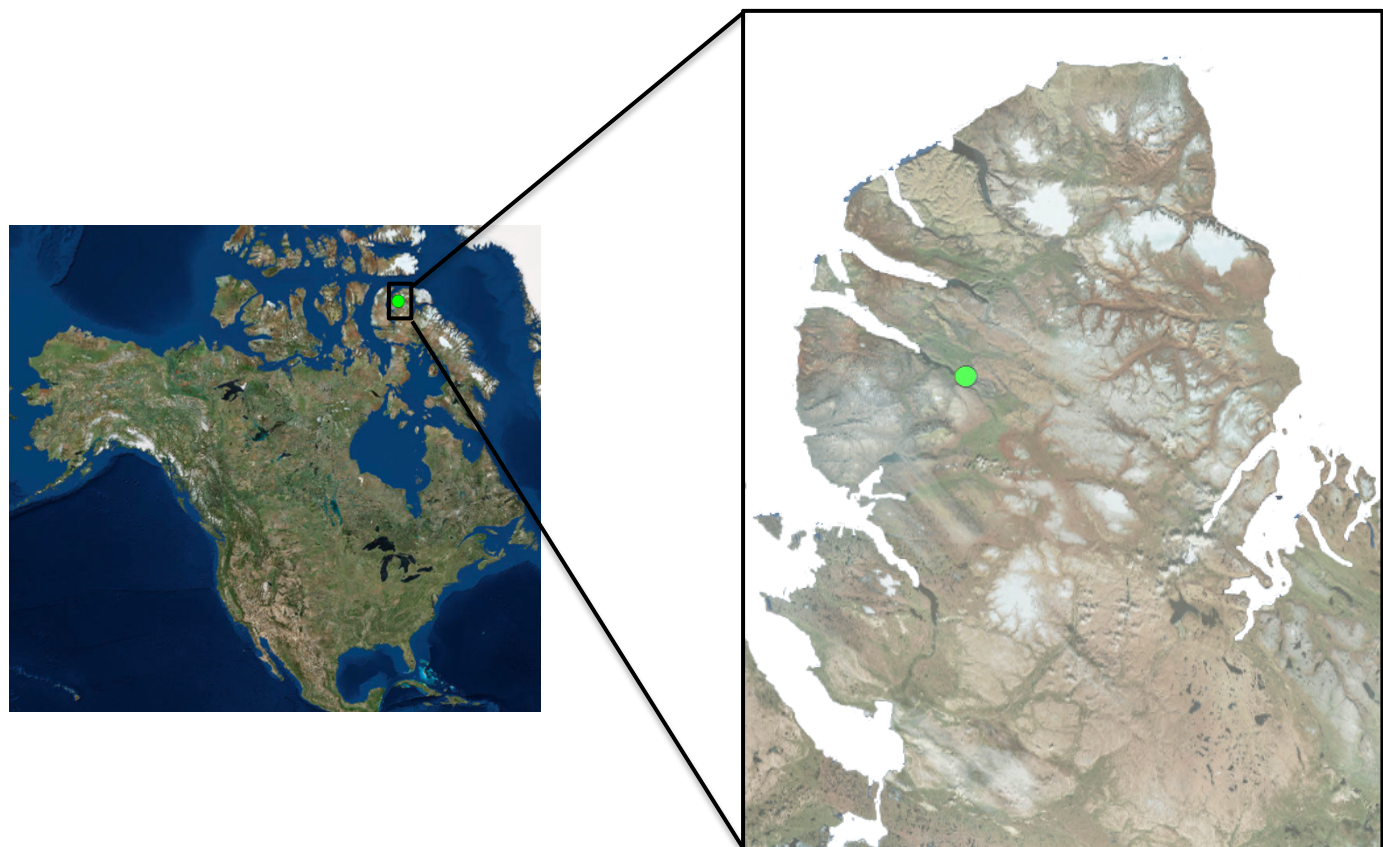


**Figure 4. Blow up of the Borden Rift Basin of Arctic Canada, of location with respect to North America. The green circle represents the location of the Arctic Bay Formation**

## METHODS

### Sample Collection

A large number of organic-rich black shales were collected from field outcrops and drill core to create a large sample base spanning the Paleoproterozoic to the Neoproterozoic. These samples were obtained from the greater McArthur basin, N.T, the Amadeus Basin N.T, and the Adelaide Rift Complex, S.A. A further sample set was acquired from the Bylot Supergroup of Canada. The samples were collected at small intervals, to obtain a high-resolution data set.

### Crushing

All samples were crushed to a fine powder (~100g) using a ‘Rocklabs’ tungsten carbide ring mill. Between each sample, the mill was cleaned using high pressure air and ethanol to ensure no cross contamination occurred. The rock powders were transferred to 50mL Corning CentriStar tubes.

### Source Rock Analyser (SRA)

Powdered samples were weighed out between 75-85mg into crucibles and loaded onto a Weatherford Source Rock Analyser, which ran pyrolysis on all samples. Alternate standards of Weatherford SRA rock standard, an Adelaide shale standard and the international standard, Green River Shale, were run every 10 samples. TOC, S1, S2, T<sub>max</sub>, HI, OI and PI results for each sample were produced from the Source Rock Analyser (SRA). Explanations of source rock parameters can be found in the following table (Table 2).

**Table 2. Definitions reproduced from Jarrett et al. (2018b).**

Acronyms	Definitions	Units
<b>TOC</b>	Total organic carbon (TOC), measure of the whole rock's organic richness.	wt. %
<b>S1</b>	The number of free hydrocarbons in a rock sample. Volatile hydrocarbon content.	mg Hydrocarbon/ g rock
<b>S2</b>	The number of hydrocarbons generated through cracking of kerogen. Remaining hydrocarbon generative potential.	mg Hydrocarbon/ g rock
<b>T<sub>max</sub></b>	Thermal maximum, the temperature during pyrolysis at which the maximum rate of hydrocarbons generated from cracking of kerogen (S2 peak).	°C
<b>HI</b>	Hydrogen Index. Number of hydrocarbons released during pyrolysis. Associated with residual organic matter. (S2x100)/TOC.	mg Hydrocarbon/ g TOC
<b>OI</b>	Oxygen Index. O <sub>2</sub> released from carbon dioxide during pyrolysis. Associated with organic matter. (S3x100)/TOC.	mg CO <sub>2</sub> / g TOC
<b>PI</b>	Production Index. Extent kerogen has converted to oil and gas. Used to measure maturity of rock. S1/(S1+S2).	-

### Acidification

All samples for carbon and nitrogen isotope analysis were acidified to remove any carbonate from shale powders. ~3-4mL of 3 molar hydrochloric acid was added to ~0.5-3g of rock powder in 15mL Corning CentriStar tubes. The powder and acid were thoroughly mixed using a centrifuge vibrator before being placed in the Eppendorf Centrifuge 5804, for 10 minutes at 4000 rpm. The hydrochloric acid was tipped off, and ~6mL of RO water was added, thoroughly mixed, and placed in the centrifuge again for 10 minutes at 4000 rpm. The RO water was tipped off and samples were placed in the oven (40-45°C) until dry.

### Isotope Ratio Mass Spectrometry (IRMS)

The dry, acid-treated samples were weighed (10-60mg), depending on their TOC, into EuroVector pressed tin capsules that were folded to seal the contents. The tin capsules were loaded and run through the Euro EA (Elemental Analyzer) which combusted the samples at 1030°C, where the resultant gases passed through the Nu-Horizon mass-

spectrometry IRMS to measure  $\delta^{15}\text{N}$  and  $\delta^{13}\text{C}$  isotopes along with standards of Glycine, Glutamic Acid, TPA and Green River Shale.

### **Major and Trace Elemental Analysis**

Bulk elemental analysis was analysed by Bureau Veritas. Major elements were analysed by X-ray fluorescence (XRF) using a Panalytical Axios 1<sup>TM</sup> spectrometer. XRF analysis were conducted on 40mm diameter fused beads prepared from a 1:10 sample/lithium tetraborate mixture (12:22 tetraborate/metaborate) from calcined powder. Calibration regression lines were prepared using Spec pure oxides and certified reference materials. Corrections for mass absorption effects were applied on concentration values using a combination of alpha coefficients and/or Compton scatter. The accuracy for silica is within 0.5% absolute, within 1% for other majors and within 5% for trace elements.

Trace elements were analysed on an Agilent 7900 ICP-MS. Analysis was performed on ~0.15g of rock powder which underwent mixed acid digestion ( $\text{HNO}_3$ ,  $\text{HClO}_4$  and HF) and made up to 10ml analytical volume. Rh and Ir were used as an internal standard for drift correction. The generation of oxides and doubly charged species was monitored using the mass ratios Th/ThO with on-line interference correction and internal standard correction carried out. To assess accuracy of the digestion process and analysis, certified reference materials (CRMs) Rmad25, Rmad 500 (A set), Rref25, Rref500 (B set) were run. Analytical reproducibility was assessed by repeat analysis of these CRMs throughout the run and repeat analysis of a random selection of solutions at the end of the run.

Further extended methods can be found in Appendix-A.

## RESULTS

### ca. 1.74 Ga

#### WOLLOGORANG FORMATION

Carbon isotopes ( $\delta^{13}\text{C}$ ) range from -28.77‰ to -31.25‰ with an average of -30.54‰.

Mo and V concentrations range from <0.5 ppm to 62.50 ppm, with an average of 18.31 ppm, and 20 ppm to 310 ppm, with an average of 106.07 ppm, respectively. Hydrogen indices (HI) range from 2 mg HC/g TOC to 64 mg HC/g TOC with an average of 28.43 mg HC/g TOC, classifying these shales as mature to over-mature (Jarrett *et al.*, 2018).

TOC values range from 0.27 wt. % to 8.49 wt. % with an average of 1.59 wt. %.

### ca. 1.64 Ga

#### FRAYNES FORMATION

Carbon and nitrogen isotopes ( $\delta^{13}\text{C}$ ,  $\delta^{15}\text{N}$ ) range from -29.99‰ to -33.83‰ (with an average of -32.55‰) and 1.24‰ to 6.58‰ (with an average of 4.82‰) respectively. Mo concentrations vary between <0.5 ppm and 101 ppm, with an average of 12.55 ppm. V concentrations range between 10 ppm and 250 ppm, with an average of 119.68 ppm. HI values range between 15.66 HC/g TOC and 86 HC/g TOC with an average value of 32.34 HC/g TOC, categorising the Fraynes shales as mature to over-mature (Jarrett *et al.*, 2018b). TOC values vary between 0.84 wt. % and 8.39 wt. %, with an average value of 2.88 wt. %.

#### BARNEY CREEK FORMATION

Carbon isotopes range between -28.67‰ and -34.79‰, averaging -32.84‰. Nitrogen isotope range between 2.91‰ and 8.37‰ averaging 5.85‰. Mo and V concentrations

range from 0.2 ppm to 23.3 ppm, with an average value of 4.85 ppm, and from 20.30 ppm to 212 ppm, with an average of 76.88 ppm, respectively. HI range between 15.66 HC/g TOC and 86 HC/g TOC, and an average of 32.34 HC/g TOC. Therefore, Barney Creek samples are classified as mature to over-mature (Jarrett et al., 2018b). TOC values range from 0.84 wt. % to 8.39 wt. % with an average value of 2.88 wt. %.

### **ca. 1.5 Ga to ca. 1.4 Ga**

#### **MAINORU FORMATION**

Carbon and nitrogen isotopes range between -19.89‰ and -32.43‰, with an average of -39.76‰, and 2.18‰ and 10.83‰, with an average of 4.66‰, respectively. Mo concentrations vary from <0.5 ppm to 3 ppm and an average of 0.55 ppm. V concentrations range from 70 ppm to 130 ppm and average 99.18 ppm. HI values range between 20 HC/g TOC and 136 HC/g TOC, with an average value of 60.15 HC/g TOC, classifying as mature to over-mature (Jarrett et al., 2018b). TOC values vary between 0.11 wt. % and 0.89 wt. %, with an average of 0.35 wt.%.

#### **CRAWFORD FORMATION**

Carbon isotope values range between -29.87‰ and -30.92‰ and average -30.44‰. Nitrogen isotopes range from 3.43‰ to 4.40‰ and average 4.07‰. Mo and V concentrations vary between <0.5 ppm to 1.5 ppm, with an average of 0.58‰, and 90 ppm to 190 ppm with an average of 130 ppm, respectively. HI values range between 24 HC/g TOC to 58 HC/g TOC and average 35.33 HC/g TOC, classifying these shales as mature to over-mature (Jarrett et al., 2018b). The TOC values range between 0.26 wt. % and 0.77 wt. % with an average value of 0.51 wt. %.

## JALBOI FORMATION

Carbon and nitrogen isotopes range from -27.85‰ and -31.30‰, with an average of -29.67‰, and 3.5‰ and 7.34‰, with an average of 4.29‰, respectively. Mo concentrations range from <0.5 ppm to 1.5 ppm and average 0.5 ppm. V concentrations range from 80 ppm to 130 ppm, with an average value of 94.29 ppm. HI values range between 26 HC/g TOC and 450 HC/g TOC and average 118.86 HC/g TOC, indicating the Jalboi formation as mature to over-mature (Jarrett et al., 2018b). TOC values range from 0.04 wt. % to 0.42 wt. %, averaging 0.25 wt. %.

## **ca. 1.38 Ga**

### VELKERRI FORMATION

Carbon isotopes for the Velkerri Formation range from -32.45‰ to -35.47‰, averaging -33.67‰. Nitrogen isotopes range between 0.79‰ and 4.94‰ with an average value of 3.64‰. Mo and V concentrations range from 0.20 ppm to 102 ppm, averaging at 14.04 ppm, and 50 ppm to 740 ppm, with an average value of 191.29 ppm, respectively. HI values range between 3 HC/g TOC and 551 HC/g TOC, with an average of 155.66 HC/g TOC, classifying as mature to over-mature (Jarrett et al., 2018b). TOC values range from 0.57 wt. % to 8.64 wt. % and averages 4.26 wt. %.

## **ca. 1.33 Ga**

### KYALLA FORMATION

Carbon and nitrogen isotopes range between -21.36‰ and -31.71‰, with an average of -29.80‰, and 1.44‰ to 3.14‰, averaging 2.48‰, respectively. Mo and V concentrations vary from; 0.37 ppm to 5ppm, averaging 1.63 ppm, and 65 ppm to 141

ppm, with an average of 109.33 ppm, respectively. HI values range from 35 HC/g TOC to 437.69 HC/g TOC, averaging at 104.43 HC/g TOC, classifying the Kyalla Formation's thermal maturity as mature to over-mature (Jarrett et al., 2018b). The TOC values range from 0.51 wt. % to 3.02 wt. % with an average value of 0.96 wt. %.

### **ca. 1.1 Ga**

#### ARCTIC BAY FORMATION

Carbon isotopes range from -26.6‰ to -32.07‰, averaging -29.64‰. Nitrogen isotopes range between 0.83‰ and 4.84‰ with an average value of 2.54‰. Mo and V concentrations range between 0.08 ppm to 50.30 ppm, with an average value of 13.99 ppm, and 28.34 ppm to 877.62 ppm, averaging at 210.65 ppm, respectively. TOC values vary from 0.28 wt. % to 16.64 wt. % with an average value of 5.06 wt. %.

### **ca. 0.80 Ga**

#### GILLEN FORMATION

Carbon isotopes range from -22.46‰ to -29.61‰, averaging at -25.82‰. Nitrogen isotopes vary between 3.71‰ to 8.26‰, with an average of 4.81‰. Mo and V concentrations range between <0.5 ppm to 2 ppm, averaging at 0.69 ppm, and 20 ppm to 170 ppm, with an average of 119.41 ppm, respectively. The HI values range between 1 HC/g TOC to 25 HC/g TOC, averaging 7.79 HC/g TOC, therefore classifying them as over-mature (Jarrett et al., 2018b). TOC values vary between 0.36 wt. % to 7.36 wt. %, with an average of 1.73 wt. %.

## ca. 0.66 Ga

### TAPLEY HILL FORMATION

Carbon and nitrogen isotopes vary between -28.21‰ to -29.45‰, averaging -28.95‰, and 0.98‰ to 2.03‰, with an average of 1.57‰, respectively. Mo concentrations range from 3.28 ppm to 22.38 ppm, averaging 7.32 ppm. V concentrations vary from 52.43 ppm to 142.10 ppm, with an average value of 89.60 ppm. HI values range between 2 HC/g TOC and 33 HC/g TOC, averaging at 12.36 HC/g TOC, classifying the Tapley Hill formation as over-mature (Jarrett et al., 2018b). TOC values range from 0.28 wt. % to 0.82 wt. %, averaging at 0.63 wt. %.

## ca. 0.635 Ga

### TENT HILL FORMATION

Carbon isotopes of the Tent Hill Formation range between -25.49‰ to -27.01‰ with an average of -26.33‰. Nitrogen isotopes vary from 2.21‰ to 5.45‰, averaging 3.80‰. Mo and V values range from 0 ppm to 5.23 ppm, averaging 0.62 ppm, and 73.75 ppm to 126.93 ppm, with an average of 103.10‰, respectively. HI values range from 5 HC/g TOC to 900 HC/g TOC, averaging 157 HC/g TOC classifying as immature to over-mature in thermal maturity (Jarrett et al., 2018b). TOC values range between 0.02 wt. % to 0.23 wt. %, with an average value of 0.13 wt. %.

Full organic and inorganic geochemical characterisations can be found in Appendix-B.

## DISCUSSION

### Assessment of alteration in carbon and nitrogen isotopes

C% vs. N% expresses the relationship between nitrogen and organic carbon, where data trending at the origin (0,0) provides evidence that nitrogen is exclusively associated with organic matter (C%) (Anbar & Knoll, 2002). This trend can be seen in Figure 5, indicating the nitrogen measured in these rock samples are organic rather than inorganic nitrogen. The Arctic Bay Formation however, does not follow such trend and therefore may carry a contribution from inorganic sources.

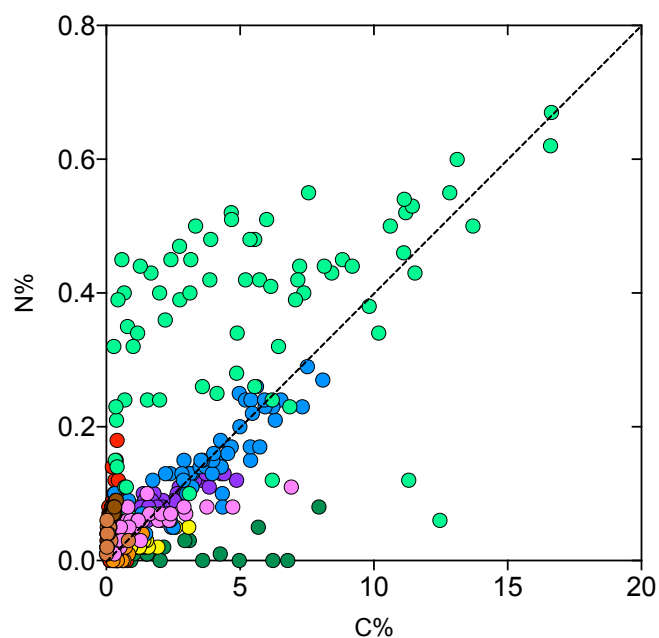


**Figure 5.** C% vs. N% of Tent Hill (light brown), Tapley Hill (dark brown), Gillen (pink), Arctic Bay (light green), Kyalla (orange), Velkerri (blue), Lower Roper Group (red), Fraynes (purple), Barney Creek (yellow) and Wollogorang formations (dark green).

Carbon (C%) and nitrogen (N%) concentrations characterise the abundance of carbon and nitrogen in the rock. Figure 6 shows the relationship between carbon and nitrogen abundances, where their isotopic composition can be used to ascertain the loss or gain of carbon and/or nitrogen via devolatilization and any effect on the isotope ratios of the samples. As a loss or gain of carbon and/or nitrogen will affect C% and N%, any isotope effect should be observed as a trend in either plots. No significant trends exist within the samples, signifying any carbon and/or nitrogen loss via devolatilization has not altered the  $\delta^{13}\text{C}$  or  $\delta^{15}\text{N}$  of the samples. Thus, observed changes in  $\delta^{13}\text{C}$  or  $\delta^{15}\text{N}$  are likely to reflect a primary marine signal.

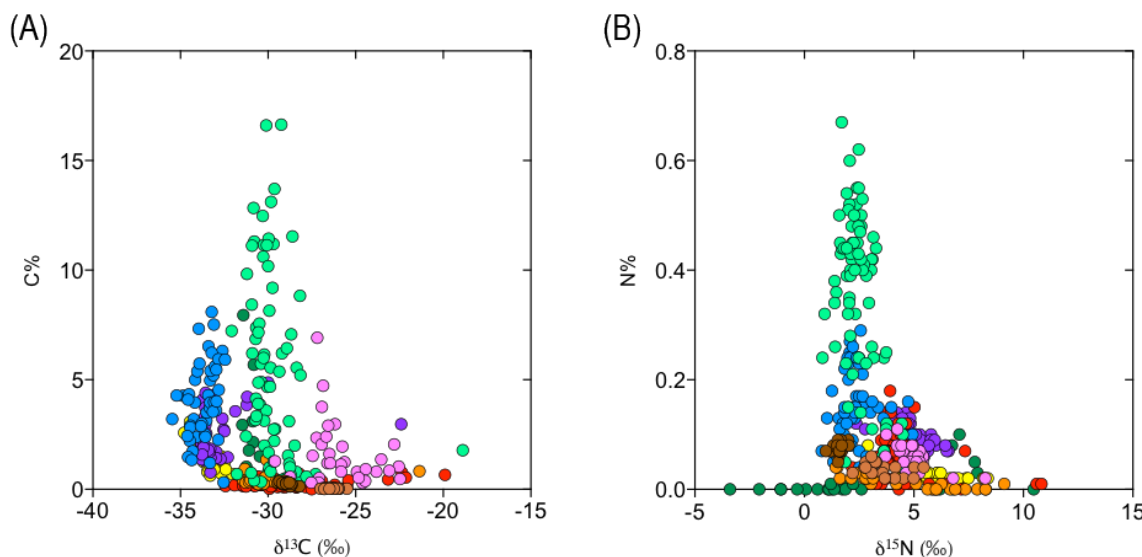


**Figure 6a**  $\delta^{13}\text{C}$  vs. C% of formations Tent Hill (light brown), Tapley Hill (dark brown), Gillen (pink), Arctic Bay (light green), Kyalla (orange), Velkerri (blue colour), Lower Roper Group (red colour), Fraynes (purple), Barney Creek (yellow) and Wollogorang (dark green). **Figure 6b**  $\delta^{15}\text{N}$  vs. N% of formations Tent Hill (light brown), Tapley Hill (dark brown), Gillen (pink), Arctic Bay (light green), Kyalla (orange), Velkerri (blue colour), Lower Roper Group (red colour), Fraynes (purple), Barney Creek (yellow) and Wollogorang (dark green).

Characteristics such as hydrogen indices (HI) and  $T_{max}$  are used to indicate the level of thermal maturity of organic matter (Peters, Kacewicz, & Curry, 2012). Figure 7 displays the  $\delta^{13}C$  associated with these indices. HI and  $T_{max}$  classifications of the samples give similar yet slightly different results. With this in mind, it is therefore essential to use HI and  $T_{max}$  in conjunction when determining thermal maturity. As seen in (Figure 7a & 7b) no relationship between thermal maturity and  $\delta^{13}C$  is observed, suggesting that thermal maturity of the rock has not affected the primary isotopic signature. Production Index (PI) and the measured amount of free hydrocarbons (S1), when used in conjunction, give an indication of hydrocarbon generation and/or migration and when compared together with  $\delta^{13}C$ , allow us to assess any alteration of primary isotopic signals due to generation and/or migration. As shown (Figure 7) no relationship between either PI or S1 and  $\delta^{13}C$  is observed, indicating that neither migration or generation has altered the  $\delta^{13}C$  ratio of the rock samples.

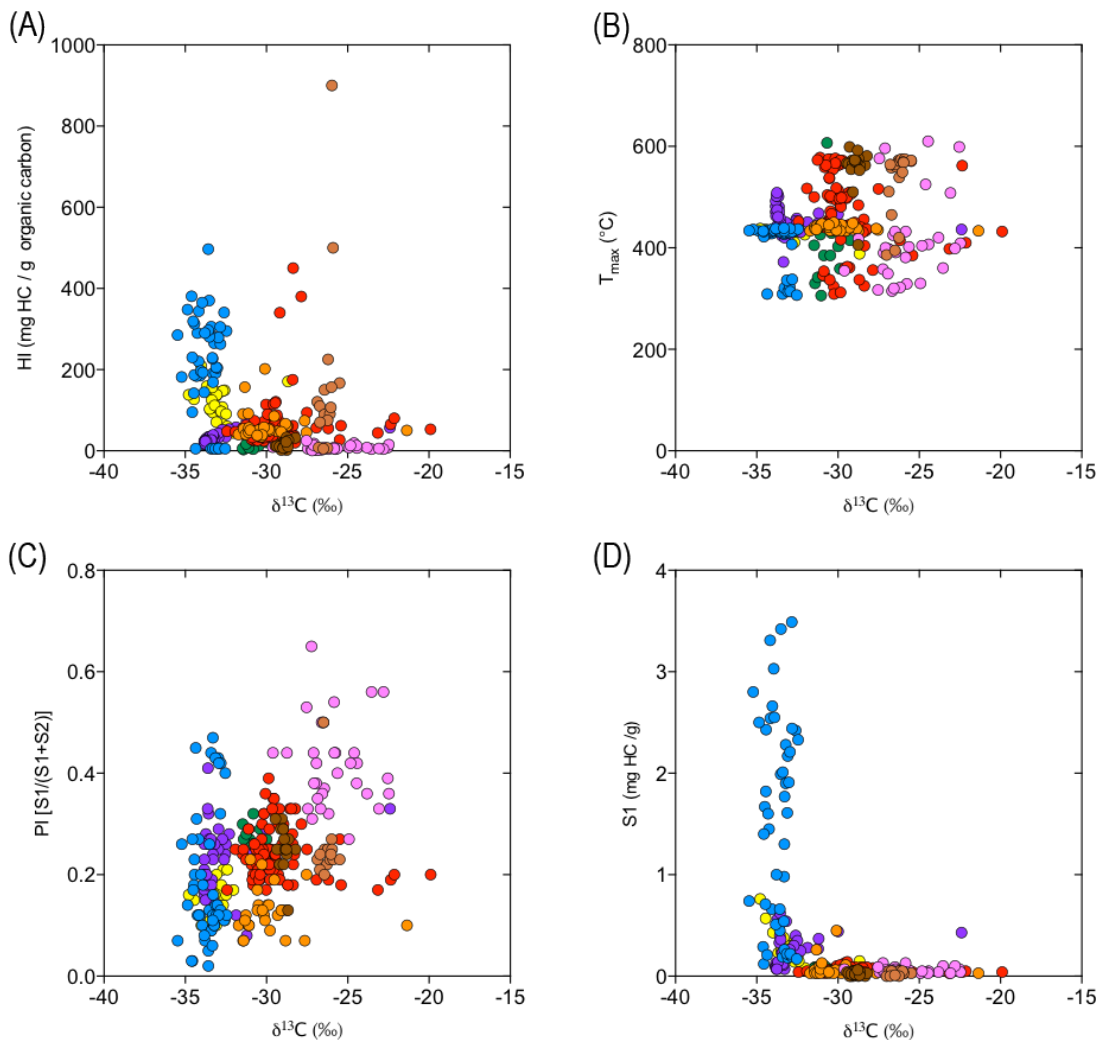


**Figure 7.** Carbon isotope alteration plots, shown by  $\delta^{13}\text{C}$  (‰), with formations; Tent Hill (light brown), Tapley Hill (dark brown), Gillen (pink), Kyalla (orange), Velkerri (blue), Lower Roper Group (red), Fraynes (purple), Barney Creek (yellow) and Wollogorang (dark green) formations. Figure 7a  $\delta^{13}\text{C}$  (‰) vs. Hydrogen Index (HI). Figure 7b  $\delta^{13}\text{C}$  (‰) vs. Thermal maximum ( $T_{max}$ ). Figure 7c  $\delta^{13}\text{C}$  (‰) vs. hydrocarbon Production Index (PI). Figure 7d  $\delta^{13}\text{C}$  (‰) vs. free hydrocarbons ( $S_1$ ). For further explanations see Table 2.

Figure 8a and 8b show the relationship and potential alteration of  $\delta^{15}\text{N}$  by thermal maturity. However, as both plots do not show any significant relationship, thermal maturity of the samples has not altered the primary  $\delta^{15}\text{N}$  of the samples. These plots are consistent with Figure 7, further reinforcing the lack of isotope fractionation associated with variations in thermal maturity. Figure 8c and 8d show no significant trends between  $\delta^{15}\text{N}$  and hydrocarbon production and migration. These plots are again consistent with Figure 7, further emphasizing that migration and generation of hydrocarbons has not altered the isotopic composition of the samples.

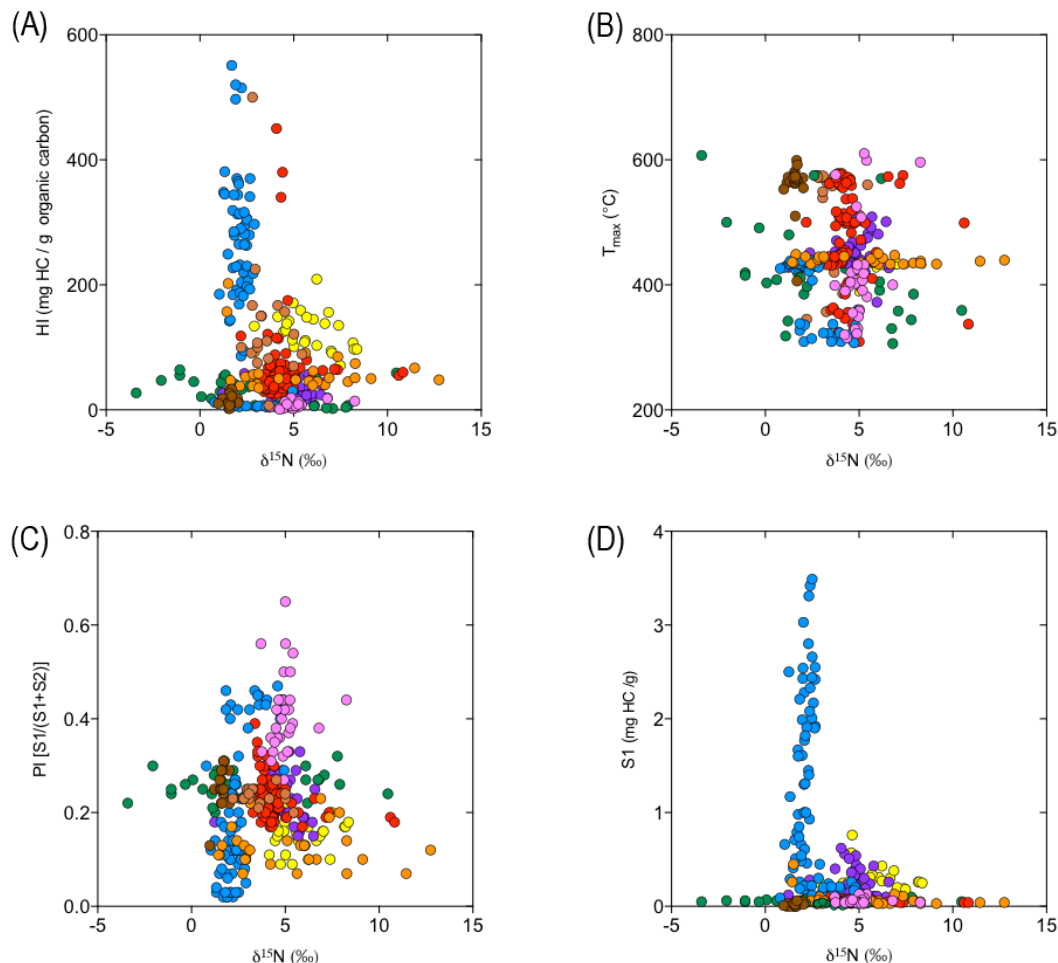


**Figure 8. Nitrogen isotope alteration plots, shown by  $\delta^{15}\text{N}$ , all showing formations; Tent Hill (light brown), Tapley Hill (dark brown), Gillen (pink), Kyalla (orange), Velkerri (blue), Lower Roper Group (red), Fraynes (purple), Barney Creek (yellow) and Wollogorang (dark green) formations. Figure 8a  $\delta^{15}\text{N}$  vs. Hydrogen Index (HI). Figure 8b  $\delta^{15}\text{N}$  vs. Thermal maximum, Tmax. Figure 8c  $\delta^{15}\text{N}$  vs. hydrocarbon Production Index (PI). Figure 8d  $\delta^{15}\text{N}$  vs. free hydrocarbons, S1. For further explanations see Table 2.**

### Organic carbon isotope record ( $\delta^{13}\text{C}$ )

Whilst the  $\delta^{13}\text{C}$  record throughout this time period is dynamic, an overall trend to isotopically heavier  $\delta^{13}\text{C}_{\text{org}}$  values is observed (Figure 9). The typical interpretation of this trend is that it reflects increasing organic carbon burial (Hayes et al., 1999). Organic carbon burial can be quantified using a carbon isotope mass balance approach (e.g. Equation 5):

$$f_{\text{org}} = \frac{(\delta^{13}\text{C}_{\text{org}} + \Delta_{\text{org-carb}} + \delta^{13}\text{C}_{\text{in}})}{\Delta_{\text{org-carb}}} \quad (\text{Equation 5})$$

The increase in  $f_{\text{org}}$  between ca. 1.64 Ga ( $f_{\text{org}} = 0.12$ ) and ca. 0.63 Ga ( $f_{\text{org}} = 0.33$ ) represents nearly a three-fold increase in organic carbon burial. A consequence of this increase in organic carbon burial would be net production of oxygen across the Proterozoic.

Despite this overall trend to increasingly heavy  $\delta^{13}\text{C}$ , variations exist (Figure 9). The lighter  $\delta^{13}\text{C}$  values within the Velkerri formation are likely due to significant contributions of chemotrophic biomass within buried organic matter ( $f_{\text{org}}$ ), indicated by recent bio-marker studies, i.e. (Jarrett et al., 2018a). While the Tapley Hill and Tent Hill formations are the youngest samples in this study, their relatively light  $\delta^{13}\text{C}$  values are lower than expected. This is possibly due to their association with the glacial intervals of the Sturtian and Marinoan, periods in time known to cause major carbon cycle perturbations (Hoffman et al., 2017). Despite this, these  $\delta^{13}\text{C}$  values are still consistent with overall increasing organic carbon burial.

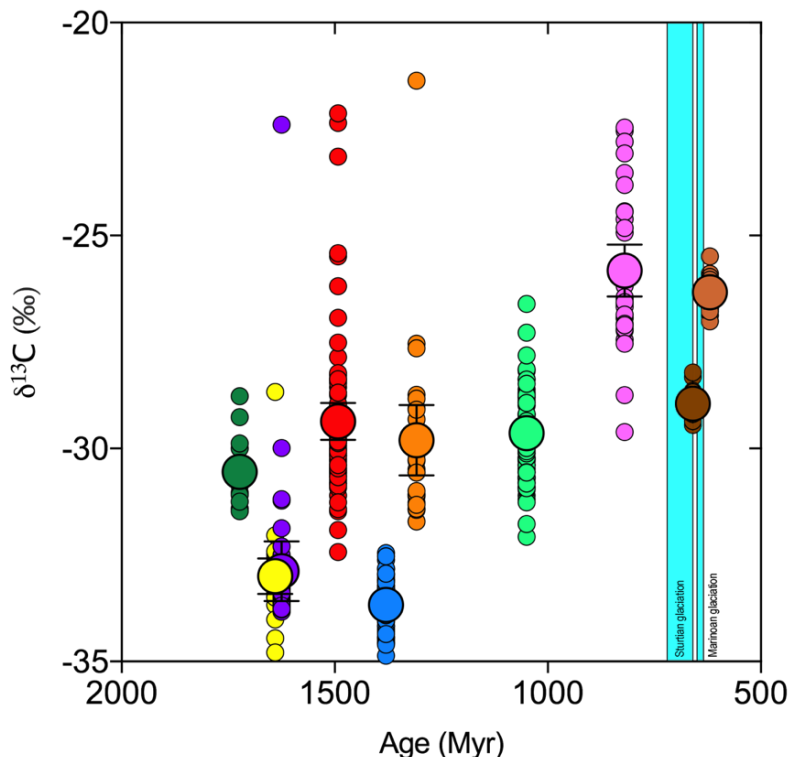


**Figure 9.**  $\delta^{13}\text{C}_{\text{org}}$  (‰) of Tent Hill (light brown), Tapley Hill (dark brown), Gillen (pink), Arctic Bay (light green), Kyalla (orange), Velkerri (blue), Lower Roper Group (red), Fraynes (purple), Barney Creek (yellow) and Wollogorang (dark green) formations, plotted against their estimated ages. The larger circles for each formation represent the bootstrapped average of each formation. Confidence intervals of 95% can be seen as error bars on these bootstrapped points. Where confidence intervals cannot be seen, the error bars are smaller than the size of the point. It is important to note that where each formation plots, may not be to their exact formation ages. This was done to ensure formations would be able to be seen, rather than overlapping. The larger of the blue lines represents the time of the Sturtian glaciation, and the smaller represents the Marinoan glaciation.

While equating changes in  $\delta^{13}\text{C}$  to changes in  $f_{\text{org}}$  may be a first order control on variations observed in  $\delta^{13}\text{C}$ , other factors should be considered. One possibility is a reduction in chemotrophic contribution to organic carbon burial. As chemotrophs incorporate light  $\delta^{13}\text{C}$ , the presence of heavier isotopes could indicate a reduction in chemotrophic re-working of organic matter. A second possibility would include increasing sea surface temperatures. Freeman & Hayes (1992) showed that an increase in  $\delta^{13}\text{C}$  can be caused by increasing surface water temperatures. This is due to the temperature dependence between dissolved  $\text{CO}_2$  and dissolved bicarbonate (DIC) with a

fractionation factor of ~0.12‰ per degree of temperature change (Freeman & Hayes, 1992). The overall increase in  $\delta^{13}\text{C}_{\text{org}}$  of ~6.66‰ in this data set would require a 50°C change in sea surface temperatures across this time which seems unlikely. While these other interpretations may be contributing to the overall isotopic signature, the most influential factor is likely organic carbon burial. A consequence of such an increase would be an increase in the net production of O<sub>2</sub>, assuming long term production of carbon is relatively constant. This explanation is further supported by the trace elemental data.

### **Redox sensitive trace metal record**

Widely used proxies for basin redox are the redox sensitive trace metals of molybdenum and vanadium. These trace metal proxies are used as they are redox sensitive, such that, under reducing conditions they are enriched in sediments, and under oxic conditions are depleted in sediments (Piper & Calvert, 2009). Under mildly reducing to sub-oxic conditions, V is reduced first and its concentration in sediments increases (Tribouillard et al., 2006). Therefore, the V/Mo ratio increases under such conditions. Within sub-oxic to anoxic conditions, Mo starts to reduce along with V where the V/Mo will then decrease (Algeo & Maynard, 2004). Under euxinic (sulphidic) conditions, Mo reacts strongly with hydrogen sulphide such that it is removed from sea and pore-waters and enriched in sediments (Wanty & Goldhaber, 1992), therefore, decreasing V/Mo ratios and increasing Mo values within sediments. Therefore, looking at V/Mo ratios independently may result in an unclear interpretation of whether there is a transition from sub-oxic to oxic conditions, or anoxic to euxinic conditions. Both trends could be argued for without further context from absolute Mo abundances.

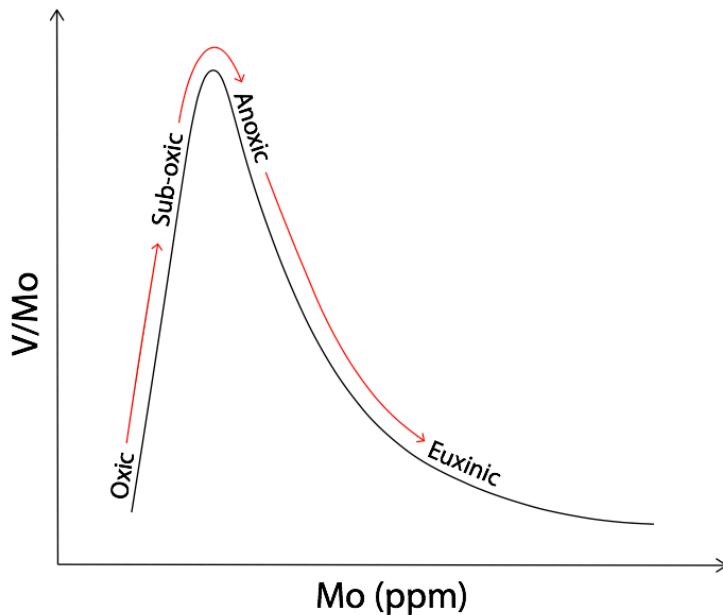


**Figure 10.** Without comparing V/Mo ratios to Mo abundances, it is unclear which side of the curve a potential gradient represents as either oxic to sub-oxic or anoxic to euxinic trends could be argued for. Knowing the trend in Mo abundances gives an accurate interpretation of the V/Mo proxy.

Therefore, it is vital to compare the trace metal trend (V/Mo) against absolute Mo values to interpret the correct trend. High Mo values definitively indicate euxinic environments, as Mo becomes enriched in sediments under such conditions, compared to low Mo values which would indicate an oxic environment (as Mo is enriched in the water column under such conditions, Figure 10).

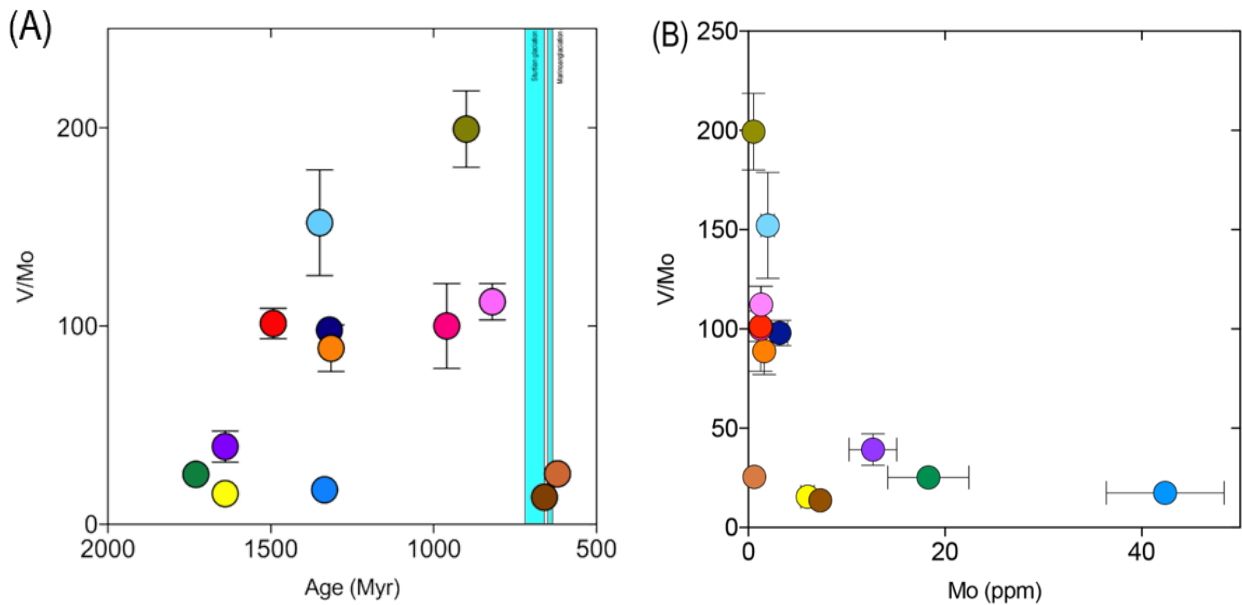


**Figure 11a** V/Mo bootstrapped average values for the Tent Hill (light brown), Tapley Hill (dark brown), Gillen (light pink), Hayfield (olive green), Jamison (dark pink), Kyalla (orange), Upper Velkerri (dark blue), Middle Velkerri (medium blue), Lower Velkerri (light blue), Lower Roper Group (red), Fraynes (purple), Barney Creek (yellow) and Wollogorang (dark green) formations plotted with respect to their depositional ages. Confidence intervals of 95% can be seen as error bars on these bootstrapped points. Where confidence intervals cannot be seen, the error bars are smaller than the size of the point. The larger of the blue lines represents the time of the Sturtian glaciation, and the smaller represents the Marinoan glaciation. **Figure 11b** V/Mo vs. Mo (ppm), bootstrapped data of said formations. Confidence intervals of 95% can be seen as error bars on these bootstrapped points. Where confidence intervals cannot be seen, the error bars are smaller than the size of the point.

With reference to Figure 11a, it is apparent that, while variability exists within sedimentary V/Mo ratios, a trend of increasing V/Mo ratios is evident. Throughout such time (Paleoproterozoic to Neoproterozoic), Mo becomes less abundant in sediments and increasingly enriched within seawaters. An obvious outlier to this trend is the middle Velkerri, where Mo values are particularly high. This is interpreted to be the result of large increases in organic carbon production and export resulting in local euxinic conditions. Complicating the overall picture are samples from the Cryogenian; the Tapley Hill and Tent Hill formations, where a significant drop in V/Mo ratios towards the Tapley Hill Formation indicate a time of more anoxic sea-waters. This formation is intimately associated with the Sturtian glaciation, a time of known anoxic conditions

(Hoffman et al., 2017). However, V/Mo ratios along with absolute Mo abundances for the Tent Hill Formation are consistent with sub-oxic conditions. While subtle, there is again an increasing trend in V/Mo ratios from the Tapley Hill to the Tent Hill formation, indicating more oxic sea-waters conditions. This is further supported by the Mo abundances within the samples.

The most significant trend is the overall increasing V/Mo ratios coupled to decreasing Mo abundances broadly characterising the Paleoproterozoic to Neoproterozoic (Figure 11b). This trend is entirely consistent with a Paleoproterozoic to Neoproterozoic transition from dominantly euxinic/anoxic to sub-oxic conditions, albeit with significant variability. This trace metal data, when viewed in conjunction with  $\delta^{13}\text{C}$  supports a model of increasing oxygenation within seawaters throughout the Proterozoic.

### Organic nitrogen isotope record ( $\delta^{15}\text{N}$ )

The nitrogen isotope record gives increasingly more nuanced insights into the Proterozoic with regards to ocean redox. In broad terms,  $\delta^{15}\text{N}$  values  $\sim < 2\text{\textperthousand}$  indicate a marine nitrogen cycle dominated by  $\text{N}_2$  fixation, with values between  $-1\text{\textperthousand}$  and  $+2\text{\textperthousand}$  suggesting Mo-based nitrogenase fixation (Zhang et al., 2014). Furthermore,  $\delta^{15}\text{N}$  values less than  $-1\text{\textperthousand}$  would suggest that, not only is  $\text{N}_2$  fixation the dominant process, but that seawaters are persistently low in dissolved Mo (i.e.  $< 10 \mu\text{M}$ ; (Zerkle, House, Cox, & Canfield, 2006)), requiring that fixation is somewhat ‘forced’ to use the less efficient V and Fe based nitrogenases (Stüeken, Kipp, Koehler, & Buick, 2016; Zhang et al., 2014). However, within the dataset, there is no observed  $\delta^{15}\text{N}$  values consistent with V and Fe based nitrogenases (Figure 12). Therefore, while pervasive euxinic conditions have been reported to be an important feature of Proterozoic oceans (Reinhard et. al. 2013), our  $\delta^{15}\text{N}$  record suggests that dissolved Mo concentrations were never low enough see the widespread use of alternative V and Fe nitrogenases. This interpretation is consistent with our Mo data set, showing that with increasingly lower measured Mo abundances within sediments, Mo must be enriched in seawater, supporting Mo-based isozyme as the dominant nitrogenase within the fixation process.

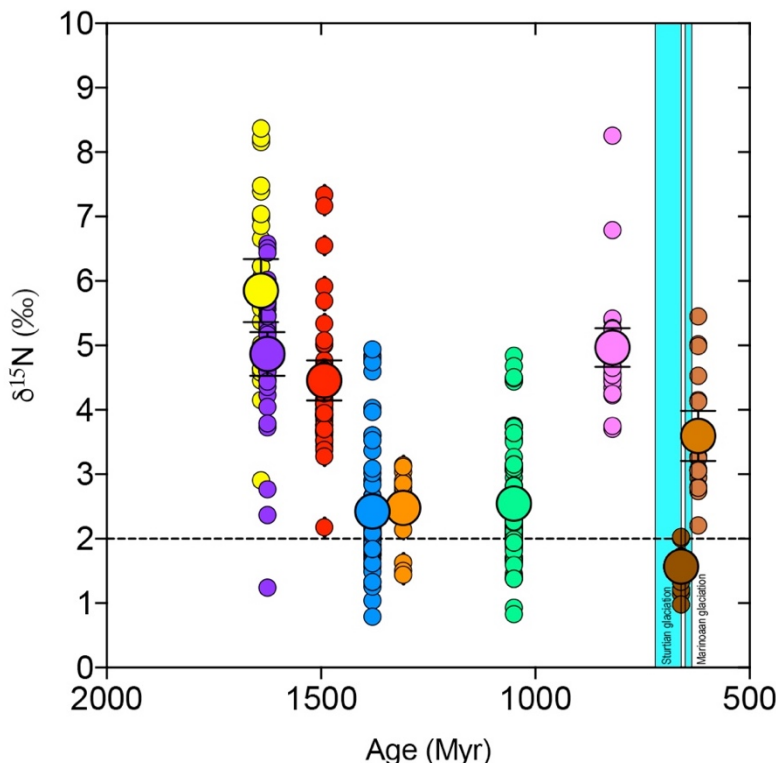


**Figure 12.**  $\delta^{15}\text{N}$  of Tent Hill (light brown), Tapley Hill (dark brown), Gillen (pink), Arctic Bay (light green), Kyalla (orange), Velkerri (blue), Lower Roper Group (red), Fraynes (purple) and Barney Creek (yellow), plot against their ages. The larger circles seen represent the bootstrapped average of all the points with 95% confidence intervals. Where confidence intervals cannot be seen is due to error bars being smaller than the size of the point. It is important to note that where each formation plots, may not be to their exact formation ages. This was done to ensure formations would be able to be seen, rather than overlapping data. The dashed line at  $\delta^{15}\text{N} = 2\text{\textperthousand}$  represents fractionation believed to be associated with nitrogen fixation. The larger of the blue lines represents the time of the Sturtian glaciation, and the smaller represents the Marinoan glaciation.

### What can cause more positive $\delta^{15}\text{N}$ values?

In this data set,  $\delta^{15}\text{N}$  values are consistently above  $+2\text{\textperthousand}$ . While such values may represent partial assimilation or nitrification (as nitrogen is generally the limiting nutrient in primary productivity) assimilation and nitrification go to completion in the modern ocean, and consequently their large fractionations are not expressed. It is widely held that Precambrian oceans were likely characterised by lower bioavailable nitrogen than their Phanerozoic equivalents (Stüeken et al., 2016). Therefore, it is considered

unlikely that assimilation and/or nitrification would not also go to completion in Precambrian oceans (Stüeken et al., 2016).

Considering that partial assimilation and/or nitrification are unlikely to be responsible for the isotopically heavy  $\delta^{15}\text{N}$ , denitrification and anammox are therefore most likely to be involved. The processes of denitrification and anammox are complex and their rates are not just a function of nitrogen availability but are also influenced by the size and distribution of the ocean chemocline (influenced by redox conditions), availability of nitrites and nitrates (also influenced by redox conditions), and an overall availability of organic matter. Therefore, denitrification and anammox are considered partial processes that could potentially cause the large observed positive fractionations.

### **Denitrification and anammox as dominant processes**

$\delta^{15}\text{N}$  values for most individual samples, as well as formation averages, plot predominantly above +2‰, suggesting the dominance of denitrification and/or anammox processes over Mo-based fixation throughout the late Paleoproterozoic to early Mesoproterozoic, as fractionation factors associated with  $\text{N}_2$  fixation generally reach a maximum of +2‰ (Zhang et al., 2014). This indicates the water column must be experiencing high enough redox potentials to exhibit aerobic nitrogen cycling, as denitrification and anammox require enough oxygen to drive these processes (as  $\text{NO}_2^-$  and  $\text{NO}_3^-$  are essential to drive such reactions, Figure 2).

## N<sub>2</sub> fixation vs. denitrification – what makes one dominant over the other?

As we have ruled out the possibility of Fe or V isozymes as the dominant nitrogenase for N<sub>2</sub> fixation based on the observed data (Figure 12), Mo-based fixation therefore must be the dominant expression of N<sub>2</sub> fixation. As both Mo-based fixation and denitrification/anammox are indicative of oxic environments, the question stands as to why one would be expressed over the other if oxic seawaters are a necessity for both processes? For denitrification/anammox to be dominant over fixation comes down to one of two potential causes. The first potential cause requires low enough Mo abundances within seawater during the late Paleoproterozoic to early Mesoproterozoic to restrict the most efficient form of nitrogen fixation, Mo-based nitrogenase. Studies have shown that between 5-10µM of Mo (an estimated concentration of dissolved Mo in early Proterozoic oceans (Reinhard et al., 2017)), nitrogen fixation's efficiency is decreased by up to ~80% (Zerkle et al., 2006). However, our Mo abundances indicate that from ~1.64 Ga onwards, dissolved Mo abundances have increased (Figure 11). Therefore, from ~1.64 Ga, the restriction of Mo for Mo-based fixation is most likely not determining the lack of expression of Mo-based fixation within δ<sup>15</sup>N values. The other possibility of a less dominant role for nitrogen fixation is the increased availability of nitrites and nitrates, driving high rates of denitrification/anammox. As δ<sup>15</sup>N values plot above +2‰, this must be indicative of the latter, that denitrification and anammox are dominant processes compared to nitrogen fixation.

## Trends in $\delta^{15}\text{N}$

Two trends could potentially be argued for with reference to Figure 12. An overall trend to lighter  $\delta^{15}\text{N}$  values throughout the late Paleoproterozoic through to early Neoproterozoic (which we will refer to as Interpretation 1). The other trend that could be argued for is a decrease to lighter  $\delta^{15}\text{N}$  values within the late Paleoproterozoic to late Mesoproterozoic (~1.33 Ga, e.g. Kyalla Formation, Figure 12) followed by an upwards trend to heavier  $\delta^{15}\text{N}$  values seen in the late Mesoproterozoic to early Neoproterozoic (Interpretation 2).

### INTERPRETATION 1

While displaying some variability, an overall decreasing trend in  $\delta^{15}\text{N}$  can be seen between the late Paleoproterozoic to early Neoproterozoic (Figure 13). Suggesting during this time  $\text{N}_2$  fixation is becoming increasingly more efficient over the denitrification/anammox processes, with two outliers being the Gillen Formation and the Tent Hill Formation.

Interpretation 1 trend is unlikely, as discussed before, trace metal data (Figure 11) suggests that Mo abundances are relatively high within seawater from ~1.64 Ga onwards. This therefore overrides the interpretation of trend 1 as we know Mo-based fixation is not being restricted, and that denitrification and anammox processes are becoming increasingly more dominant. This trend therefore cannot be sustained as we have previously ruled out the possibility of increased Mo-based  $\text{N}_2$  fixation efficiency. This leaves us with interpretation 2.

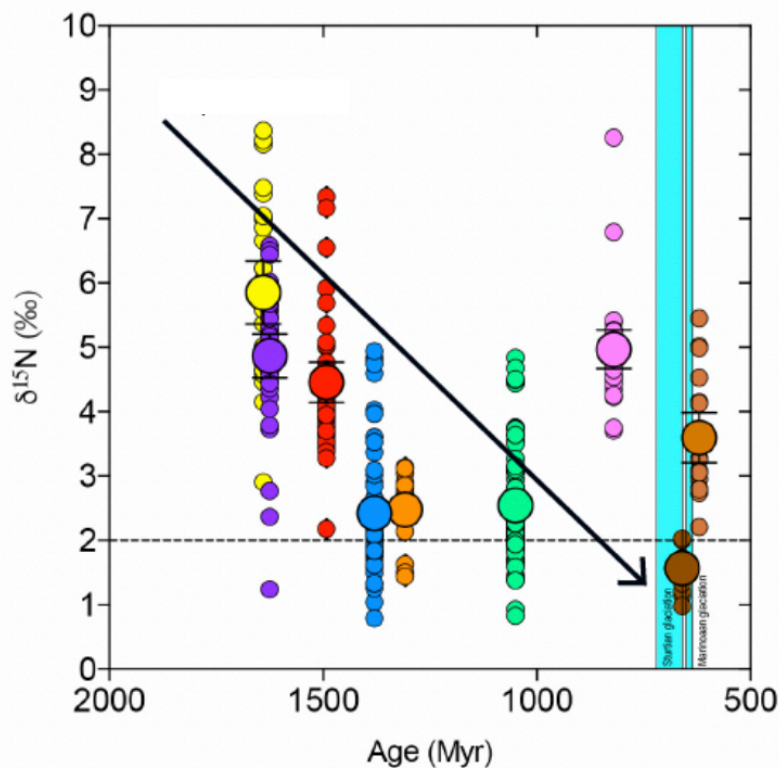


Figure 13.  $\delta^{15}\text{N}$  vs age plot as seen before in Figure 12. The black arrow here represents the potential overall trend of 'Interpretation 1'.

## INTERPRETATION 2

While displaying some variability, the  $\delta^{15}\text{N}$  record shows decreasing values from the late Paleoproterozoic to the early Mesoproterozoic, a mid-Mesoproterozoic low in  $\delta^{15}\text{N}$ , followed by increasing  $\delta^{15}\text{N}$  from ~1.1 Ga through to the Neoproterozoic, with an outlier of the Tapley Hill Formation—however, its close association to the Sturtian glaciation acquires nuances within the data (Figure 14).

The initial downwards trend observed during the Paleoproterozoic to the early Mesoproterozoic is interpreted as a progressive increase in the strength of Mo-based  $\text{N}_2$  fixation. Consequently, while denitrification and anammox are still ongoing processes, their impact on  $\delta^{15}\text{N}$  would be reduced due to increasing strength of Mo-based fixation. However, ‘Interpretation 2’ takes on greater importance when increasingly dissolved Mo concentrations within seawater are considered. Redox sensitive trace metals present a clear picture of decreasing sedimentary Mo abundances—indicating an increase in dissolved Mo concentrations (Figure 11b). This data is broadly consistent with values of increased Mo abundances throughout the Paleoproterozoic to Neoproterozoic (Reinhard et al., 2017). Therefore, from ~1.1 Ga dissolved Mo abundances are increasing, however  $\delta^{15}\text{N}$  values are not reflective of Mo-based fixation. This interpretation (Interpretation 2, Figure 14) therefore aligns with the interpretation that, while dissolved Mo abundances are increasing with time, this is not substantial of the overwhelmingly available, abundant nitrates/nitrites powering the denitrification and anammox processes dominance over Mo-based fixation. This is further supported by the Tapley Hill Formation, as we know is closely associated with the Sturtian glaciation, and thus, represents a relatively anoxic environment (as supported by our Mo abundance data, Figure X). The Tapley Hill Formation therefore is indicative of an outlier to

'Interpretation 2', rather than an outlier to 'Interpretation 1', as we have previously interpreted the Mesoproterozoic to Neoproterozoic to be reflective of abundant nitrates/nitrites (i.e. relatively more oxic conditions).

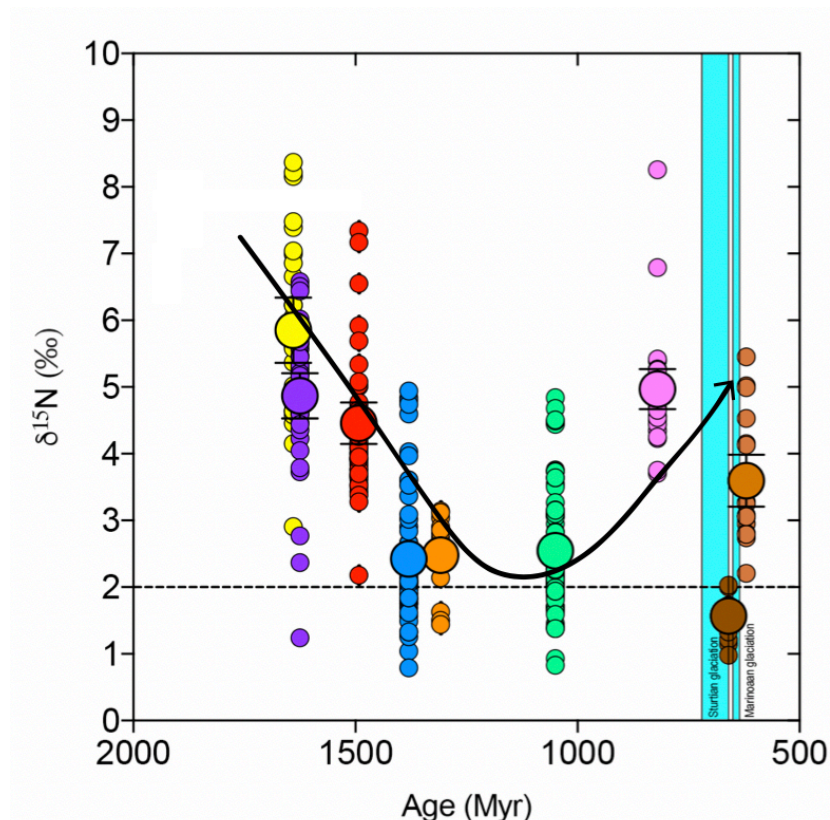


**Figure 14.**  $\delta^{15}\text{N}$  vs age plot as seen before in Figure 12. The black arrow here represents the potential overall trend of 'Interpretation 2'.

The interpretation that increasing oxygen within seawaters from ~1.1 Ga onwards to sustain high rates of aerobic nitrogen cycling is supported by the carbon isotope and V/Mo vs. Mo data provided (Figures 9 and 11 respectively). Therefore, an increase in oxygenation with increasingly younger time is supported by all data sets.

## CONCLUSION

A relatively comprehensive, coupled data set of carbon and nitrogen isotopes along with redox sensitive trace metal data spanning the Proterozoic was established, providing further understanding of marine redox throughout this time. This data set is some of the first redox proxies investigated throughout the Proterozoic, in particular the Mesoproterozoic and Neoproterozoic.

Carbon isotope data in this study overwhelmingly suggests an overall net increase in produced oxygen from the late Paleoproterozoic to Neoproterozoic. A 3-fold increase in  $f_{org}$  is supported by variations in carbon isotopes. Assuming constant or increasing total production of organic carbon, this 3-fold increase in  $f_{org}$  supports net oxygen production throughout the Proterozoic. Trace metal data supports the carbon isotope interpretation that increasingly heavier  $\delta^{13}\text{C}$  is a result of organic carbon burial, a consequence of which is increasing production of oxygen. Not only does the data support each other here, but the increasing oxygenation of sediments recorded in V/Mo ratios is likely a direct result of the increased oxygen production, indicated via  $\delta^{13}\text{C}$  values. Considering evidence for increasing oxygenation of marine sediments, and consequently higher dissolved seawater Mo concentrations, this coupled data then supports nitrogen isotope results. With increased dissolved Mo abundances, Mo-based fixation must be at its highest working potential, which is seen for some time (Paleoproterozoic to Mesoproterozoic). However, increasingly heavier  $\delta^{15}\text{N}$  values from the Mesoproterozoic to Neoproterozoic are associated with increasing dominance of denitrification and anammox, a consequence of increasingly available nitrates/nitrites

(hence increasing availability of oxic waters for such large quantities of aerobic nitrogen cycling to produce such positive  $\delta^{15}\text{N}$  values).

As all proxies point to the same interpretation, it is supportive of overall increasing oxygenation throughout the Paleoproterozoic to the Neoproterozoic.

It has previously been predicted that after the GOE, atmospheric oxygen essentially ‘flat-lined’ until the Neoproterozoic Oxygenation Event. However, compared to the GOE, which represents a relatively sharp, sudden increase in atmospheric oxygen, a singular ‘MOE’ or ‘NOE’ is not supported by this study, rather carbon and nitrogen isotopes along with redox sensitive trace metals present evidence of an overall steady increase in oxygenation throughout the Proterozoic. However, throughout the Proterozoic, redox is dynamic, there are no perfect trends seen in any of the data sets, there are outliers to overall trends and two major global glaciations that complicate our understanding of these proxies. There is however, convincing overall trends of increasing oxygenation of seawaters, and thus increasing atmospheric  $\text{O}_2$  is a distinct, if not likely consequence.

## ACKNOWLEDGMENTS

Firstly, I would like to thank the project grant providers ARC Linkage for funding this thesis. I give thanks to GSA, GSSA, NTGS, Santos and Origin for access to core. A special thanks to my supervisor Grant Cox, thank you for all your help, support and encouragement throughout the year, it would not have been the same without you, and to my co-supervisors Morgan Blades and Alan Collins.

Thank you to my fellow honours students, particularly Eilidh Cassidy, Gabrielle Redden, Tiah Bampton, Dion Higbie and Alexander Otasevic, your support and help towards me and this thesis this year is very much appreciated. I would like to say thank you to the lab assistants who helped me tremendously along the way, Tony Hall, Mark Rollog and particularly Kristine Nielson, thank you for all your hard work. And to Amber Jarrett, Marcus Kunzmann, Malcom Hodgskiss and Pierre Sansjofre for providing me with additional data when needed.

## REFERENCES

- ADER, M., THOMAZO, C., SANSJOFRE, P., BUSIGNY, V., PAPINEAU, D., LAFFONT, R.,...  
HALVERSON, G. P. (2016). Interpretation of the nitrogen isotopic composition of Precambrian sedimentary rocks: Assumptions and perspectives. *Chemical Geology*, 429, 93-110.
- ALGEO, T. J., & MAYNARD, J. B. (2004). Trace-element behaviour and redox facies in core shales of Upper Pennsylvanian Kansas-type cycloths. *Chemical Geology*, 206(289-318).
- ANBAR, A. D., DUAN, Y., LYONS, T. W., ARNOLD, G. L., KENDALL, B., CREASER, R. A.,... ROGER, B. (2007). A Whiff of Oxygen Before the Great Oxidation Event? *Science*, 317(5846), 1903-1906.
- ANBAR, A. D., & KNOLL, A. H. (2002). Proterozoic Ocean Chemistry and Evolution: A Bioinorganic Bridge? *Science*, 297(5584), 1137-1142.
- BEKKER, A., HOLLAND, D., WANG, P., RUMBLE, D., STEIN, H. J., HANNAH, J. L.,... BEUKES, N. J. (2004). Dating the rise of atmospheric oxygen. *Nature*, 427, 117-120.
- BLAUSTEIN, R. (2016). The Great Oxidation Event. *BioScience*, 66(3), 189-195.
- BREIT, G. N., & WANTY, R. B. (1991). Vanadium accumulation in carbonaceous rocks: A review of geochemical controls during deposition and diagensis. *Chemical Geology*, 91, 83-97.
- BUICK, I. S., STORKEY, A., & WILLIAMS, I. S. (2008). Timing relationships between pegmatite emplacement, metamorphism and deformation during the intra-plate Alice Springs Orogeny, central Australia. *Journal of Metamorphic Geology*, 26, 915-936.
- BULLEN, M. (2017). *Depositional Environment and Paleo-Redox Conditions of the Greater McArthur Basin, Northern Territory*. (Honours), The University of Adelaide, Adelaide.
- CAPONE, D. G. (2008). The Marine Nitrogen Cycle. *Microbe*, 3(4), 186-192.
- COLE, D. B., REINHARD, C. T., WANG, X., GUEGUEN, B., HALVERSON, G. P., GIBSON, T.,... PLANAVSKY, N. J. (2016). A shale-hosted Cr isotope record of low atmospheric oxygen during the Proterozoic. *Geology*, 44(7), 555-558.
- DAVISON, A. C., & HINKLEY, D. V. (1997). *Bootstrap Methods and Their Application*: Cambridge University Press.
- FREEMAN, K. H., & HAYES, J. M. (1992). Fractionation of carbon isotopes by phytoplankton and estimates of ancient CO<sub>2</sub> levels. *Global Biogeochemical Cycles*, 6(2), 185-198.
- GALBRAITH, E. D., SIGMAN, D. M., ROBINSON, R. S., & PEDERSEN, T. F. (2008). Nitrogen in Past Marine Environments. In *Nitrogen in the Marine Environment* (pp. 1497-1535).
- GIBSON, T. M., SHIH, P. M., CUMMING, V. M., FISCHER, W. W., CROCKFORD, P. W., HODGSKISS, M. S. W.,... HALVERSON, G. P. (2017). Precise age of Bangiomorpha pubescens dates the origin of eukaryotic photosynthesis. *Geology*, 46, 135-138.
- GILLEAUDEAU, G. J., FREI, R., KAUFMAN, A. J., KAH, L. C., AZMY, K., BARTLEY, J. K.,... KNOLL, A. H. (2016). Oxygenation of the mid-Proterozoic atmosphere: clues from chromium isotopes in carbonates. *Geochemical Perspective Letters*, 2, 178-187.

- HAINES, P. W., TURNER, S. P., KELLEY, S. P., WARTHO, J., & SHERLOCK, S. C. (2004). 40Ar-39Ar dating of detrital muscovite in provenance investigations: a case study from the Adelaide Rift Complex, South Australia. *Earth and Planetary Science Letters*, 227, 297-311.
- HAYES, J. M., STRAUSS, H., & KAUFMAN, A. J. (1999). The abundance of in marine organic matter and isotopic fractionation in the global biogeochemical cycle of carbon during the past 800 Ma. *Chemical Geology*, 161(1-3), 103-125.
- HOFFMAN, P. F., ABBOT, D. S., ASHKENAZY, Y., BENN, D. I., BROCKS, J. J., COHEN, P. A., ... WARREN, S. G. (2017). Snowball Earth climate dynamics and Cryogenian geology-geobiology. *Science Advances*, 3(11), 1-43.
- HUTCHINS, D. A., MULHOLLAND, M. R., & FU, F. (2009). Nutrient Cycles and Marine Microbes in a CO<sub>2</sub>-Enriched Ocean. *Oceanography*, 22(4), 128-145.
- JARRETT, A., COX, G. M., BROCKS, J. J., GROSJEAN, E., BOREHAM, C. J., & EDWARDS, D. S. (2018a). Microbial assemblage and paleoenvironmental reconstruction of the 1.4 Ga Velkerri Formation, McArthur Basin, northern Australia. *Geobiology*.
- JARRETT, A., COX, G. M., SOUTHBY, C., HONG, Z., PALATTY, P., CARR, L., & HENSON, P. (2018b). Source rock geochemistry of the McArthur Basin, northern Australia: Rock-Eval pyrolysis data release. *Geoscience Australia, Canberra*, 1-25.
- KAH, L. C., SHERMAN, A. G., NARBONNE, G. M., KNOLL, A. H., & KAUFMAN, A. J. (1999). d<sup>13</sup>C stratigraphy of the Proterozoic Bylot Supergroup, Baffin Island, Canada: implications for regional lithostratigraphic correlations. *Canadian Journal of Earth Sciences*, 36, 313-332.
- KENDALL, B., CREASER, R. A., GORDON, G. W., & ANBAR, A. D. (2009). Re-Os and Mo isotope systematics of black shales from the Middle Proterozoic Velkerri and Wollogorang Formations, McArthur Basin, northern Australia. *Geochimica et Cosmochimica Acta*, 73, 2534-2558.
- KENDALL, B., CREASER, R. A., & SELBY, D. (2006). Re-Os geochronology of postglacial black shales in Australia: Constraints on the timing of "Sturtian" glaciation. *Geology*, 34, 729-732.
- KNOLL, A. H., WALTER, M. R., NARBONNE, G. M., & CHRISTIE-BLICK, N. (2006). The Ediacaran Period: a new addition to the geological time scale. *Lethaia*, 39, 13-30.
- LEWAN, M. D., & MAYNARD, J. B. (1982). Factors controlling enrichment of vanadium and nickel in the bitumen of organic sedimentary rocks. *Geochimica et Cosmochimica Acta*, 46, 2547-2560.
- LYONS, T. W., REINHARD, C. T., & PLANAVSKY, N. J. (2014). The rise of oxygen in Earth's early ocean and atmosphere. *Nature*, 506(7488), 307-315.
- MACDONALD, F. A., SCHMITZ, M. D., CROWLEY, J. L., ROOTS, C. F., JONES, D. S., MALOOF, A. C., ... SCHRAG, D. P. (2010). Calibrating the Cryogenian. *Science*, 327, 1241-1243.
- MAHAN, K. H., WERNICKE, B. P., & JERCINOVIC, M. J. (2010). Th-U-total Pb geochronology of authigenic monazite in the Adelaide rift complex, South Australia, and implications for the age of the type Sturtian and Marinoan glacial deposits. *Earth and Planetary Science Letters*, 289, 76-86.
- MUNSON, T. J. (2016). Sedimentary characterisation of the Wilton package, greater McArthur Basin, Northern Territory. *Northern Territory Geological Survey, Record, 2016-003*.

- NORMINGTON, V. J., & EDGOOSE, C. J. (2018). *Neoproterozoic stratigraphic revisions to key drillholes in the Amadeus Basin - implications for basin palaeogeography and petroleum and minerals potential.* Paper presented at the Annual Geoscience Exploration Seminar (AGES) Proceedings, Alice Springs, Northern Territory.
- OCH, L. M., & SHIELDS-ZHOU, G. A. (2012). The Neoproterozoic oxygenation event: Environmental perturbations and biogeochemical cycling. *Earth-Science Reviews*, 110, 26-57.
- PAGE, R. W., & SWEET, I. P. (1998). Geochronology of basin phases in the western Mt Isa Inlier, and correlation with the McArthur Basin. *Australian Journal of Earth Science*, 45, 219-232.
- PETERS, K. E., KACEWICZ, M., & CURRY, D. J. (2012). An Overview of Basin and Petroleum System Modeling: Definitions and Concepts. *The American Association of Petroleum Geologists*, 4, 1-16.
- PIPER, D. Z., & CALVERT, S. E. (2009). A marine biogeochemical perspective on black shale deposition. *Earth-Science Reviews*, 95, 63-96.
- PLANAVSKY, N. J., REINHARD, C. T., WANG, X., THOMSON, D., McGOLDRICK, P., RAINBIRD, R. H., ... LYONS, T. W. (2014). Low Mid-Proterozoic atmospheric oxygen levels and the delayed rise of animals. *Science*, 346(6209), 635-638.
- PLUMMER, P. (2018). *Seismic shift in regional Neoproterozoic correlation, Amadeus Basin, central Australia.* Paper presented at the Annual Geoscience Exploration Seminar (AGES) Proceedings, Alice Springs, Northern Territory.
- PREISS, W. V. (2000). The Adelaide Geosyncline of South Australia and its significance in Neoproterozoic continental reconstruction. *Precambrian Research*, 100, 21-63.
- REINHARD, C. T., PLANAVSKY, N. J., GILL, B. C., OZAKI, K., ROBBINS, L. J., LYONS, T. W., ... KONHAUSER, K. O. (2017). Evolution of the global phosphorus cycle. *Nature*, 541, 386-389.
- ROBERTS, E. A., & HOUSEMAN, G. A. (2018). Geodynamics of central Australia during the intraplate Alice Springs Orogeny: thin viscous sheet models. *Geological Society of London*, 184(139-164).
- SCHRAG, D. P., HIGGINS, J. A., MACDONALD, F. A., & JOHNSTON, D. T. (2013). Authigenic Carbonate and the History of the Global Carbon Cycle. *Science*, 339(6119), 540-543.
- SCOTT, C., LYONS, T. W., BEKKER, A., SHEN, Y., POULTON, S. W., CHU, X., & ANBAR, A. D. (2008). Tracing the stepwise oxygenation of the Proterozoic ocean. *Nature*, 452, 456-459.
- SHERIDAN, M., JOHNS, D. R., JOHNSON, H. D., & MENPES, S. (2018). The stratigraphic architecture, distribution and hydrocarbon potential of the organic-rich Kyalla and Velkerri shales of the Upper Roper Group (McArthur Basin). *The APPEA Journal*, 58, 858-864.
- SHIOZAKI, T., IJICHI, M., ISOBE, K., HASHIHAMA, F., NAKAMURA, K.-I., EHAMA, M., ... FURUYA, K. (2016). Nitrification and its influence on biogeochemical cycles from the equatorial Pacific to the Arctic Ocean. *International Society for Microbial Ecology*, 10, 2184-2197.

- SPINKS, S. C., SCHMID, S., & PAGÈS, A. (2016). Delayed euxinia in Paleoproterozoic intracontinental seas: Vital havens for the evolution of eukaryotes? *Precambrian Research*, 287, 108-114.
- STÜKEN, E. E., KIPP, M. A., KOEHLER, M. C., & BUICK, R. (2016). The evolution of Earth's biogeochemical nitrogen cycle. *Earth-Science Reviews*, 160, 220-239.
- SWANSON-HYSELL, N. L., ROSE, C. V., CALMET, C. C., HALVERSON, G. P., HURTGEN, M. T., & MALOOF, A. C. (2010). Cryogenian Glaciation and the Onset of Carbon-Isotope Decoupling. *Science*, 328(5978), 608-611.
- TRIBOVILLARD, N., ALGEO, T. J., LYONS, T., & RIBOULLEAU, A. (2006). Trace metals as paleoredox and paleoproductivity proxies: An update. *Chemical Geology*, 232, 12-32.
- WANTY, R. B., & GOLDHABER, M. B. (1992). Thermodynamics and kinetics of reactions involving vanadium in natural systems: Accumulation of vanadium in sedimentary rocks. *Geochimica et Cosmochimica Acta*, 56, 1471-1483.
- WARD, B. B. (1996). Nitrification and Denitrification: Probing the Nitrogen Cycle in Aquatic Environments. *Microbial Ecology*, 32, 247-261.
- WELLS, A. T., FORMAN, D. J., RANFORD, L. C., & COOK, P. J. (1970). Geology of the Amadeus basin, central Australia. *Bureau of Mineral Resources, Geology and Geophysics*, 1-196.
- WORDEN, A. Z., FOLLOWS, M. J., GIOVANNONI, S. J., WILKEN, S., ZIMMERMAN, A. E., & KEELING, P. J. (2015). Rethinking the marine carbon cycle: Factoring in the multifarious lifestyles of microbes. *Science*, 347(6223), 1-10.
- YANG, B., SMITH, T. M., COLLINS, A. S., MUNSON, T. J., SCHOEMAKER, B., NICHOLLS, D., ... GLORIE, S. (2018). Spatial and temporal variation in detrital zircon age provenance of the hydrocarbon-bearing upper Roper Group, Beetaloo Sub-basin, Northern Territory, Australia. *Precambrian Research*, 304, 140-155.
- ZEHR, J. P., & KUDELA, R. M. (2011). Nitrogen Cycle of the Open Ocean: From Genes to Ecosystems. *Annual Review of Marine Science*, 3, 197-225.
- ZERKLE, A. L., HOUSE, C. H., COX, R. P., & CANFIELD, D. E. (2006). Metal limitation of cyanobacterial N<sub>2</sub> fixation and implications for the Precambrian nitrogen cycle. *Geobiology*, 4, 285-297.
- ZHANG, S., WANG, X., WANG, H., BJERRUM, C. J., HAMMARLUND, E. U., COSTA, M. M., ... CANFIELD, D. E. (2016). Sufficient oxygen for animal respiration 1,400 million years ago. *PNAS*, 113(7), 1-6.
- ZHANG, X., SIGMAN, D. M., FRANÇOIS, M. M., MOREL, A., & KRAEPIEL, M. L. (2014). Nitrogen isotope fractionation by alternative nitrogenases and past ocean anoxia. *PNAS*, 111(13), 4782-4787.

## APPENDIX A: EXTENDED METHODS

### Bootstrapping

Estimates of means and their variance (95% confidence intervals and in some cases standard deviations) were conducted using the Monte Carlo Bootstrap Simulation. These calculations were conducted in MATLAB™ using the “bootstrp” and “bootci” commands. Details of MATLAB’s implementation of Monte Carlo Bootstrap Simulation can be found at: <https://au.mathworks.com/help/stats/bootstrp.html>. Details on the theoretical basis of this analysis can be found in Davison and Hinkley (1997).

### Carbon and Nitrogen IRMS

Powdered sample material (~75-85 mg) was weighed into tin capsules. Samples were analysed at the University of Adelaide on a EuroVector Euro EA in-line with a Nu Instruments Continuous Flow Isotope Ratio Mass Spectrometer (CF-IRMS). In-house isotope standards run alongside were glycine ( $^{13}\text{C} = -31.2\text{\textperthousand}$   $^{15}\text{N} = +1.32\text{\textperthousand}$ ), and glutamic acid ( $^{13}\text{C} = -16.72\text{\textperthousand}$   $^{15}\text{N} = -6.18\text{\textperthousand}$ ). Certified reference material for elemental concentration was Triphenyl Amine (TPA; C:N = 18:1).

## APPENDIX B: FULL ORGANIC AND INORGANIC GEOCHEMICAL CHARACTERISATIONS

### Carbon and Nitrogen Isotope Data

**Table 3. Carbon and Nitrogen isotope data of the Tent Hill Formation.**

Rock ID	Depth (m)	d15N (per mil)	d15N err (per mil)	d13C (per mil)	d13C err (per mil)	N (%)	C (%)
MSDP02	24.0	3.65	0.27	-26.28	0.22	0.04	0.04
MSDP02	37.3	5.02	0.27	-26.87	0.22	0.04	0.05
MSDP02	58.0	3.57	0.27	-26.71	0.22	0.03	0.07
MSDP02	71.0	5.45	0.27	-26.44	0.22	0.04	0.05
MSDP02	82.0	3.28	0.08	-26.43	0.22	0.05	0.07
MSDP02	93.0	2.95	0.27	-26.20	0.22	0.05	0.06
MSDP02	105.0	2.74	0.08	-26.09	0.22	0.04	0.04
MSDP02	112.3	3.06	0.08	-26.23	0.22	0.04	0.04
MSDP02	118.0	2.81	0.08	-25.90	0.22	0.05	0.04
MSDP02	125.2	3.25	0.27		0.21	0.05	0.12
MSDP02	132.0	2.21	0.27		0.21	0.03	0.83
MSDP02	133.1	3.08	0.27		0.21	0.03	0.17
MSDP02	136.4	2.79	0.08	-25.49	0.22	0.04	0.03
MSDP02	137.38	4.15	0.27		0.21	0.04	0.08
MSDP02	143.4	4.53	0.27	-25.99	0.22	0.02	0.03
MSDP02	146.3		0.08	-25.97	0.22	0.04	0.04
MSDP02	147.8	3.06	0.08	-26.04	0.22	0.06	0.03
MSDP02	153.6	4.13	0.27	-27.01	0.22	0.02	0.03
MSDP02	158.0	3.67	0.27	-26.24	0.22	0.02	0.03
MSDP02	162.2	4.99	0.27	-26.70	0.22	0.02	0.04
MSDP02	187.0		0.08	-26.78	0.22	0.01	0.02
MSDP02	199.9		0.08	-26.50	0.22	0.02	0.03

**Table 4. Carbon and Nitrogen isotope data of the Tapley Hill Formation.**

Rock ID	Depth (m)	d15N (per mil)	d15N err (per mil)	d13C (per mil)	d13C err (per mil)	N (%)	C (%)
MSDP02	238.8	1.15	0.08	-28.32	0.22	0.07	0.15
MSDP02	246.7	1.57	0.08	-28.21	0.22	0.06	0.14
MSDP02	252.5	1.69	0.08	-28.76	0.22	0.07	0.18
MSDP02	254.6	1.57	0.08	-28.65	0.22	0.08	0.22
MSDP02	259.4	1.54	0.08	-28.74	0.22	0.05	0.14
MSDP02	265.5	1.22	0.08	-29.15	0.22	0.07	0.22
MSDP02	267.7	1.70	0.08	-29.05	0.22	0.07	0.28
MSDP02	270.85	1.59	0.08	-29.08	0.22	0.07	0.27
MSDP02	276.15	2.00	0.08	-28.98	0.22	0.09	0.36
MSDP02	283.0	1.73	0.08	-29.45	0.22	0.08	0.31
MSDP02	284.88	1.33	0.08	-29.22	0.22	0.08	0.27
MSDP02	288.9	1.67	0.08	-29.29	0.22	0.08	0.32
MSDP02	296.3	1.67	0.08	-29.12	0.22	0.09	0.38
MSDP02	297.1	1.53	0.08	-29.35	0.22	0.09	0.37
MSDP02	300.8	1.58	0.08	-29.11	0.22	0.07	0.29
MSDP02	306.5	2.03	0.08	-29.19	0.22	0.08	0.28
MSDP02	309.1	1.60	0.08	-28.84	0.22	0.07	0.32
MSDP02	315.85	1.63	0.08	-28.95	0.22	0.07	0.30
MSDP02	319.95	1.51	0.08	-28.91	0.22	0.08	0.29
MSDP02	324.15	1.59	0.08	-28.96	0.22	0.07	0.26
MSDP02	324.2	0.98	0.08	-28.68	0.22	0.07	0.26
MSDP02	335.7	1.71	0.08	-28.78	0.22	0.08	0.31

**Table 5. Carbon and Nitrogen isotope data of the Gillen Formation.**

Rock ID	Depth (m)	d15N (per mil)	d15N err (per mil)	d13C (per mil)	d13C err (per mil)	N (%)	C (%)
BL002	60.30	5.02	0.04	-23.53	0.07	0.06	1.36
BL002	62.00	5.39	0.04	-22.54	0.07	0.05	1.04
BL002	62.50	4.69	0.04	-22.46	0.07	0.06	0.47
BL002	65.00	4.57	0.04	-23.81	0.07	0.06	0.81
BL002	67.00	3.71	0.04	-22.80	0.07	0.06	2.05
BL002	72.00	4.93	0.04	-24.93	0.07	0.06	0.79
BL002	74.00	4.78	0.04	-25.76	0.07	0.06	1.95
BL002	75.00	4.88	0.04	-26.18	0.07	0.07	2.97
BL002	77.00	4.81	0.04	-25.63	0.07	0.06	1.24
BL002	77.50	5.42	0.04	-25.84	0.07	0.06	1.13
BL002	80.10	5.18	0.04	-24.43	0.07	0.06	0.92
BL002	84.40	4.93	0.04	-26.60	0.07	0.06	1.20
BL002	86.00	5.27	0.04	-26.49	0.07	0.07	1.62
BL002	87.40	3.75	0.04	-27.45	0.07	0.10	1.53
BL002	90.00	5.01	0.04	-27.23	0.07	0.06	2.35
BL002	92.10	5.18	0.04	-26.45	0.07	0.06	1.19
BL002	93.10	4.50	0.04	-26.94	0.07	0.07	2.05
BL002	95.50	4.35	0.04	-26.67	0.07	0.07	2.41
BL002	96.70	4.23	0.04	-26.56	0.07	0.08	2.91
BL002	97.50	4.96	0.04	-26.93	0.07	0.08	3.76
BL002	99.00	4.44	0.04	-26.85	0.07	0.08	4.73
BL002	102.00	4.25	0.04	-27.19	0.07	0.11	6.92
BL002	105.00	4.92	0.04	-25.83	0.07	0.08	0.80
BL002	108.30	4.86	0.04	-24.61	0.10	0.05	0.30
BL002	108.50	5.27	0.04	-24.45	0.07	0.05	0.38
BL002	110.00	5.12	0.04	-23.07	0.07	0.05	0.85
BL002	113.70	4.54	0.04	-24.82	0.07	0.05	0.53
BL002	122.00	6.79	0.04	-27.07	0.07	0.02	0.52
BL002	123.10	8.26	0.04	-27.10	0.07	0.02	0.31
BL002	128.30			-27.54	0.10	0.01	0.31
BL002	150.10	4.65	0.04	-29.61	0.07	0.03	1.28
BL002	155.15	5.25	0.04	-28.75	0.07	0.03	0.57

**Table 6. Carbon and Nitrogen isotope data of the Arctic Bay Formation.**

Rock ID	Depth (m)	d15N (per mil)	d15N err (per mil)	d13C (per mil)	d13C err (per mil)	N (%)	C (%)
T1413	<b>350.50</b>	3.08	0.22	-31.10	0.33		
T1413	<b>347.00</b>	4.45	0.14	-30.79	0.03	0.12	11.31
T1413	<b>342.60</b>	3.56	0.03	-30.30	0.33	0.06	12.47
T1413	<b>333.90</b>	4.44	0.22	-30.25	0.33		11.15
T1413	<b>328.40</b>	1.90	0.22	-30.70	0.33	0.23	6.86
T1413	<b>325.20</b>	3.76	0.36	-29.20	0.77	0.12	6.21
T1413	<b>317.60</b>	3.50	0.22	-29.20	0.33		
T1413	<b>310.30</b>	3.64	0.12	-30.89	0.13	0.24	6.21
T1413	<b>306.90</b>	3.74	0.13	-30.69	0.01	0.25	4.14
T1413	<b>298.70</b>	2.95	0.22	-30.38	0.33	0.34	4.89
T1413	<b>282.20</b>	3.11	0.22	-30.39	0.33	0.42	5.73
T1413	<b>275.00</b>	3.07	0.22	-30.46	0.33	0.42	3.87
T1413	<b>268.60</b>	3.08	0.22	-28.37	0.33	0.26	5.55
T1413	<b>259.60</b>	3.27	0.07	-32.07	0.16	0.44	7.23
T1413	<b>245.00</b>	3.05	0.06	-30.67	0.13	0.40	7.38
T1413	<b>226.50</b>	2.72	0.22	-30.22	0.33	0.41	6.15
T1413	<b>213.00</b>	2.13	0.22	-30.26	0.33	0.51	5.99
T1413	<b>204.50</b>	2.41	0.36	-30.50	0.10	0.55	7.56
T1413	<b>196.90</b>	2.38	0.27	-30.03	0.57	0.52	4.67
T1413	<b>192.50</b>	2.16	0.14	-29.86	0.02	0.48	5.55
T1413	<b>187.10</b>	2.20	0.22	-26.60	0.33		
T1413	<b>166.40</b>	2.59	0.09	-30.27	0.24	0.50	10.62
T1413	<b>163.20</b>	2.19	0.22	-28.18	0.33	0.45	8.83
T1413	<b>158.90</b>	1.67	0.22	-28.61	0.33	0.43	11.54
T1413	<b>154.70</b>	2.16	0.22	-28.15	0.33	0.42	5.21
T1413	<b>149.40</b>	2.07	0.22	-29.82	0.33	0.60	13.12
T1413	<b>140.00</b>	1.94	0.22	-28.68	0.33	0.39	7.07
T1413	<b>134.70</b>	1.72	0.22	-29.74	0.33	0.44	9.19
T1413	<b>129.70</b>	2.06	0.22	-29.69	0.33	0.52	11.19
T1413	<b>126.50</b>	1.70	0.21	-29.25	0.09	0.67	16.64
T1413	<b>112.30</b>	1.46	0.22	-29.64	0.33	0.36	2.21
T1413	<b>105.70</b>	2.48	0.22	-28.86	0.33	0.24	1.54
T1413	<b>101.00</b>	1.70	0.22	-29.20	0.33		
T1413	<b>94.90</b>	2.33	0.04	-28.99	0.03	0.32	0.28
T1413	<b>90.60</b>	2.30	0.22	-29.20	0.33		
T1413	<b>76.40</b>	2.09	0.22	-30.55	0.33	0.28	4.87
T1413	<b>67.20</b>	1.38	0.02	-31.20	0.03	0.38	9.83
T1413	<b>25.60</b>	1.86	0.15	-29.92	0.03	0.05	0.99
T1413	<b>16.30</b>	2.00	0.22	-30.40	0.33	0.15	0.34
PWC1405	<b>636.50</b>	2.02	0.15	-29.88	0.28	0.51	4.68
PWC1405	<b>600.50</b>	2.83	0.06	-29.59	0.44	0.39	2.75
PWC1405	<b>479.80</b>	2.20	0.25	-28.91	0.24	0.21	0.38
PWC1405	<b>458.60</b>	1.41	0.14	-30.11	0.04	0.26	3.59
PWC1405	<b>388.00</b>	2.57	0.40	-30.80	0.36	0.14	0.41
PWC1405	<b>340.00</b>	3.10	0.03	-31.77	0.35	0.11	0.70
PWC1405	<b>257.50</b>	3.73	0.09	-30.97	0.36	0.11	0.75
PWC1405	<b>216.00</b>	3.64	0.32	-18.88	0.79	0.07	1.78
PWC1405	<b>110.50</b>	4.84	0.12	-29.85	0.58	0.07	0.82
PWC1405	<b>74.00</b>	4.49	0.30	-28.80	0.44	0.10	3.11
PWC1405	<b>45.10</b>	4.68	0.52	-29.35	0.18	0.04	0.41
PWC1405	<b>23.10</b>	4.51	0.38	-28.99	0.28	0.04	0.50

**Table 7. Carbon and Nitrogen isotope data of the Arctic Bay Formation continued.**

Rock ID	Depth (m)	d15N (per mil)	d15N err (per mil)	d13C (per mil)	d13C err (per mil)	N (%)	C (%)
<b>MB1401</b>	<b>465.50</b>	3.16	0.18	-27.28	0.26	0.24	0.70
<b>MB1401</b>	<b>441.50</b>	2.82	0.13	-28.14	0.08	0.23	0.36
<b>MB1401</b>	<b>167.20</b>	2.06	0.40	-28.38	0.28	0.35	0.79
<b>MB1401</b>	<b>160.00</b>	1.64	0.27	-27.81	0.29	0.45	0.58
<b>MB1401</b>	<b>150.00</b>	2.11	0.27	-28.71	0.29	0.40	0.67
<b>MB1401</b>	<b>140.00</b>	2.11	0.22	-29.19	0.17	0.39	0.44
<b>MB1401</b>	<b>132.00</b>	2.05	0.15	-28.79	0.23	0.34	1.17
<b>MB1401</b>	<b>120.20</b>	2.66	0.71	-30.21	0.35	0.40	3.13
<b>MB1401</b>	<b>113.70</b>	2.30	0.06	-30.21	0.19	0.40	1.99
<b>MB1401</b>	<b>107.60</b>	2.12	0.21	-29.96	0.18	0.43	1.67
<b>MB1401</b>	<b>102.80</b>	2.58	0.22	-30.55	0.33	0.42	7.16
<b>MB1401</b>	<b>96.70</b>	2.43	0.33	-30.72	0.39	0.45	3.16
<b>MB1401</b>	<b>91.00</b>	1.81	0.33	-29.68	0.20	0.44	1.27
<b>MB1401</b>	<b>85.00</b>	1.99	0.22	-28.75	0.21	0.32	1.01
<b>MB1401</b>	<b>79.00</b>	3.15	0.56	-30.91	0.87	0.46	11.12
<b>MB1401</b>	<b>75.00</b>	2.25	0.18	-31.26	0.75	0.45	2.42
<b>MB1401</b>	<b>69.40</b>	2.47	0.14	-30.93	0.80	0.43	8.43
<b>MB1401</b>	<b>66.00</b>	2.27	0.02	-30.66	0.84	0.50	3.34
<b>MB1401</b>	<b>61.90</b>	2.65	0.16	-29.96	0.37	0.53	11.44
<b>MB1401</b>	<b>56.40</b>	2.48	0.19	-30.11	0.67	0.62	16.61
<b>MB1401</b>	<b>49.00</b>	2.48	0.21	-30.82	0.72	0.55	12.84
<b>MB1401</b>	<b>44.20</b>	2.60	0.43	-29.35	0.17	0.48	5.37
<b>MB1401</b>	<b>40.50</b>	2.47	0.04	-30.56	0.96	0.48	3.91
<b>MB1401</b>	<b>36.60</b>	1.94	0.39	-30.06	0.51	0.54	11.14
<b>MB1401</b>	<b>31.00</b>	2.55	0.09	-29.68	0.12	0.47	2.74
<b>MB1401</b>	<b>25.80</b>	1.94	0.22	-29.92	0.58	0.44	8.15
<b>MB1401</b>	<b>21.40</b>	1.59	0.73	-29.63	0.36	0.50	13.70
<b>MB1401</b>	<b>16.00</b>	1.38	0.40	-29.99	0.22	0.34	10.18
<b>MB1401</b>	<b>10.00</b>	0.93	0.28	-28.93	0.33	0.32	6.44
<b>MB1401</b>	<b>6.40</b>	0.83	0.13	-28.48	0.23	0.24	1.99

**Table 8. Carbon and Nitrogen isotope data of the Kyalla Formation**

Rock ID	Depth (m)	d15N (per mil)	d15N err (per mil)	d13C (per mil)	d13C err (per mil)	N (%)	C (%)
Elliot 1	672.00			-28.74	0.76	0.00	0.39
Elliot 1	681.35			-27.54	0.76	0.00	0.42
Elliot 1	690.66			-27.65	0.76	0.00	0.44
Elliot 1	696.40			-29.52	0.76	0.00	0.31
Elliot 1	709.33			-21.36	0.76	0.01	0.83
Elliot 1	717.95			-29.05	0.76	0.00	0.45
Elliot 1	721.80			-28.83	0.76	-0.01	0.53
Elliot 1	758.36			-31.71	0.76	0.00	0.66
Elliot 1	766.84			-29.31	0.76	-0.01	0.29
Elliot 1	780.20			-30.49	0.76	0.00	0.43
Elliot 1	797.17			-29.93	0.76	0.01	0.47
Elliot 1	805.90			-31.44	0.76	0.00	0.59
Elliot 1	820.56	2.74	0.74	-31.41	0.76	0.02	0.41
Elliot 1	849.36	3.04	0.74	-31.27	0.76	0.01	0.31
Elliot 1	857.10			-29.79	0.76	0.01	0.37
Elliot 1	876.40	2.90	0.74	-31.12	0.76	0.02	0.72
Elliot 1	891.60	2.43	0.74	-29.86	0.76	0.03	0.45
Elliot 1	899.13	2.81	0.74	-30.56	0.76	0.02	0.28
Elliot 1	907.84			-31.09	0.76	0.01	0.35
Elliot 1	918.70	3.14	0.74	-30.29	0.76	0.02	0.24
Elliot 1	929.70	2.86	0.74	-31.07	0.76	0.03	0.77
Elliot 1	936.50			-31.00	0.76	0.00	0.42
Elliot 1	944.35	3.12	0.74	-30.14	0.76	0.03	0.56
Elliot 1	962.42	1.63	0.74	-29.09	0.76	0.02	0.42
Balmain 1	1013.37	1.50	0.74	-30.09	0.76	0.04	1.35
Balmain 1	1018.90	1.44	0.74	-31.32	0.76	0.04	0.93
Balmain 1	1040.10			-30.26	0.76	0.00	0.25
Balmain 1	1043.80	2.14	0.74	-30.56	0.76	0.02	0.24

**Table 9. Carbon and Nitrogen isotope data of the Velkerri Formation.**

Rock ID	Depth (m)	d15N (per mil)	d15N err (per mil)	d13C (per mil)	d13C err (per mil)	N (%)	C (%)
Altree 2	617.12	2.19	0.03			0.09	0.83
Altree 2	621.84	2.31	0.03	-34.24	0.10	0.13	3.20
Altree 2	640.98	1.04	0.03	-34.07	0.10	0.13	2.39
Altree 2	650.50	2.00	0.05	-34.42	0.07	0.15	2.90
Altree 2	655.27	1.57	0.03	-34.46	0.10	0.13	2.22
Altree 2	661.98	1.26	0.05	-34.86	0.07	0.18	4.27
Altree 2	664.69	1.75	0.03	-34.51	0.10	0.10	4.34
Altree 2	669.51	2.67	0.05			0.15	5.39
Altree 2	674.32	2.02	0.05	-34.16	0.07	0.20	4.99
Altree 2	679.11	1.97	0.03	-33.52	0.10	0.13	3.14
Altree 2	688.61	2.04	0.05	-33.95	0.07	0.23	7.33
Altree 2	697.90	2.66	0.05	-32.61	0.07	0.21	6.32
Altree 2	707.31	2.49	0.05	-33.39	0.07	0.24	6.53
Altree 2	722.05	2.64	0.05	-33.22	0.07	0.23	6.23
Altree 2	736.33	2.08	0.05	-33.22	0.07	0.27	8.10
Altree 2	746.02	2.07	0.05	-33.30	0.07	0.25	4.97
Altree 2	760.33	1.97	0.05	-33.12	0.07	0.24	5.21
Altree 2	769.64	2.09	0.05	-33.28	0.07	0.24	5.40
Altree 2	783.81	2.22	0.05	-33.02	0.07	0.26	5.62
Altree 2	793.37	2.57	0.05	-33.09	0.07	0.29	7.52
Altree 2	802.74	2.49	0.05	-32.82	0.07	0.23	5.94
Altree 2	812.11	2.39	0.05	-32.45	0.07	0.24	5.92
Altree 2	821.78	1.84	0.05	-32.95	0.07	0.22	5.46
Altree 2	831.21	2.37	0.05			0.17	4.67
Altree 2	845.48	2.39	0.05	-33.51	0.07	0.14	3.50
Altree 2	854.93	2.33	0.05	-34.17	0.07	0.15	3.96
Altree 2	873.77	1.76	0.03	-34.30	0.10	0.12	1.74
Altree 2	883.63	2.14	0.03	-34.44	0.10	0.13	2.83
Altree 2	898.25	2.13	0.03			0.08	4.35
Altree 2	912.37	2.51	0.03	-32.84	0.10	0.07	2.26
Altree 2	922.05	2.51	0.05	-34.04	0.07	0.17	5.38
Altree 2	926.59	2.33	0.05	-34.56	0.07	0.15	4.09
Altree 2	931.53	2.66	0.05	-33.91	0.07	0.17	5.74
Altree 2	940.69	2.30	0.05	-35.22	0.07	0.14	4.28

**Table 10. Carbon and Nitrogen isotope data of the Vekkerri Formation continued.**

Rock ID	Depth (m)	d15N (per mil)	d15N err (per mil)	d13C (per mil)	d13C err (per mil)	N (%)	C (%)
Marmbulligan 1	129.00	2.52	0.14	-34.56	0.17	0.04	1.47
Marmbulligan 1	135.50	1.33	0.14	-34.60	0.17	0.05	2.43
Marmbulligan 1	139.65	2.22	0.14			NA	NA
Marmbulligan 1	144.20	1.90	0.14			NA	NA
Marmbulligan 1	149.00	1.69	0.14			NA	NA
Marmbulligan 1	173.50	1.90	0.14			NA	NA
Marmbulligan 1	206.00	2.91	0.14	-33.57	0.17	0.05	2.51
Marmbulligan 1	214.30	1.49	0.14	-33.58	0.17	0.06	2.40
Marmbulligan 1	314.00	1.76	0.14		NA	NA	NA
Marmbulligan 1	316.00	2.84	0.14	-33.31	0.17	0.06	1.21
Marmbulligan 1	324.50	2.07	0.14			NA	NA
Marmbulligan 1	341.60	1.33	0.14			NA	NA
Marmbulligan 1	347.00	2.10	0.14			NA	NA
Marmbulligan 1	350.00	2.36	0.14			NA	NA
Marmbulligan 1	355.00	1.80	0.14			NA	NA
Marmbulligan 1	364.00						
Marmbulligan 1	374.50	2.17	0.14			NA	NA
Marmbulligan 1	384.00	1.81	0.14	-33.79	0.17	0.10	3.00
Marmbulligan 1	514.00	1.62	0.14	-35.47	0.17	0.11	3.21
Marmbulligan 1	589.00	1.93	0.14	-33.83	0.17	0.12	2.88
Amungee NW1	2239.00	3.02	0.14	-33.32	0.17	0.14	3.73
Amungee NW1	2241.12	2.06	0.14		0.17	NA	NA
Amungee NW1	2245.25	3.61	0.14		0.17	NA	NA
Amungee NW1	2247.32	4.84	0.14		0.17	NA	NA
Amungee NW1	2249.38	4.03	0.14		0.17	NA	NA
Amungee NW1	2251.44	4.60	0.14		0.17	NA	NA
Amungee NW1	2253.58	1.84	0.14	-33.41	0.17	0.14	4.30
Amungee NW1	2255.62	3.61	0.14	-33.30	0.17	0.13	3.96
Amungee NW1	2259.76	4.80	0.14		0.17	NA	NA
Amungee NW1	2261.80	3.97	0.14	-33.08	0.17	0.15	3.98
Amungee NW1	2263.86	2.09	0.14		0.17	NA	NA
Amungee NW1	2265.94	3.37	0.14	-32.96	0.17	0.15	3.60
Amungee NW1	2268.00	1.84	0.14	-33.15	0.17	0.15	3.54
Amungee NW1	2270.13	2.47	0.14		0.17	NA	NA
Amungee NW1	2272.24	3.09	0.14	-32.81	0.17	0.16	4.54
Amungee NW1	2274.30	4.74	0.14	-32.94	0.17	0.16	4.02
Amungee NW1	2275.58	3.53	0.14		0.17	NA	NA
Tanumbirini 1	3198.00	4.94	0.14	-32.53	0.17	0.10	0.32
Tanumbirini 1	3199.00	0.79	0.14	-34.35	0.17	0.07	1.34

**Table 11. Carbon and Nitrogen isotope data of the Lower Roper Group: Jalboi and Crawford formations.**

Rock ID	Depth (m)	d15N (per mil)	d15N err (per mil)	d13C (per mil)	d13C err (per mil)	N (%)	C (%)
Urapunga 5	118.50	3.87	0.02	-31.10	0.20	0.05	0.19
Urapunga 5	119.30	7.34	0.02	-30.57	0.20	0.07	0.24
Urapunga 5	120.20	4.60	0.02	-30.81	0.20	0.05	0.17
Urapunga 5	120.55	3.90	0.02	-29.80	0.20	0.05	0.21
Urapunga 5	123.55	3.98	0.02	-30.38	0.20	0.07	0.19
Urapunga 5	130.60	4.25	0.02	-29.73	0.20	0.06	0.23
Urapunga 5	139.90	3.65	0.02	-29.29	0.20	0.07	0.23
Urapunga 5	139.95	3.50	0.02	-29.57	0.20	0.09	0.39
Urapunga 5	149.10	3.62	0.02	-29.43	0.20	0.07	0.33
Urapunga 5	149.50	3.91	0.02	-30.27	0.20	0.09	0.24
Urapunga 5	150.50	4.35	0.02	-29.81	0.20	0.07	0.23
Urapunga 5	157.95	4.41	0.02	-27.85	0.20	0.07	0.10
Urapunga 5	160.50	4.68	0.02	-28.38	0.20	0.08	0.09
Urapunga 5	169.80	4.08	0.02	-28.36	0.20	0.07	0.11
Urapunga 5	326.20	3.43	0.15	-30.04	0.18	0.05	0.32
Urapunga 5	334.50	3.71	0.15	-30.82	0.18	0.09	0.39
Urapunga 5	341.30	4.25	0.15	-30.92	0.18	0.09	0.45
Urapunga 5	347.80	4.08	0.15	-30.16	0.18	0.08	0.48
Urapunga 5	348.00	4.24	0.15	-30.49	0.18	0.06	0.34
Urapunga 5	354.70	3.68	0.15	-30.39	0.18	0.06	0.28
Urapunga 5	356.90	3.93	0.15	-30.17	0.18	0.07	0.40
Urapunga 5	361.90	4.00	0.15	-30.16	0.18	0.06	0.37
Urapunga 5	369.50	4.24	0.15	-30.57	0.18	0.08	0.31
Urapunga 5	375.20	4.14	0.15	-30.30	0.18	0.06	0.35
Urapunga 5	380.10	4.30	0.15	-30.52	0.18	0.08	0.41
Urapunga 5	381.30	4.38	0.15	-30.65	0.18	0.09	0.57
Urapunga 5	382.40	4.12	0.15	-30.55	0.18	0.10	0.58
Urapunga 5	387.30	4.39	0.15	-30.41	0.18	0.08	0.39
Urapunga 5	391.70	3.93	0.15	-30.82	0.18	0.05	0.19
Urapunga 5	392.50	4.03	0.15	-30.65	0.18	0.06	0.23
Urapunga 5	393.10	4.40	0.15	-29.87	0.18	0.04	0.20

**Table 12. Carbon and Nitrogen isotope data of the Lower Roper Group: Mainoru Formation.**

Rock ID	Depth (m)	d15N (per mil)	d15N err (per mil)	d13C (per mil)	d13C err (per mil)	N (%)	C (%)
Urapunga 5	396.80	4.17	0.15	-30.00	0.18	0.05	0.26
Urapunga 5	399.30	4.58	0.02	-30.11	0.20	0.07	0.23
Urapunga 5	399.90	5.34	0.15	-29.69	0.18	0.06	0.21
Urapunga 5	401.50	3.94	0.02	-29.27	0.20	0.07	0.17
Urapunga 5	403.00	3.75	0.02	-30.10	0.20	0.07	0.19
Urapunga 5	403.50	4.73	0.02	-29.46	0.20	0.07	0.20
Urapunga 5	405.70	5.01	0.02	-30.25	0.20	0.07	0.26
Urapunga 5	412.40	4.38	0.02	-30.46	0.20	0.07	0.27
Urapunga 5	416.05	4.18	0.02	-30.02	0.20	0.07	0.19
Urapunga 5	421.50	4.01	0.02	-29.36	0.20	0.06	0.17
Urapunga 5	428.00	4.33	0.02	-29.18	0.20	0.06	0.12
Urapunga 5	431.10	4.53	0.02	-30.16	0.20	0.08	0.21
Urapunga 5	435.70	4.58	0.02	-29.86	0.20	0.08	0.20
Urapunga 5	439.65	4.10	0.02	-29.58	0.20	0.07	0.18
Urapunga 5	442.75	4.65	0.02	-30.53	0.20	0.06	0.19
Urapunga 5	448.50	4.77	0.74	-31.47	0.76	0.01	0.16
Urapunga 5	449.50	5.92	0.74	-32.43	0.76	0.00	0.15
Urapunga 5	453.50		0.05	-26.19	0.08	0.01	0.21
Urapunga 5	459.50		0.05	-29.81	0.08	0.03	0.23
Urapunga 5	464.50		0.05	-29.83	0.08	0.02	0.16
Urapunga 5	479.10	3.77	0.74	-31.91	0.76	0.02	0.18
Urapunga 5	486.15		0.05	-29.93	0.08	0.03	0.03
Urapunga 5	487.50	2.18	0.74	-29.45	0.76	0.04	0.10
Urapunga 5	498.60		0.05	-27.51	0.08	0.01	0.01
Urapunga 5	505.10	3.83	0.15	-28.28	0.18	0.05	0.16
Urapunga 5	507.00	3.77	0.15	-25.49	0.18	0.05	0.14
Urapunga 5	516.10		0.05	-29.03	0.08	0.02	0.09
Urapunga 5	535.00		0.05	-28.41	0.08	0.02	0.12
Urapunga 5	535.60		0.05	-28.75	0.08	0.02	0.13
Urapunga 5	540.60		0.05	-28.98	0.08	0.02	0.17
Urapunga 5	541.20	3.67	0.74	-31.42	0.76	0.02	0.17
Urapunga 5	544.80		0.05	-28.56	0.08	0.04	0.57
Urapunga 5	547.80		0.05	-28.23	0.08	0.05	0.72
Urapunga 5	563.10	3.65	0.15	-28.95	0.18	0.07	0.41
Urapunga 5	567.00	3.54	0.15	-29.44	0.18	0.06	0.38
Urapunga 5	571.20		0.05	-29.22	0.08	0.02	0.31
Urapunga 5	574.00		0.05	-29.54	0.08	0.01	0.30
Urapunga 5	578.90		0.05	-29.26	0.08	0.00	0.14
Urapunga 5	583.90		0.05	-29.64	0.08	0.03	0.50
Urapunga 5	587.70	3.53	0.74	-28.46	0.76	0.01	0.29
Urapunga 5	591.40		0.05	-30.06	0.08	0.01	0.29
Urapunga 5	597.80	3.38	0.15	-29.87	0.18	0.06	0.31
Urapunga 6	78.70	4.32	0.74	-30.74	0.76	0.00	0.15
Urapunga 6	232.90	5.03	0.08	-26.93	0.12	0.15	0.37
Urapunga 6	234.20	4.66	0.08	-30.51	0.12	0.12	0.33
Urapunga 6	234.70	4.40	0.08	-28.37	0.12	0.10	0.29
Urapunga 6	237.40	10.60	0.74	-29.78	0.76	0.01	0.16
Urapunga 6	239.60	3.92	0.08	-30.87	0.12	0.18	0.40
Urapunga 6	243.90	4.29	0.08	-23.15	0.12	0.12	0.45
Urapunga 6	245.60	3.70	0.08	-30.67	0.12	0.14	0.28
Urapunga 6	247.05	4.26	0.74	-25.41	0.76	0.01	0.41
Urapunga 6	248.35	4.62	0.74	-29.84	0.76	0.01	0.13
Urapunga 6	249.60	5.08	0.74	-30.46	0.76	0.02	0.21
Urapunga 6	250.80	3.95	0.08	-30.39	0.12	0.14	0.23
Urapunga 6	251.40	3.28	0.74	-19.89	0.76	0.01	0.66
Urapunga 6	256.00	7.17	0.74	-22.35	0.76	0.00	0.76
Urapunga 6	267.60	5.69	0.74	-22.13	0.76	0.01	0.54
Urapunga 6	269.30	10.83	0.74	-28.69	0.76	0.01	0.18
Urapunga 6	422.10	6.55	0.74	-31.26	0.76	0.01	0.13

**Table 13. Carbon and Nitrogen isotope data of the Fraynes Formation**

Rock ID	Depth (m)	d15N (per mil)	d15N err (per mil)	d13C (per mil)	d13C err (per mil)	N (%)	C (%)
MBSI	721.36	2.37	0.08	-31.87	0.11	0.12	3.56
MBSI	721.69	2.77	0.08	-31.22	0.11	0.11	3.85
MBSI	722.55	4.85	0.08	-29.99	0.11	0.12	4.87
MBSI	722.79	4.72	0.08	-32.53	0.11	0.11	2.73
MBSI	722.99	4.64	0.08	-31.19	0.11	0.14	4.22
MBSI	723.15	3.73	0.08	-32.60	0.11	0.12	3.23
MBSI	723.36	4.87	0.08	-32.50	0.11	0.10	2.65
MBSI	723.57	5.57	0.08	-32.95	0.11	0.08	1.71
MBSI	780.77	4.60	0.08	-32.30	0.11	0.07	1.46
MBSI	781.70	5.78	0.08	-22.40	0.11	0.10	2.97
MBSI	782.58	5.27	0.08	-32.71	0.11	0.10	1.38
MBSI	783.54	6.58	0.08	-32.96	0.11	0.07	1.43
MBSI	784.65	5.07	0.08	-33.58	0.11	0.10	2.94
MBSI	785.46	4.83	0.08	-33.19	0.11	0.13	4.30
MBSI	786.26	4.76	0.08	-33.60	0.11	0.12	3.30
MBSI	786.54	4.23	0.08	-33.73	0.11	0.14	4.10
MBSI	786.91	4.05	0.08	-33.56	0.11	0.13	4.40
MBSI	787.31	4.47	0.08	-33.57	0.11	0.13	3.73
MBSI	787.81	4.60	0.08	-33.52	0.11	0.09	2.54
MBSI	788.31	4.87	0.08	-33.47	0.11	0.09	1.61
MBSI	788.71	4.76	0.08	-33.30	0.11	0.08	1.85
MBSI	789.12	4.36	0.08	-33.42	0.11	0.08	1.62
MBSI	789.46	5.33	0.08	-33.28	0.11	0.09	1.44
MBSI	865.80	6.02	0.08	-33.63	0.11	0.08	1.31
MBSI	867.20	6.51	0.08	-33.28	0.11	0.07	0.77
MBSI	867.50	4.93	0.08	-33.71	0.11	0.08	1.77
MBSI	867.90	3.79	0.08	-33.82	0.11	0.08	1.93
MBSI	868.15	5.77	0.08	-33.81	0.11	0.09	2.12
MBSI	868.49	5.21	0.08	-33.62	0.11	0.07	1.73
MBSI	868.66	5.09	0.08	-33.81	0.11	0.10	1.78
MBSI	868.75	5.47	0.08	-33.82	0.11	0.06	1.54
MBSI	868.90	5.64	0.08	-33.83	0.11	0.07	1.75
MBSI	869.30	5.45	0.08	-33.74	0.11	0.07	1.42
MBSI	869.58	6.44	0.08	-33.66	0.11	0.08	2.11
MBSI	869.77	5.17	0.08	-33.78	0.11	0.07	1.36
MBSI	870.10	5.95	0.08	-33.36	0.11	0.09	1.69
MBSI	871.22	1.24	0.08	-33.39	0.11	0.07	1.78
MBSI	871.48	4.44	0.08	-33.69	0.11	0.08	1.91
MBSI	872.93	5.68	0.08	-33.76	0.11	0.08	1.58

**Table 14. Carbon and Nitrogen isotope data of the Barney Creek Formation.**

Rock ID	Depth (m)	d15N (per mil)	d15N err (per mil)	d13C (per mil)	d13C err (per mil)	N (%)	C (%)
GR4	95.30	4.97	0.18	-28.67	0.27	0.01	0.15
GR4	111.00	5.02	0.18	-33.47	0.27	0.02	0.81
GR4	118.00	5.37	0.18	-33.67	0.27	0.02	1.25
GR4	125.70	4.75	0.18	-33.41	0.27	0.02	1.00
GR4	128.80	7.39	0.18	-33.09	0.27	0.02	0.97
GR4	140.60	6.23	0.18	-34.01	0.27	0.02	1.93
GR4	148.50	2.91	0.08	-33.14	0.11	0.08	1.15
GR4	153.40	6.99	0.18	-33.30	0.27	0.01	0.63
GR7	599.50	6.05	0.18	-32.83	0.27	0.03	1.49
GR7	605.80	4.15	0.18	-32.57	0.27	0.02	1.40
GR7	616.90	5.62	0.18	-33.28	0.27	0.02	1.37
GR7	628.50	5.69	0.18	-32.67	0.27	0.03	1.50
GR7	638.00	6.66	0.18	-33.05	0.27	0.02	1.51
GR7	647.10	4.46	0.18	-33.37	0.27	0.03	1.14
GR7	657.60	6.86	0.18	-33.34	0.27	0.02	1.57
GR7	668.40	8.16	0.18	-33.12	0.27	0.02	1.20
GR7	678.00	6.23	0.18	-33.50	0.27	0.03	1.50
GR7	771.20	5.58	0.18	-32.71	0.27	0.03	1.41
GR7	792.00	8.22	0.18	-32.81	0.27	0.02	1.21
GR7	802.00	4.93	0.18	-33.19	0.27	0.02	0.99
GR7	812.60	8.37	0.18	-32.78	0.27	0.02	1.05
GR7	824.00	5.91	0.18	-32.04	0.27	0.01	0.70
GR7	850.00	7.04	0.18	-32.48	0.27	0.02	1.24
GR7	860.00	4.58	0.18	-34.45	0.27	0.05	3.08
GR7	870.10	4.64	0.18	-34.79	0.27	0.05	2.58
GR7	881.00	4.97	0.18	-32.68	0.27	0.03	0.72
GR7	891.00	7.48	0.18	-33.08	0.27	0.02	0.91
GR7	901.00	4.64	0.18	-32.41	0.27	0.02	0.90

**Table 15. Carbon isotope data of the Wollogorang Formation.**

Rock ID	Depth (m)	d13C (per mil)	d13C err (per mil)	N (%)	C (%)
Mt Young 2	52.40		0.08	0.00	4.97
Mt Young 2	57.20	-30.67	0.08	0.00	0.43
Mt Young 2	58.00	-30.47	0.08	0.00	0.43
Mt Young 2	59.40		0.08	0.00	0.27
Mt Young 2	60.40		0.08	0.00	0.62
Mt Young 2	62.40		0.08	0.00	3.60
Mt Young 2	63.80	-30.84	0.08	0.02	2.15
Mt Young 2	65.80	-31.04	0.08	0.00	0.60
Mt Young 2	66.80		0.08	0.01	4.26
Mt Young 2	67.90	-30.87	0.08	0.03	3.11
Mt Young 2	70.20	-30.00	0.08	0.00	0.78
Mt Young 2	71.40		0.08	0.00	0.92
Mt Young 2	72.00	-30.47	0.08	0.01	1.50
Mt Young 2	74.30	-30.81	0.08	0.05	5.68
Mt Young 2	76.30			0.10	
Mt Young 2	77.05	-31.41	0.08	0.08	7.95
Mt Young 2	79.40	-31.47	0.08	0.03	2.94
Mt Young 2	80.20	-31.09	0.08	0.01	1.77
Mt Young 2	82.00		0.08	0.00	2.02
Mt Young 2	84.00		0.08	0.00	6.78
Mt Young 2	84.50	-28.77	0.08	0.00	0.36
Mt Young 2	85.90	-30.40	0.08	0.00	0.29
Mt Young 2	88.30	-29.88	0.08	0.00	0.35
Mt Young 2	89.00	-29.26	0.08	0.00	0.28
Mt Young 2	90.20	-31.25	0.08	0.01	1.03
Mt Young 2	92.20		0.08	0.01	1.53
Mt Young 2	94.00		0.08	0.00	6.23
Mt Young 2	96.00		0.08	0.00	0.65

**Table 16. Carbon and Nitrogen isotope data of the standards used for the IRMS.**

Standard	Weight	d15N	d15N error	d13C	d13C error	%N	%C
Glutamic Acid	939	-6.68	0.27	-16.99	0.21	8.90	40.75
Glutamic Acid	975	-5.90	0.14	-16.40	0.17	10.81	40.97
Glutamic Acid	976	-6.30	0.15	-16.46	0.18	9.26	39.53
Glutamic Acid	983	-6.10	0.27	-16.91	0.21	8.93	41.81
Glutamic Acid	985	-6.15	0.14	-16.88	0.17	9.19	40.38
Glutamic Acid	988	-5.49	0.74	-16.88	0.76	9.65	37.84
Glutamic Acid	1003	-6.23	0.18	-16.70	0.27	8.55	39.48
Glutamic Acid	1031	-6.40	0.74	-17.13	0.76	9.48	36.44
Glutamic Acid	1032	-6.34	0.14	-16.99	0.17	9.60	40.31
Glutamic Acid	1036	-5.58	0.27	-16.28	0.21	9.24	43.62
Glutamic Acid	1060	-5.34	0.74	-17.05	0.76	9.58	36.02
Glutamic Acid	912	-6.17	0.08	-20.00	0.11	9.38	33.58
Glutamic Acid	992	-6.04	0.08	-16.58	0.11	9.62	39.48
Glutamic Acid	978	-6.31	0.08	-16.86	0.11	9.72	39.87
Green River Shale	4271	17.90	0.08	NA	NA	0.83	NA
Green River Shale	3535	17.43	0.08	NA	NA	0.82	NA
Green River Shale	3255	17.51	0.08	NA	NA	0.83	NA
Green River Shale	3	17.51	0.08	NA	NA	0.83	NA
Green River Shale	4	17.43	0.08	NA	NA	0.82	NA
Green River Shale	4	17.90	0.08	NA	NA	0.83	NA
Green River Shale	3409	16.28	0.14	NA	NA	0.83	NA
Green River Shale	3882	17.28	0.14	NA	NA	0.83	NA
TPA	491	-0.71	0.74	-28.33	0.76	3.52	77.89
TPA	514	-1.03	0.14	-29.32	0.17	4.92	93.58
TPA	525	-0.06	0.14	-28.67	0.17	4.94	86.33
TPA	525	-0.11	0.18	-29.80	0.27	4.86	90.97
TPA	529	-0.57	0.27	-29.40	0.21	5.27	94.87
TPA	533	-0.21	0.27	-29.47	0.21	5.01	89.09
TPA	543	-0.62	0.27	-29.08	0.21	5.81	108.11
TPA	543	-1.40	0.74	-28.05	0.76	4.08	74.00
TPA	558	-0.71	0.14	-29.17	0.17	4.70	90.93
TPA	573	-0.45	0.15	-29.20	0.18	5.44	80.56
TPA	515	-0.64	0.08	-29.20	0.11	6.64	84.52
TPA	516	-0.36	0.08	-29.22	0.11	6.15	77.37
TPA	502	-0.59	0.08	-29.22	0.11	6.63	84.61

## Trace metal data

**Table 17. Trace metal data of the Tent Hill Formation**

Rock ID	Depth (m)	TOC (wt %)	P (ppm)	P/TOC (ppm/ wt%)	V (ppm)	Mo (ppm)	V/Mo	Mo/TOC (ppm/ wt%)	V/Mo /TOC (per wt %)	Fe (molar)	Al (molar)	Fe/Al	Cr (ppm)	Ti (ppm)	Cr/Ti
MSDP02	30.65		2194.76		119.68	0.00				0.08	0.30	0.27	118.03	7687.63	0.02
MSDP02	31.40		1686.53		106.79	3.84	27.81			0.09	0.32	0.27	155.64	7446.95	0.02
MSDP02	32.23		1415.59		105.43	0.00				0.07	0.31	0.24	101.07	7627.52	0.01
MSDP02	33.40		1563.31		73.16	0.00				0.08	0.31	0.25	80.72	7856.16	0.01
MSDP02	34.40		1396.72		100.64	0.00				0.08	0.31	0.26	75.86	7463.87	0.01
MSDP02	35.41		1320.69		98.61	0.00				0.08	0.29	0.26	77.62	7448.09	0.01
MSDP02	36.40		1406.77		92.86	0.00				0.08	0.30	0.27	101.85	7657.68	0.01
MSDP02	37.41	0.14	1374.04	9814.57	104.38	0.00		0.00	0.00	0.08	0.32	0.26	101.04	7498.26	0.01
MSDP02	38.40		1279.07		73.75	3.58	20.60			0.08	0.32	0.26	98.58	7580.38	0.01
MSDP02	39.40		1295.14		94.01	0.00				0.08	0.32	0.26	91.01	7828.59	0.01
MSDP02	40.40		1332.57		110.53	0.00				0.08	0.32	0.25	59.59	7754.62	0.01
MSDP02	41.40		1356.76		94.21	0.00				0.07	0.29	0.26	74.20	8238.95	0.01
MSDP02	45.40		1566.95		105.75	3.61	29.29			0.08	0.30	0.26	93.62	7943.12	0.01
MSDP02	46.00		1472.76		91.99	0.00				0.08	0.29	0.28	123.61	7632.84	0.02
MSDP02	47.35		1608.12		106.15	0.00				0.09	0.31	0.28	143.96	7947.44	0.02
MSDP02	48.70		1499.16		108.55	0.00				0.08	0.30	0.27	117.46	8005.11	0.01
MSDP02	50.06		1480.81		97.56	0.00				0.08	0.31	0.27	138.51	8116.07	0.02
MSDP02	51.40		1409.87		95.22	0.00				0.08	0.29	0.27	91.62	7904.30	0.01
MSDP02	52.40		1461.16		102.60	0.00				0.08	0.29	0.26	0.00	7794.72	0.00
MSDP02	53.40		1651.54		91.61	0.00				0.08	0.29	0.27	104.12	7245.83	0.01
MSDP02	54.41		1429.91		111.49	0.00				0.07	0.28	0.27	102.55	7623.31	0.01
MSDP02	56.40		1410.04		95.84	3.45	27.78			0.08	0.28	0.28	73.20	7792.54	0.01
MSDP02	58.40	0.10	1463.00	14630.00	107.92	3.33	32.41	33.30	324.08	0.08	0.28	0.28	80.03	7421.37	0.01
MSDP02	60.40		1313.12		88.68	0.00				0.08	0.28	0.27	137.35	7509.14	0.02
MSDP02	61.90		1386.38		88.96	4.09	21.75			0.08	0.28	0.27	122.02	7923.70	0.02
MSDP02	63.40		1421.07		108.61	0.00				0.08	0.29	0.26	91.10	7647.18	0.01
MSDP02	64.15		1368.10		93.03	0.00				0.08	0.29	0.28	114.02	7970.60	0.01
MSDP02	64.90		1394.24		89.38	0.00				0.08	0.30	0.27	95.13	7754.64	0.01
MSDP02	65.66		1424.01		99.09	0.00				0.08	0.30	0.26	144.71	7654.56	0.02
MSDP02	66.40		1507.27		103.36	5.02	20.59			0.09	0.32	0.29	156.83	7995.43	0.02
MSDP02	67.40		1383.61		95.24	0.00				0.08	0.30	0.27	112.34	7078.13	0.02
MSDP02	68.41		1370.36		118.36	0.00				0.08	0.30	0.25	72.61	7400.63	0.01
MSDP02	69.40		1398.41		97.50	0.00				0.08	0.31	0.26	107.45	8119.21	0.01
MSDP02	70.40		1318.78		86.76	0.00				0.08	0.31	0.26	116.27	8200.22	0.01
MSDP02	71.41	0.09	1345.39	14948.78	107.45	0.00		0.00	0.00	0.08	0.30	0.26	80.47	7980.96	0.01
MSDP02	72.40		1350.40		111.43	0.00				0.08	0.30	0.26	126.16	8106.88	0.02
MSDP02	73.20		1386.18		92.96	3.86	24.08			0.08	0.30	0.25	134.38	7916.61	0.02
MSDP02	74.00		1187.06		109.74	0.00				0.08	0.29	0.26	85.55	7526.90	0.01
MSDP02	75.40		1371.47		116.47	0.00				0.08	0.31	0.26	114.36	7694.41	0.01
MSDP02	75.80		1339.79		110.88	0.00				0.08	0.31	0.27	95.40	7992.34	0.01
MSDP02	76.40		1304.15		97.05	0.00				0.08	0.31	0.26	107.32	7712.96	0.01
MSDP02	78.40		1263.40		116.01	0.00				0.08	0.31	0.27	66.59	7491.82	0.01
MSDP02	79.41		1168.78		110.71	0.00				0.08	0.31	0.26	77.84	7727.02	0.01
MSDP02	80.40		1154.87		91.26	0.00				0.08	0.31	0.26	129.69	7826.96	0.02
MSDP02	81.40		1126.63		110.82	0.00				0.08	0.29	0.28	69.71	7693.45	0.01

**Table 18. Trace metal data of the Tent Hill Formation continued.**

Rock ID	Depth (m)	TOC (wt %)	P (ppm)	P/TOC (ppm/wt%)	V (ppm)	Mo (ppm)	V/Mo	Mo/TOC (ppm/wt%)	V/Mo / TOC (per wt %)	Fe (molar)	Al (molar)	Fe/Al	Cr (ppm)	Ti (ppm)	Cr/Ti
MSDP02	82.01	0.06	1242.18	20703.00	94.04	0.00		0.00	0.00	0.08	0.29	0.27	148.87	7824.02	0.02
MSDP02	82.60		1128.29		128.87	0.00				0.08	0.29	0.27	68.52	7893.36	0.01
MSDP02	84.40		1181.56		140.13	0.00				0.08	0.30	0.27	113.97	7630.20	0.01
MSDP02	85.40		1164.08		126.93	0.00				0.08	0.29	0.27	118.41	7839.04	0.02
MSDP02	86.40		1280.73		150.98	0.00				0.08	0.30	0.27	0.00	7690.91	0.00
MSDP02	87.41		1356.33		96.94	0.00				0.08	0.30	0.26	106.11	7217.88	0.01
MSDP02	88.60		1343.30		82.20	0.00				0.07	0.31	0.24	111.50	7060.91	0.02
MSDP02	89.80		1263.54		106.48	3.43	31.04			0.08	0.30	0.26	93.21	8017.27	0.01
MSDP02	90.41		1305.44		117.67	0.00				0.08	0.31	0.25	96.99	7321.40	0.01
MSDP02	91.61		1169.69		98.97	0.00				0.08	0.31	0.25	80.67	7764.70	0.01
MSDP02	92.81		1231.96		77.34	0.00				0.08	0.31	0.25	99.90	7112.40	0.01
MSDP02	93.40	0.04	1222.59	30564.75	108.42	4.24	25.57	106.00	639.27	0.08	0.30	0.27	97.88	7004.43	0.01
MSDP02	94.40		1201.54		103.97	0.00				0.08	0.31	0.25	112.73	7200.91	0.02
MSDP02	95.40		1195.22		111.66	5.13	21.77			0.08	0.31	0.24	101.97	7130.06	0.01
MSDP02	96.40		1209.43		90.07	0.00				0.08	0.31	0.25	113.64	7449.64	0.02
MSDP02	97.40		1273.26		104.62	4.11	25.45			0.07	0.32	0.23	127.26	7323.90	0.02
MSDP02	98.41		1172.08		90.15	0.00				0.08	0.32	0.24	126.08	7464.69	0.02
MSDP02	99.40		1209.25		101.96	0.00				0.07	0.30	0.25	114.17	7064.39	0.02
MSDP02	100.40		1104.83		106.96	0.00				0.08	0.29	0.27	142.47	7307.65	0.02
MSDP02	101.41		1166.82		115.97	0.00				0.08	0.31	0.26	81.30	7382.68	0.01
MSDP02	102.40		1167.32		84.78	0.00				0.07	0.29	0.26	131.84	6950.09	0.02
MSDP02	103.40		1527.29		97.16	0.00				0.08	0.32	0.26	107.62	6403.40	0.02
MSDP02	104.40		1225.15		83.38	0.00				0.08	0.31	0.26	107.63	7317.25	0.01
MSDP02	105.40	0.11	1089.17	9901.55	97.96	0.00		0.00	0.00	0.08	0.29	0.27	118.71	6927.73	0.02
MSDP02	106.40		1135.35		104.34	0.00				0.08	0.32	0.26	136.75	7143.80	0.02
MSDP02	107.40		1186.23		89.25	0.00				0.08	0.31	0.26	76.15	7677.31	0.01
MSDP02	108.41		1110.94		114.53	0.00				0.08	0.31	0.26	105.26	7386.87	0.01
MSDP02	109.40		1105.16		100.32	0.00				0.08	0.29	0.27	123.59	7157.35	0.02
MSDP02	110.41		1166.02		102.70	0.00				0.08	0.31	0.27	138.53	7262.57	0.02
MSDP02	111.40		1173.28		84.11	0.00				0.08	0.30	0.27	126.28	7379.90	0.02
MSDP02	112.40	0.20	1153.25	5766.25	97.79	0.00		0.00	0.00	0.08	0.32	0.26	75.67	7598.91	0.01
MSDP02	113.41		1126.58		102.57	0.00				0.08	0.32	0.25	131.67	7378.18	0.02
MSDP02	114.41		1248.06		102.25	0.00				0.08	0.33	0.25	126.06	6936.02	0.02
MSDP02	115.40		1082.45		76.57	0.00				0.08	0.33	0.25	150.71	7239.18	0.02
MSDP02	116.40		1022.46		91.48	0.00				0.08	0.32	0.26	111.45	7463.70	0.01
MSDP02	117.40		1117.18		120.15	0.00				0.08	0.31	0.27	122.93	7455.10	0.02
MSDP02	118.40	0.02	989.42	49471.00	110.92	0.00		0.00	0.00	0.08	0.32	0.26	128.80	7300.89	0.02
MSDP02	119.40		1038.15		97.00	0.00				0.08	0.33	0.25	159.14	6857.15	0.02
MSDP02	120.40		1062.35		119.94	0.00				0.09	0.33	0.26	121.68	7480.44	0.02
MSDP02	121.41		924.16		121.90	0.00				0.09	0.31	0.27	89.96	7366.34	0.01
MSDP02	122.41		937.26		144.71	0.00				0.08	0.31	0.24	92.13	7020.95	0.01
MSDP02	123.40		1549.77		115.04	0.00				0.08	0.27	0.30	118.13	6283.12	0.02
MSDP02	124.40		1119.98		111.09	4.19	26.51			0.08	0.31	0.26	83.60	7021.97	0.01
MSDP02	125.41	0.06	969.71	16161.83	110.87	0.00		0.00	0.00	0.08	0.32	0.26	106.57	7057.65	0.02
MSDP02	126.40		1105.13		99.23	5.23	18.97			0.09	0.34	0.26	142.02	7353.30	0.02
MSDP02	127.40		1116.95		112.56	3.94	28.57			0.09	0.34	0.26	138.30	7421.90	0.02
MSDP02	128.40		992.84		123.94	0.00				0.08	0.32	0.26	81.03	7496.97	0.01
MSDP02	129.40		984.16		93.46	0.00				0.08	0.32	0.26	108.04	7262.88	0.01
MSDP02	130.91		1040.78		105.80	0.00				0.08	0.33	0.25	77.30	7449.98	0.01
MSDP02	131.65		1033.08		78.26	0.00				0.08	0.33	0.26	124.82	7483.61	0.02
MSDP02	132.40	0.10	913.33	9133.30	102.30	0.00		0.00	0.00	0.08	0.30	0.26	106.07	6764.04	0.02
MSDP02	133.41	0.10	853.00	8530.00	81.10	0.00		0.00	0.00	0.07	0.29	0.24	70.30	6351.80	0.01
MSDP02	134.40		871.64		116.66	0.00				0.07	0.31	0.24	94.94	6109.99	0.02
MSDP02	135.40		884.38		125.73	0.00				0.07	0.31	0.23	62.18	6173.58	0.01

**Table 19. Trace metal data of the Tapley Hill Formation.**

Rock ID	Depth (m)	TOC (wt %)	P (ppm)	P/TOC (ppm/wt%)	V (ppm)	Mo (ppm)	V/Mo	Mo/TOC (ppm/wt%)	V/Mo /TOC (per wt %)	Fe (molar)	Al (molar)	Fe/Al	Cr (ppm)	Ti (ppm)	Cr/Ti
MSDP02	225.50		698.46		61.49	8.22	7.48			0.06	0.17	0.37	178.43	4650.18	0.04
MSDP02	226.50		804.02		92.88	9.03	10.29			0.06	0.18	0.33	159.15	5241.45	0.03
MSDP02	227.50		785.21		68.29	8.17	8.36			0.06	0.18	0.33	170.78	5895.86	0.03
MSDP02	228.12		896.71		63.31	6.08	10.41			0.06	0.18	0.32	143.72	5997.30	0.02
MSDP02	228.50		712.99		75.94	5.96	12.74			0.05	0.18	0.31	113.77	4530.63	0.03
MSDP02	229.67		685.10		65.92	5.25	12.56			0.06	0.17	0.34	157.01	4765.05	0.03
MSDP02	230.83		729.45		76.65	6.29	12.19			0.06	0.18	0.31	122.80	5139.52	0.02
MSDP02	232.01		758.97		82.38	5.63	14.63			0.06	0.20	0.29	132.42	5016.13	0.03
MSDP02	233.25		827.85		85.81	6.17	13.91			0.06	0.19	0.30	105.79	5101.54	0.02
MSDP02	234.50		748.60		80.14	3.33	24.07			0.06	0.19	0.31	118.37	4763.10	0.02
MSDP02	236.01		757.88		58.46	5.50	10.63			0.06	0.20	0.29	131.43	4772.67	0.03
MSDP02	237.51		788.61		69.14	4.24	16.31			0.06	0.19	0.30	122.01	4774.77	0.03
MSDP02	239.01		794.33		63.94	5.20	12.30			0.06	0.20	0.29	123.35	4775.30	0.03
MSDP02	240.50		697.75		84.69	5.78	14.65			0.06	0.20	0.31	136.63	4454.01	0.03
MSDP02	241.50		780.06		47.84	4.79	9.99			0.06	0.19	0.30	132.05	4838.76	0.03
MSDP02	242.51		892.90		77.31	6.01	12.86			0.06	0.19	0.29	146.30	4859.46	0.03
MSDP02	243.50		759.38		77.11	0.00				0.05	0.17	0.30	117.06	4497.16	0.03
MSDP02	244.51		711.28		85.87	4.57	18.79			0.05	0.18	0.29	139.91	4302.35	0.03
MSDP02	245.50		790.23		109.87	5.17	21.25			0.06	0.19	0.31	124.79	4816.21	0.03
MSDP02	246.51	0.28	747.67	2670.25	77.74	4.33	17.95	15.46	64.12	0.06	0.18	0.31	163.61	4382.21	0.04
MSDP02	247.70		866.11		82.31	4.11	20.03			0.06	0.20	0.30	149.81	4643.55	0.03
MSDP02	248.90		728.53		78.09	5.78	13.51			0.06	0.20	0.29	176.75	4463.07	0.04
MSDP02	250.10		742.36		96.23	6.31	15.25			0.06	0.19	0.30	146.84	4461.50	0.03
MSDP02	251.30		839.55		82.40	4.89	16.85			0.07	0.19	0.35	119.68	4386.26	0.03
MSDP02	252.51	0.49	874.75	1785.20	87.07	5.27	16.52	10.76	33.72	0.06	0.21	0.30	134.56	4536.79	0.03
MSDP02	253.70		766.85		93.37	4.76	19.62			0.06	0.20	0.31	148.23	4646.95	0.03
MSDP02	254.90	0.43	723.34	1682.19	91.68	8.93	10.27	20.77	23.88	0.06	0.21	0.30	155.23	4852.29	0.03
MSDP02	256.10		767.81		75.42	7.88	9.57			0.06	0.21	0.29	91.02	4518.99	0.02
MSDP02	257.30		711.47		52.43	4.22	12.42			0.06	0.21	0.28	132.47	4818.78	0.03
MSDP02	258.50		771.95		104.30	3.36	31.04			0.06	0.20	0.30	180.03	4305.04	0.04
MSDP02	259.70	0.43	720.49	1675.56	131.03	5.30	24.72	12.33	57.49	0.06	0.21	0.29	148.54	4566.16	0.03
MSDP02	260.90		882.02		110.75	6.63	16.70			0.06	0.20	0.30	122.84	4923.83	0.02
MSDP02	262.10		674.64		123.17	5.21	23.64			0.06	0.20	0.30	142.69	4845.23	0.03
MSDP02	263.30		708.46		125.59	5.99	20.97			0.06	0.20	0.29	105.97	4695.35	0.02
MSDP02	264.51		747.86		115.71	5.20	22.25			0.06	0.21	0.29	110.93	4928.55	0.02
MSDP02	265.51	0.51	786.99	1543.12	72.38	6.08	11.90	11.92	23.34	0.06	0.22	0.29	154.71	5123.85	0.03
MSDP02	266.50		827.87		102.80	6.13	16.77			0.06	0.21	0.30	122.25	4878.10	0.03
MSDP02	267.50	0.60	770.16	1283.60	115.43	6.41	18.01		30.01	0.06	0.21	0.29	81.05	4928.15	0.02
MSDP02	269.50		641.64		94.80	4.90	19.35	8.17		0.06	0.21	0.29	111.50	4624.01	0.02
MSDP02	271.51		756.66		96.09	3.84	25.02			0.07	0.24	0.30	111.87	4531.85	0.02
MSDP02	272.50		810.15		88.27	5.04	17.51			0.07	0.26	0.29	146.20	4201.95	0.03
MSDP02	273.50		821.58		98.92	6.42	15.41			0.07	0.23	0.30	113.71	4670.05	0.02
MSDP02	273.51		697.88		89.92	5.23	17.19			0.06	0.21	0.29	114.71	4729.71	0.02
MSDP02	274.61		787.00		89.68	7.85	11.42			0.06	0.23	0.28	159.67	4725.31	0.03
MSDP02	275.39		837.48		85.01	6.50	13.08			0.07	0.25	0.28	124.67	4450.87	0.03
MSDP02	276.50	0.68	822.96	1210.24	66.82	5.74	11.64	8.44	17.12	0.08	0.27	0.31	142.86	3980.27	0.04
MSDP02	277.54		757.54		68.72	6.26	10.98			0.08	0.26	0.30	145.10	4267.99	0.03
MSDP02	278.58		785.94		55.33	5.86	9.44			0.07	0.23	0.30	129.97	4529.49	0.03
MSDP02	279.51		784.81		102.55	5.81	17.65			0.07	0.23	0.29	138.02	4729.09	0.03
MSDP02	280.30		776.33		89.49	4.74	18.88			0.06	0.23	0.28	109.35	5023.44	0.02
MSDP02	281.46		783.90		83.79	6.27	13.36			0.06	0.22	0.29	131.54	4720.22	0.03
MSDP02	282.51	0.74	811.44	1096.54	91.98	5.29	17.39	7.15	23.50	0.06	0.22	0.30	126.12	4740.91	0.03
MSDP02	283.50		725.07		88.96	4.31	20.64			0.06	0.22	0.29	119.96	4963.88	0.02
MSDP02	284.50	0.60	736.46	1227.43	79.09	4.82	16.41	8.03	27.35	0.06	0.21	0.28	74.47	4908.26	0.02
MSDP02	285.50		723.81		77.41	4.66	16.61			0.06	0.21	0.28	139.01	4972.76	0.03
MSDP02	286.60		759.96		96.09	4.96	19.37			0.06	0.22	0.27	131.06	4885.99	0.03
MSDP02	287.39		741.51		122.09	7.93	15.40			0.06	0.21	0.29	127.48	5076.06	0.03
MSDP02	288.51	0.60	723.38	1205.63	104.07	3.28	31.73	5.47	52.88	0.06	0.21	0.30	111.19	4644.99	0.02
MSDP02	289.55		695.22		102.82	6.47	15.89			0.06	0.21	0.29	143.58	4929.27	0.03
MSDP02	290.61		649.41		79.11	0.00				0.06	0.21	0.28	105.84	4713.03	0.02
MSDP02	291.50		753.22		87.02	3.37	25.82			0.06	0.21	0.29	141.74	4896.70	0.03
MSDP02	292.55		816.57		78.21	6.41	12.20			0.06	0.22	0.29	146.07	5012.32	0.03
MSDP02	293.62		852.27		82.36	6.58	12.52			0.06	0.22	0.30	109.92	5099.34	0.02
MSDP02	294.51		797.79		90.74	5.10	17.79			0.06	0.22	0.29	129.57	4889.40	0.03
MSDP02	295.44		808.40		66.82	5.50	12.15			0.06	0.21	0.29	110.26	4764.58	0.02
MSDP02	296.39	0.70	646.65	923.79	102.28	5.63	18.17	8.04	25.95	0.06	0.21	0.29	108.11	5053.79	0.02
MSDP02	297.50	0.74	708.30	957.16	72.63	8.73	8.32	11.80	11.24	0.06	0.22	0.29	130.73	5128.77	0.03
MSDP02	299.00		852.91		84.99	4.69	18.12			0.06	0.22	0.29	152.58	4882.10	0.03
MSDP02	300.51	0.64	693.22	1083.16	83.36	5.00	16.67	-7.81	26.05	0.06	0.21	0.29	153.06	4835.64	0.03
MSDP02	301.70		811.26		66.59	11.66	5.71			0.07	0.22	0.34	189.39	5010.31	0.04
MSDP02	302.90		857.05		81.92	9.06	9.04			0.07	0.22	0.30	156.18	5170.56	0.03
MSDP02	304.11		915.71		78.65	7.25	10.85			0.07	0.23	0.29	151.21	5162.97	0.03
MSDP02	305.30		823.37		77.87	4.56	17.08			0.07	0.23	0.32	152.26	4618.22	0.03
MSDP02	306.50	0.66	733.07	1110.71	99.16	4.04	24.54</								

**Table 20. Trace metal data of the Tapley Hill Formation continued.**

Rock ID	Depth (m)	TOC (wt %)	P (ppm)	P/TOC (ppm/wt%)	V (ppm)	Mo (ppm)	V/Mo	Mo/TOC (ppm/wt%)	V/Mo /TOC (per wt %)	Fe (molar)	Al (molar)	Fe/Al	Cr (ppm)	Ti (ppm)	Cr/Ti
MSDP02	312.51		855.03		81.30	4.38	18.56			0.07	0.23	0.31	180.61	5153.47	0.04
MSDP02	313.50		822.54		78.85	5.54	14.23			0.07	0.23	0.30	144.27	4949.22	0.03
MSDP02	314.50		871.44		87.10	7.00	12.44			0.07	0.23	0.30	138.31	5240.59	0.03
MSDP02	315.50	0.76	850.94	1119.66	91.21	8.41	10.85	11.07	14.27	0.07	0.23	0.31	179.64	5150.17	0.03
MSDP02	316.51		877.71		79.46	10.54	7.54			0.07	0.23	0.31	178.42	5183.35	0.03
MSDP02	317.50		864.24		79.29	9.97	7.95			0.07	0.23	0.30	152.42	5203.61	0.03
MSDP02	318.50		789.37		78.99	7.38	10.70			0.08	0.24	0.32	145.07	4848.05	0.03
MSDP02	319.50	0.80	680.86	851.07	96.91	6.09	15.91	7.61	19.89	0.07	0.23	0.32	150.92	4580.59	0.03
MSDP02	320.50		825.88		93.02	12.63	7.37			0.09	0.25	0.35	193.69	4867.80	0.04
MSDP02	321.50		720.28		95.70	9.33	10.26			0.09	0.25	0.34	197.65	4421.63	0.04
MSDP02	322.51		737.59		72.14	7.88	9.15			0.07	0.23	0.32	182.10	4753.60	0.04
MSDP02	323.50		735.66		77.55	8.66	8.95			0.07	0.24	0.31	174.38	4769.11	0.04
MSDP02	324.50	0.76	808.37	1063.64	71.70	8.76	8.18	11.53	10.77	0.08	0.24	0.32	154.73	4843.63	0.03
MSDP02	325.70		738.29		88.71	8.41	10.55			0.07	0.24	0.30	147.50	5078.85	0.03
MSDP02	326.90		889.18		104.24	7.58	13.75			0.07	0.23	0.29	166.81	5084.37	0.03
MSDP02	328.10		886.97		87.96	7.13	12.34			0.07	0.22	0.30	153.22	4989.23	0.03
MSDP02	329.30		807.21		81.65	6.88	11.87			0.07	0.24	0.30	152.64	5171.56	0.03
MSDP02	330.50		758.27		87.25	3.72	23.45			0.07	0.23	0.30	138.59	4766.61	0.03
MSDP02	331.70		811.19		87.14	7.92	11.00			0.07	0.22	0.31	139.02	5104.96	0.03
MSDP02	332.90		740.01		73.17	8.64	8.47			0.07	0.23	0.31	155.24	5140.67	0.03
MSDP02	334.10		748.96		82.13	5.57	14.75			0.07	0.23	0.30	113.39	4965.92	0.02
MSDP02	335.30	0.82	788.88	962.05	67.04	6.89	9.73	8.40	11.87	0.07	0.22	0.31	160.85	5083.89	0.03
MSDP02	336.50		803.55		113.06	7.14	15.83			0.08	0.25	0.33	143.67	5118.53	0.03
MSDP02	337.51		784.16		111.98	4.21	26.60			0.09	0.28	0.32	133.98	4619.72	0.03
MSDP02	338.50		771.12		123.75	6.97	17.75			0.09	0.28	0.31	186.78	4935.14	0.04
MSDP02	339.50		817.50		138.84	6.62	20.97			0.09	0.29	0.32	149.55	4595.48	0.03
MSDP02	340.71		813.15		156.63	6.61	23.70			0.09	0.28	0.31	143.93	4882.50	0.03
MSDP02	341.91		736.58		105.56	8.84	11.94			0.09	0.28	0.33	215.59	5150.71	0.04
MSDP02	342.50		828.42		115.32	10.22	11.28			0.09	0.28	0.33	177.23	5285.56	0.03
MSDP02	343.50		818.56		121.60	7.54	16.13			0.07	0.24	0.30	155.56	5536.76	0.03
MSDP02	344.50		847.93		114.65	5.50	20.85			0.07	0.24	0.31	128.85	5328.15	0.02
MSDP02	345.50		825.99		129.74	6.07	21.37			0.07	0.24	0.31	113.68	5194.84	0.02
MSDP02	346.50		850.06		93.36	5.67	16.47			0.07	0.23	0.30	140.39	5793.12	0.02
MSDP02	347.50		815.66		80.96	7.35	11.01			0.07	0.22	0.30	134.82	5374.73	0.03
MSDP02	348.51		754.46		115.05	6.87	16.75			0.07	0.24	0.31	179.80	5666.41	0.03
MSDP02	349.62		788.58		105.96	7.39	14.34			0.07	0.23	0.30	125.37	5870.54	0.02
MSDP02	350.56		776.39		99.84	4.63	21.56			0.07	0.23	0.29	114.70	5351.34	0.02
MSDP02	351.50		882.66		90.16	4.24	21.26			0.07	0.23	0.30	125.47	5443.21	0.02
MSDP02	354.50		791.51		109.77	8.40	13.07			0.07	0.22	0.31	141.66	5489.40	0.03
MSDP02	355.50		798.07		87.80	8.38	10.48			0.07	0.23	0.30	177.55	5423.95	0.03
MSDP02	356.50		852.86		96.26	5.21	18.48			0.07	0.22	0.30	154.24	5374.61	0.03
MSDP02	357.51		752.71		126.79	9.79	12.95			0.08	0.24	0.32	175.07	5660.98	0.03
MSDP02	358.62		868.22		59.66	7.96	7.49			0.08	0.24	0.32	202.32	5928.53	0.03
MSDP02	359.56		731.97		77.94	8.08	9.65			0.07	0.23	0.31	175.31	5718.30	0.03
MSDP02	360.50		781.64		122.99	7.63	16.12			0.07	0.22	0.33	171.43	5480.08	0.03
MSDP02	361.50		780.30		90.78	9.33	9.73			0.07	0.22	0.32	158.00	5357.95	0.03
MSDP02	362.50		729.34		98.07	5.78	16.97			0.07	0.23	0.31	207.06	5550.20	0.04
MSDP02	363.51		745.41		102.99	11.01	9.35			0.07	0.21	0.33	112.41	5338.62	0.02
MSDP02	365.01		745.93		91.35	10.38	8.80			0.07	0.22	0.32	164.01	5466.33	0.03
MSDP02	366.50		755.87		77.79	10.56	7.37			0.08	0.23	0.33	174.76	5259.23	0.03
MSDP02	367.51		715.38		104.86	10.97	9.56			0.08	0.23	0.33	147.77	5273.60	0.03
MSDP02	368.50		743.26		100.42	11.19	8.97			0.08	0.23	0.34	163.81	5175.12	0.03
MSDP02	369.50		840.70		96.76	11.05	8.76			0.07	0.23	0.33	148.66	5598.62	0.03
MSDP02	370.86		851.46		136.65	10.01	13.65			0.07	0.22	0.32	152.90	5972.24	0.03
MSDP02	372.50		722.87		97.81	10.13	9.66			0.08	0.22	0.33	157.49	5626.04	0.03
MSDP02	373.50		825.22		76.90	10.38	7.41			0.07	0.21	0.34	160.59	5307.84	0.03
MSDP02	374.51		817.32		92.21	13.05	7.07			0.07	0.21	0.34	192.97	5452.57	0.04
MSDP02	375.50		872.68		91.23	11.71	7.79			0.07	0.22	0.33	134.99	5087.29	0.03
MSDP02	376.70		847.33		104.00	13.39	7.77			0.08	0.23	0.35	156.15	5652.71	0.03
MSDP02	377.90		876.52		99.13	8.70	11.39			0.07	0.23	0.33	139.57	5719.81	0.02
MSDP02	379.10		809.43		83.46	10.97	7.61			0.08	0.23	0.34	214.12	5541.37	0.04
MSDP02	380.30		950.18		98.54	10.54	9.35			0.08	0.23	0.35	154.99	5342.68	0.03
MSDP02	381.51		854.75		88.12	10.62	8.30			0.08	0.23	0.35	136.78	5173.74	0.03
MSDP02	382.70		757.00		81.26	10.60	7.67			0.08	0.23	0.35	102.68	5412.31	0.02
MSDP02	383.91		690.42		76.50	8.90	8.60			0.08	0.23	0.36	155.35	5208.21	0.03
MSDP02	385.11		705.42		82.02	7.84	10.46			0.08	0.22	0.37	172.16	5317.74	0.03
MSDP02	386.30		765.25		94.39	8.87	10.64			0.08	0.24	0.34	118.92	5649.71	0.02
MSDP02	387.50		826.70		83.00	6.21	13.37			0.09	0.24	0.37	136.57	5120.34	0.03
MSDP02	388.50		753.53		80.28	11.62	6.91			0.09	0.23	0.39	157.38	5577.38	0.03
MSDP02	389.50		819.28		0.00	11.24	0.00			0.09	0.24	0.38	182.77	5798.89	0.03
MSDP02	390.51		750.59		79.66	14.42	5.52			0.09	0.22	0.40	232.68	5505.79	0.04
MSDP02	391.50		748.83		91.64	22.38	4.09			0.10	0.23	0.43	234.97	6059.39	0.04
MSDP02	392.50		841.82		69.23	18.11	3.82			0.10	0.25	0.41	227.25	5508.62	0.04
MSDP02	393.50		957.13		102.32	15.17	6.74			0.09	0.25	0.37	204.00	5328.14	0.04
MSDP02	394.70		918.07		102.92	12.19	8.44			0.09	0.24	0.36	199.75	5972.43	0.03

**Table 21. Trace metal data of the Gillen Formation.**

Rock ID	Depth (m)	TOC (wt %)	P (ppm)	P/TOC (ppm/ wt%)	V (ppm)	Mo (ppm)	V/Mo	Mo/TOC (ppm /wt%)	V/Mo /TOC (per wt %)	Fe (molar)	Al (molar)	Fe/Al	Cr (ppm)	Ti (ppm)	Cr/Ti
BL002	60.30	1.81	130.00	71.82	140.00	1.00	140.00	0.55	77.35	0.02	0.36	0.07	90.00	4614.25	0.02
BL002	62.00	1.38	120.00	86.96	140.00	2.00	70.00	1.45	50.72	0.06	0.33	0.19	90.00	4434.48	0.02
BL002	62.50	0.46	260.00	565.22	170.00	1.00	170.00	2.17	369.57	0.03	0.39	0.07	60.00	5153.58	0.01
BL002	65.00	0.93	160.00	172.04	160.00	<0.5				0.03	0.39	0.08	60.00	5333.36	0.01
BL002	67.00	2.24	90.00	40.18	100.00	2.00	50.00	0.89	22.32	0.15	0.23	0.66	60.00	3116.12	0.02
BL002	68.50	1.08	210.00	194.44	170.00	<0.5				0.03	0.41	0.07	90.00	5573.06	0.02
BL002	72.00	0.95	160.00	168.42	160.00	<0.5				0.03	0.40	0.08	90.00	5393.28	0.02
BL002	74.00	2.10	150.00	71.43	110.00	1.00	110.00	0.48	52.38	0.05	0.36	0.14	100.00	4614.25	0.02
BL002	75.00	3.16	280.00	88.61	120.00	1.00	120.00	0.32	37.97	0.03	0.36	0.10	70.00	4614.25	0.02
BL002	77.00	1.39	230.00	165.47	160.00	<0.5				0.06	0.37	0.15	90.00	5033.73	0.02
BL002	77.50	1.34	280.00	208.96	120.00	<0.5				0.06	0.36	0.18	90.00	5213.51	0.02
BL002	80.10	0.97	300.00	309.28	140.00	1.00	140.00	1.03	144.33	0.03	0.41	0.07	40.00	5453.21	0.01
BL002	84.40	1.34	280.00	208.96	140.00	1.00	140.00	0.75	104.48	0.03	0.38	0.08	60.00	5453.21	0.01
BL002	86.00	1.84	340.00	184.78	160.00	1.00	160.00	0.54	86.96	0.05	0.43	0.12	90.00	5692.91	0.02
BL002	87.40	1.60	350.00	218.75	140.00	1.00	140.00	0.63	87.50	0.05	0.40	0.12	90.00	5393.28	0.02
BL002	90.00	2.48	220.00	88.71	130.00	1.00	130.00	0.40	52.42	0.06	0.37	0.17	90.00	4494.40	0.02
BL002	92.10	1.57	260.00	165.61	100.00	<0.5				0.02	0.38	0.06	60.00	5033.73	0.01
BL002	93.10	2.22	310.00	139.64	140.00	<0.5				0.04	0.41	0.09	70.00	4913.88	0.01
BL002	95.50	2.38	280.00	117.65	130.00	1.00	130.00	0.42	54.62	0.04	0.39	0.10	60.00	4973.81	0.01
BL002	96.70	2.90	290.00	100.00	130.00	1.00	130.00	0.34	44.83	0.04	0.39	0.11	60.00	4614.25	0.01
BL002	97.50	3.86	310.00	80.31	140.00	2.00	70.00	0.52	18.13	0.05	0.39	0.13	70.00	4434.48	0.02
BL002	99.00	4.98	310.00	62.25	90.00	<0.5				0.03	0.36	0.09	60.00	4434.48	0.01
BL002	102.00	7.36	250.00	33.97	130.00	2.00	65.00	0.27	8.83	0.07	0.41	0.17	100.00	4913.88	0.02
BL002	105.00	0.82	490.00	597.56	150.00	<0.5				0.03	0.48	0.06	90.00	6771.57	0.01
BL002	108.30	0.26	410.00	1576.92	80.00	<0.5				0.03	0.40	0.07	40.00	4973.81	0.01
BL002	108.50	0.39	320.00	820.51	120.00	<0.5				0.02	0.40	0.06	40.00	5093.66	0.01
BL002	110.00	0.98	250.00	255.10	120.00	<0.5				0.03	0.43	0.08	70.00	5752.84	0.01
BL002	113.70	0.56	430.00	767.86	140.00	1.00	140.00	1.79	250.00	0.03	0.47	0.07	60.00	6112.39	0.01
BL002	122.00	0.56	290.00	517.86	50.00	<0.5				0.01	0.17	0.07	20.00	2217.24	0.01
BL002	123.10	0.36	280.00	777.78	20.00	<0.5				0.01	0.13	0.09	20.00	1498.13	0.01
BL002	128.00	1.20	210.00	175.00	80.00	2.00	40.00	1.67	33.33	0.05	0.35	0.14	60.00	5093.66	0.01
BL002	128.30	0.28	100.00	357.14	20.00	<0.5				0.01	0.06	0.17	<10	539.33	
BL002	150.10	1.05	160.00	152.38	50.00	<0.5				0.03	0.23	0.12	30.00	3235.97	0.01
BL002	155.15	0.58	220.00	379.31	110.00	1.50	73.33	2.59	126.44	0.06	0.37	0.17	60.00	4554.33	0.01

**Table 22. Trace metal data of the Arctic Bay Formation.**

Rock ID	Depth (m)	TOC (wt %)	V (ppm)	Mo (ppm)	V/Mo	Mo/TOC (ppm/ wt%)	V/Mo /TOC (per wt %)	Fe (molar)	Al (molar)	Fe/Al	Cr (ppm)	Ti (ppm)	Cr/Ti
T1413	350.50		92.39	6.12	15.10			0.03	0.00		16.511	733.20	0.02
T1413	347.00	11.31	28.34	1.82	15.61	0.16	1.38	0.02	0.00		5.903	192.46	0.03
T1413	342.60	12.47	109.26	0.13	810.33	0.01	64.98	0.04	0.00	1288.75	22.33	1052.74	0.02
T1413	333.90	11.15	33.75	2.37	14.27	0.21	1.28	0.02	0.00		5.785	255.19	0.02
T1413	328.40	6.86	49.88	1.88	26.47	0.27	3.86	0.02	0.00		15.524	713.69	0.02
T1413	325.20	6.21	86.73	5.74	15.11	0.92	2.43	0.06	0.09	0.67	25.35	1048.00	0.02
T1413	317.60		131.89	11.01	11.97			0.08	0.10	0.79	28.92	1151.64	0.03
T1413	310.30	6.21	77.70	0.08	951.64	0.01	153.19	0.03	0.00	946.02	16.13	673.85	0.02
T1413	306.90	4.14	63.57	2.78	22.89	0.67	5.52	0.05	0.04	1.43	11.58	530.41	0.02
T1413	298.70	4.89	99.69	8.20	12.16	1.67	2.48	0.07	0.03	1.97	18.13	813.33	0.02
T1413	282.20	5.73	195.36	12.25	15.95	2.14	2.78	0.08	0.11	0.68	37.73	1777.57	0.02
T1413	275.00	3.87	110.61	7.61	14.53	1.96	3.75	0.07	0.06	1.18	23.49	1122.25	0.02
T1413	268.60	5.55	284.17	17.49	16.25	3.15	2.93	0.11	0.00		36.903	1780.84	0.02
T1413	259.60	7.23	283.90	20.06	14.15	2.77	1.96	0.10	0.15	0.71	52.86	2812.34	0.02
T1413	245.00	7.38	342.57	30.16	11.36	4.09	1.54	0.08	0.10	0.79	44.35	2331.87	0.02
T1413	226.50	6.15	294.81	28.82	10.23	4.69	1.66	0.06	0.20	0.29	56.06	2833.70	0.02
T1413	213.00	5.99	300.49	17.70	16.98	2.96	2.83	0.05	0.14	0.36	48.82	2542.55	0.02
T1413	204.50	7.56	275.78	10.84	25.43	1.44	3.37	0.03	0.08	0.39	46.54	2713.14	0.02
T1413	196.90	4.67	414.27	24.28	17.06	5.20	3.66	0.04	0.11	0.37	46.34	2452.71	0.02
T1413	192.50	5.55	400.08	14.73	27.16	2.65	4.89	0.04	0.15	0.29	51.83	2369.38	0.02
T1413	187.10		342.67	42.10	8.14			0.05	0.20	0.25	57.93	2808.04	0.02
T1413	166.40	10.62	190.05	18.05	10.53	1.70	0.99	0.04	0.13	0.28	40.71	1881.34	0.02
T1413	163.20	8.83	175.76	21.18	8.30	2.40	0.94	0.05	0.13	0.41	34.98	1400.26	0.02
T1413	158.90	11.54	202.28	13.10	15.44	1.14	1.34	0.04	0.12	0.30	40.89	1774.91	0.02
T1413	154.70	5.21	290.99	50.30	5.79	9.65	1.11	0.07	0.28	0.24	80.89	3629.50	0.02
T1413	149.40	13.12	143.69	15.95	9.01	1.22	0.69	0.05	0.14	0.32	42.00	1936.18	0.02
T1413	140.00	7.07	146.09	10.50	13.91	1.48	1.97	0.06	0.19	0.32	60.66	2825.72	0.02
T1413	134.70	9.19	215.88	34.98	6.17	3.81	0.67	0.09	0.38	0.23	93.18	3925.06	0.02
T1413	129.70	11.19	253.12	26.48	9.56	2.37	0.85	0.10	0.40	0.25	101.69	4292.71	0.02
T1413	126.50	16.64	108.51	2.54	42.71	0.15	2.57	0.08	0.37	0.20	88.17	4350.01	0.02
T1413	112.30	2.21	80.16	4.89	16.39	2.21	7.40	0.08	0.21	0.41	50.86	2579.20	0.02
T1413	105.70	1.54	73.63	4.11	17.93	2.67	11.65	0.06	0.31	0.19	49.99	2957.31	0.02
T1413	101.00		140.23	0.77	181.56			0.07	0.00		90.570	5231.98	0.02
T1413	94.90	0.28	127.18	2.23	57.04	7.93	203.01	0.10	0.00		83.448	4429.88	0.02
T1413	90.60		333.28	31.06	10.73			0.06	0.19	0.32	60.88	3234.73	0.02
T1413	76.40	4.87	216.44	19.44	11.13	3.99	2.28	0.09	0.43	0.21	95.52	5321.54	0.02
T1413	67.20	9.83	364.71	33.69	10.82	3.43	1.10	0.09	0.19	0.50	64.86	2653.02	0.02
T1413	25.60	0.99	44.90	0.36	125.06	0.36	126.44	0.19	0.24	0.79	35.49	2582.46	0.01
T1413	16.30	0.34	78.63	0.31	257.28	0.90	757.14	0.10	0.41	0.25	67.74	5519.72	0.01

**Table 23. Trace metal data of the Arctic Bay Formation continued.**

Rock ID	Depth (m)	TOC (wt %)	V (ppm)	Mo (ppm)	V/Mo	Mo/TOC (ppm/ wt%)	V/Mo /TOC (per wt %)	Fe (molar)	Al (molar)	Fe/Al	Cr (ppm)	Ti (ppm)	Cr/Ti
PWC1405	636.50	4.68	274.24	26.03	10.54	5.56	2.25	0.07	0.37	0.20	88.08	4229.52	0.02
PWC1405	600.50	2.75	169.36	8.60	19.68	3.13	7.16	0.05	0.35	0.15	81.57	3700.80	0.02
PWC1405	479.80	0.38	111.43	0.51	217.18	1.36	575.21	0.11	0.37	0.31	78.63	5375.46	0.01
PWC1405	458.60	3.59	122.15	2.41	50.61	0.67	14.09	0.08	0.38	0.20	86.47	5161.05	0.02
PWC1405	388.00	0.41	103.37	0.89	116.63	2.17	285.33	0.12	0.43	0.27	83.63	6678.84	0.01
PWC1405	340.00	0.70	81.21	0.40	200.83	0.58	286.09	0.06	0.37	0.18	61.27	5293.05	0.01
PWC1405	257.50	0.75	94.89	0.41	230.51	0.55	307.94	0.15	0.25	0.60	60.48	5328.09	0.01
PWC1405	216.00	1.78	75.53	0.94	80.57	0.53	45.24	0.42	0.23	1.82	42.68	3425.84	0.01
PWC1405	110.50	0.82	107.92	1.86	58.04	2.27	70.83	0.11	0.39	0.29	70.74	5258.98	0.01
PWC1405	74.00	3.11	133.22	3.45	38.60	1.11	12.42	0.07	0.45	0.16	85.38	4854.27	0.02
PWC1405	45.10	0.41	79.52	1.37	58.04	3.36	142.41	0.08	0.36	0.21	54.34	4862.47	0.01
PWC1405	23.10	0.50	82.07	1.28	64.24	2.54	127.56	0.05	0.34	0.16	55.75	4964.64	0.01
MB1401	465.50	0.70	98.39	0.56	175.35	0.80	249.54	0.09	0.37	0.25	84.78	4697.50	0.02
MB1401	441.50	0.36	81.73	0.21	383.27	0.59	1062.42	0.09	0.35	0.26	76.72	3816.69	0.02
MB1401	167.20	0.79	118.20	1.24	95.46	1.56	120.49	0.12	0.30	0.38	95.38	5941.59	0.02
MB1401	160.00	0.58	101.51	0.92	109.86	1.60	190.81	0.12	0.32	0.39	88.27	4925.58	0.02
MB1401	150.00	0.67	113.89	0.45	253.46	0.67	378.48	0.09	0.36	0.26	92.32	5052.40	0.02
MB1401	140.00	0.44	91.75	0.23	407.68	0.52	935.24	0.08	0.34	0.25	94.02	5349.68	0.02
MB1401	132.00	1.17	120.57	1.14	105.57	0.98	90.58	0.12	0.31	0.39	98.94	5939.18	0.02
MB1401	120.20	3.13	155.16	9.63	16.11	3.08	5.15	0.09	0.37	0.24	95.24	4621.94	0.02
MB1401	113.70	1.99	117.44	3.58	32.82	1.79	16.46	0.11	0.28	0.38	71.48	3437.19	0.02
MB1401	107.60	1.67	143.48	2.26	63.52	1.35	38.04	0.08	0.33	0.24	98.68	4860.45	0.02
MB1401	102.80	7.16	286.43	27.14	10.55	3.79	1.47	0.10	0.23	0.45	58.68	2708.61	0.02
MB1401	96.70	3.16	198.71	8.34	23.81	2.64	7.53	0.08	0.36	0.22	78.27	3222.25	0.02
MB1401	91.00	1.27	148.69	2.38	62.35	1.88	49.02	0.08	0.41	0.19	99.99	5038.35	0.02
MB1401	85.00	1.01	111.38	1.42	78.48	1.40	77.37	0.12	0.38	0.33	76.57	4551.45	0.02
MB1401	79.00	11.12	526.45	47.58	11.07	4.28	1.00	0.08	0.14	0.54	61.83	2903.20	0.02
MB1401	75.00	2.42	182.62	9.28	19.68	3.84	8.14	0.08	0.38	0.20	87.44	4003.76	0.02
MB1401	69.40	8.43	514.55	44.09	11.67	5.23	1.38	0.11	0.17	0.69	62.99	3483.11	0.02
MB1401	66.00	3.34	213.21	11.53	18.50	3.46	5.55	0.09	0.39	0.24	81.23	3622.16	0.02
MB1401	61.90	11.44	500.01	43.44	11.51	3.80	1.01	0.07	0.20	0.34	54.81	2813.91	0.02
MB1401	56.40	16.61	727.07	65.55	11.09	3.95	0.67	0.05	0.19	0.28	57.01	3027.12	0.02
MB1401	49.00	12.84	877.62	84.05	10.44	6.55	0.81	0.05	0.16	0.33	61.79	3078.04	0.02
MB1401	44.20	5.37	234.97	18.41	12.76	3.43	2.38	0.07	0.12	0.58	42.66	2477.94	0.02
MB1401	40.50	3.91	368.36	24.00	15.35	6.14	3.92	0.06	0.32	0.20	77.26	3566.09	0.02
MB1401	36.60	11.14	656.36	43.69	15.02	3.92	1.35	0.06	0.29	0.20	71.60	2977.44	0.02
MB1401	31.00	2.74	157.64	4.22	37.35	1.54	13.61	0.05	0.32	0.15	81.64	3592.17	0.02
MB1401	25.80	8.15	429.29	8.60	49.90	1.06	6.12	0.03	0.16	0.21	48.83	2156.67	0.02
MB1401	21.40	13.70	687.42	34.44	19.96	2.51	1.46	0.06	0.22	0.26	78.77	3894.25	0.02
MB1401	16.00	10.18	294.62	27.17	10.84	2.67	1.07	0.06	0.27	0.24	78.37	3540.40	0.02
MB1401	10.00	6.44	83.95	2.98	28.14	0.46	4.37	0.05	0.33	0.14	90.24	4241.78	0.02
MB1401	6.40	1.99	82.37	0.17	483.44	0.09	242.33	0.06	0.37	0.15	81.06	4238.63	0.02

**Table 24. Trace metal data of the Hayfield Formation.**

Rock ID	Depth (m)	TOC (wt %)	P (ppm)	P/TOC (ppm/wt%)	V (ppm)	Mo (ppm)	V/Mo	Mo/TOC (ppm/wt%)	V/Mo /TOC (per wt %)	Fe (molar)	Al (molar)	Fe/Al	Cr (ppm)	Ti (ppm)	Cr/Ti
Balmain 1	604.00	0.03	327.31	10910.37	74.00	0.59	125.42	19.67	4180.79	0.06	0.32	0.19	66.00	4195.39	0.02
Balmain 1	609.27	0.01	545.52	54551.83	40.00	0.40	100.00	40.00	10000.00	0.08	0.23	0.33	47.00	3596.05	0.01
Balmain 1	618.51	0.01	218.21	21820.73	77.00	0.11	700.00	11.00	70000.00	0.06	0.36	0.17	68.00	4195.39	0.02
Balmain 1	623.25	0.01	218.21	21820.73	84.00	0.14	600.00	14.00	60000.00	0.07	0.38	0.18	71.30	4195.39	0.02
Balmain 1	632.81	0.05	218.21	4364.15	66.00	0.16	412.50	3.20	8250.00	0.05	0.33	0.16	61.50	4195.39	0.01
Balmain 1	637.36	0.05	109.10	2182.07	69.00	0.33	209.09	6.60	4181.82	0.07	0.36	0.19	66.60	4794.73	0.01
Balmain 1	641.95	0.02	109.10	5455.18	84.00	0.38	221.05	19.00	11052.63	0.07	0.39	0.17	70.10	4195.39	0.02
Balmain 1	646.61	0.06	109.10	1818.39	77.00	0.40	192.50	6.67	3208.33	0.06	0.36	0.16	64.80	4195.39	0.02
Balmain 1	651.27	0.04	109.10	2727.59	77.00	0.21	366.67	5.25	9166.67	0.06	0.34	0.19	60.10	4195.39	0.01
Balmain 1	656.05	0.05	109.10	2182.07	72.00	0.24	300.00	4.80	6000.00	0.06	0.36	0.17	66.00	4794.73	0.01
Balmain 1	664.94	0.04	109.10	2727.59	119.00	0.50	238.00	12.50	5950.00	0.08	0.41	0.19	99.60	4195.39	0.02
Balmain 1	670.68	0.01	109.10	10910.37	92.00	0.34	270.59	34.00	27058.82	0.11	0.34	0.32	81.10	3596.05	0.02
Balmain 1	675.59	0.01	109.10	10910.37	83.00	0.31	267.74	31.00	26774.19	0.12	0.38	0.32	64.00	3596.05	0.02
Balmain 1	679.08	0.15	109.10	727.36	66.00	0.44	150.00	2.93	1000.00	0.04	0.35	0.13	62.50	4794.73	0.01
Balmain 1	688.25	0.04			43.00	0.27	159.26	6.75	3981.48	0.03	0.28	0.10	38.60	3596.05	0.01
Balmain 1	692.72	0.00	218.21		58.00	0.24	241.67			0.09	0.40	0.22	57.20	4195.39	0.01
Balmain 1	698.50	0.37	109.10	294.87	67.00	1.21	55.37	3.27	149.65	0.24	0.33	0.74	51.80	4195.39	0.01
Balmain 1	706.53	0.37	109.10	294.87	72.00	0.34	211.76	0.92	572.34	0.07	0.40	0.18	71.70	4195.39	0.02
Balmain 1	720.31	0.06	109.10	1818.39	81.00	0.54	150.00	9.00	2500.00	0.05	0.39	0.13	67.70	4195.39	0.02
Balmain 1	724.86	0.02			43.00	0.48	89.58	24.00	4479.17	0.04	0.26	0.14	42.40	3596.05	0.01
Balmain 1	732.66	0.02	109.10	5455.18	73.00	0.52	140.38	26.00	7019.23	0.11	0.36	0.29	62.20	3596.05	0.02
Balmain 1	737.26	0.22	109.10	495.93	104.00	1.08	96.30	4.91	437.71	0.08	0.39	0.20	59.70	4794.73	0.01
Balmain 1	741.85	0.15	109.10	727.36	84.00	0.60	140.00	4.00	933.33	0.08	0.35	0.23	60.90	4794.73	0.01
Balmain 1	746.42	0.25	109.10	436.41	108.00	0.89	121.35	3.56	485.39	0.08	0.38	0.21	57.80	5394.07	0.01
Balmain 1	750.88	0.17	109.10	641.79	110.00	0.84	130.95	4.94	770.31	0.06	0.36	0.17	62.60	4794.73	0.01
Balmain 1	762.00	0.16	109.10	681.90	112.00	0.82	136.59	5.13	853.66	0.06	0.38	0.15	74.90	5394.07	0.01
Balmain 1	766.22	0.14	109.10	779.31	91.00	1.22	74.59	8.71	532.79	0.09	0.34	0.26	51.60	4195.39	0.01
Balmain 1	770.67	0.07	2072.97	29613.85	86.00	0.61	140.98	8.71	2014.05	0.20	0.30	0.66	63.50	2996.71	0.02
Balmain 1	775.50	0.02	109.10	5455.18	81.00	0.38	213.16	19.00	10657.89	0.08	0.37	0.22	57.00	4794.73	0.01
Balmain 1	779.70	0.01	109.10	10910.37	82.00	0.45	182.22	45.00	18222.22	0.05	0.40	0.13	52.70	4794.73	0.01
Balmain 1	793.38	0.06	109.10	1818.39	43.00	0.89	48.31	14.83	805.24	0.06	0.27	0.22	27.40	2397.37	0.01
Balmain 1	798.24	0.06			53.00	0.73	72.60	12.17	1210.05	0.05	0.28	0.18	30.60	2996.71	0.01
Balmain 1	802.79	0.08	109.10	1363.80	98.00	0.47	208.51	5.88	2606.38	0.05	0.39	0.14	60.30	5394.07	0.01
Balmain 1	807.32	0.07	109.10	1558.62	116.00	0.59	196.61	8.43	2808.72	0.06	0.41	0.14	57.30	5394.07	0.01
Balmain 1	812.80	0.02	109.10	5455.18	95.00	0.50	190.00	25.00	9500.00	0.06	0.36	0.16	50.40	4794.73	0.01
Balmain 1	816.60	0.04	109.10	2727.59	87.00	0.41	212.20	10.25	5304.88	0.09	0.38	0.25	57.00	4794.73	0.01
Balmain 1	820.91	0.02	109.10	5455.18	83.00	0.26	319.23	13.00	15961.54	0.04	0.35	0.13	48.90	4794.73	0.01
Balmain 1	825.05	0.02	109.10	5455.18	99.00	0.34	291.18	17.00	14558.82	0.07	0.39	0.18	59.00	4195.39	0.01
Balmain 1	834.02	0.02	109.10	5455.18	104.00	0.49	212.24	24.50	10612.24	0.07	0.39	0.19	55.90	4195.39	0.01
Balmain 1	834.06	0.04	109.10	2727.59	83.00	0.39	212.82	9.75	5320.51	0.06	0.37	0.17	50.10	4195.39	0.01
Balmain 1	838.63	0.05	109.10	2182.07	41.00	0.76	53.95	15.20	1078.95	0.03	0.31	0.10	27.80	2397.37	0.01
Balmain 1	843.20	0.15	109.10	727.36	116.00	1.31	88.55	8.73	590.33	0.05	0.44	0.12	63.60	5993.41	0.01
Balmain 1	847.81	0.08	109.10	1363.80	85.00	0.55	154.55	6.88	1931.82	0.06	0.40	0.14	54.30	4794.73	0.01
Balmain 1	852.45	0.48	218.21	454.60	98.00	1.50	65.33	3.13	136.11	0.06	0.41	0.15	54.10	5993.41	0.01

**Table 25. Trace metal data of the Jamison Formation.**

Rock ID	Depth (m)	TOC (wt %)	P (ppm)	P/TOC (ppm/wt%)	V (ppm)	Mo (ppm)	V/Mo	Mo/TOC (ppm/wt%)	V/Mo /TOC (per wt %)	Fe (molar)	Al (molar)	Fe/Al	Cr (ppm)	Ti (ppm)	Cr/Ti
Balmain 1	868.60	0.00	109.10		98.00	0.30	326.67			0.06	0.46	0.13	89.00	6591.79	0.01
Balmain 1	869.00	0.00	218.21		104.00	0.56	185.71			0.06	0.44	0.14	83.00	6591.79	0.01
Balmain 1	883.75	0.00	218.21		110.00	0.68	161.76			0.08	0.40	0.20	92.00	5393.28	0.02
Balmain 1	883.90	0.54	55.64	103.34	70.00	1.00	70.00	1.86	130.00	0.05	0.43	0.11	90.00	5692.91	0.02
Balmain 1	884.39	0.33	45.82	137.47	60.00	1.00	60.00	3.00	180.00	0.04	0.39	0.10	70.00	5333.36	0.01
Balmain 1	888.15	0.30	89.46	298.22	80.00	1.00	80.00	3.33	266.67	0.07	0.43	0.16	90.00	6232.24	0.01
Balmain 1	889.05	0.33	90.56	271.67	80.00	2.00	40.00	6.00	120.00	0.05	0.46	0.10	90.00	7790.30	0.01
Balmain 1	901.79	0.88	102.56	116.98	80.00	1.00	80.00	1.14	91.25	0.06	0.38	0.16	70.00	5213.51	0.01
Balmain 1	902.15	1.19	74.19	62.34	60.00	<0.5				0.05	0.36	0.13	50.00	5153.58	0.01
Balmain 1	902.10	0.25	109.10	436.41	130.00	1.85	70.27	7.40	281.08	0.02	0.42	0.04	69.00	5992.54	0.01
Balmain 1	911.00	1.64			109.00	1.69	64.50	1.03	39.33	0.02	0.36	0.06	57.00	5992.54	0.01
Balmain 1	911.10	0.39	313.13	805.18	130.00	2.50	52.00	6.43	133.71	0.06	0.46	0.14	90.00	7011.27	0.01
Balmain 1	918.45	0.33	31.64	94.92	50.00	1.00	50.00	3.00	150.00	0.07	0.36	0.19	70.00	4254.70	0.02
Balmain 1	919.60	0.31	52.37	167.58	120.00	2.00	60.00	6.40	192.00	0.11	0.45	0.25	160.00	7910.15	0.02

**Table 26. Trace metal data of the Kyalla Formation.**

Rock ID	Depth (m)	TOC (wt %)	P (ppm)	P/TOC (ppm/wt%)	V (ppm)	Mo (ppm)	V/Mo	Mo/TOC (ppm/wt%)	V/Mo /TOC (per wt %)	Fe (molar)	Al (molar)	Fe/Al	Cr (ppm)	Ti (ppm)	Cr/Ti
Balmain 1	939.95	1.04	109.10	104.91	122.00	1.94	62.89	1.87	60.47	0.02	0.41	0.05	66.00	5992.54	0.01
Balmain 1	944.60	0.01	109.10	10910.37	83.00	0.86	96.51	86.00	9651.16	0.04	0.44	0.08	53.00	5393.28	0.01
Balmain 1	949.21	0.01	109.10	10910.37	77.00	0.37	208.11	37.00	20810.81	0.03	0.39	0.07	34.00	4794.03	0.01
Balmain 1	953.64	0.02	109.10	5455.18	135.00	0.39	346.15	19.50	17307.69	0.03	0.42	0.08	65.00	5992.54	0.01
Balmain 1	958.20	0.23	109.10	474.36	133.00	1.12	118.75	4.87	516.30	0.03	0.43	0.06	70.00	5992.54	0.01
Balmain 1	962.53	0.31	109.10	351.95	106.00	1.40	75.71	4.52	244.24	0.03	0.34	0.09	54.00	5393.28	0.01
Balmain 1	967.08	0.50	109.10	218.21	115.00	0.84	136.90	1.68	273.81	0.02	0.38	0.04	58.00	5393.28	0.01
Balmain 1	971.55	0.83	109.10	131.45	126.00	1.59	79.25	1.92	95.48	0.03	0.39	0.07	63.00	5393.28	0.01
Balmain 1	976.11	2.66			132.00	1.72	76.74	0.65	28.85	0.06	0.37	0.15	58.00	5992.54	0.01
Balmain 1	985.37	2.68			122.00	1.61	75.78	0.60	28.27	0.04	0.35	0.10	69.00	5992.54	0.01
Balmain 1	990.01	3.02			91.00	1.71	53.22	0.57	17.62	0.03	0.30	0.10	51.00	5992.54	0.01
Balmain 1	994.52	1.49	109.10	73.22	105.00	1.09	96.33	0.73	64.65	0.02	0.40	0.06	62.00	5992.54	0.01
Balmain 1	998.91	0.24	109.10	454.60	126.00	1.14	110.53	4.75	460.53	0.02	0.42	0.06	69.00	5992.54	0.01
Balmain 1	1003.51	0.19			65.00	0.86	75.58	4.53	397.80	0.03	0.27	0.12	44.00	4194.78	0.01
Balmain 1	1007.49	1.24			122.00	1.50	81.33	1.21	65.59	0.03	0.38	0.07	54.00	5393.28	0.01
Balmain 1	1011.96	1.83	109.10	59.62	122.00	1.67	73.05	0.91	39.92	0.04	0.39	0.09	73.00	6591.79	0.01
Balmain 1	1013.37	0.11	27.28	256.39	100.00	1.50	66.67	14.10	626.67	0.04	0.40	0.11	70.00	6052.46	0.01
Balmain 1	1016.38	0.44			109.00	1.44	75.69	3.27	172.03	0.02	0.39	0.06	66.00	5992.54	0.01
Balmain 1	1018.90	0.11	29.46	274.19	100.00	1.50	66.67	13.96	620.51	0.02	0.41	0.06	110.00	6531.87	0.02
Balmain 1	1024.35	0.22	29.46	135.51	90.00	3.50	25.71	16.10	118.29	0.04	0.42	0.08	70.00	6172.31	0.01
Balmain 1	1026.95	0.23	40.37	177.62	120.00	5.00	24.00	22.00	105.60	0.03	0.46	0.06	50.00	6831.49	0.01
Balmain 1	1030.53	0.44	52.37	117.83	120.00	2.00	60.00	4.50	135.00	0.02	0.43	0.05	50.00	6651.72	0.01
Balmain 1	1036.30	0.19	38.19	206.21	110.00	3.00	36.67	16.20	198.00	0.03	0.43	0.08	70.00	7011.27	0.01
Balmain 1	1040.10	0.13	34.91	267.67	80.00	1.50	53.33	11.50	408.89	0.02	0.42	0.05	70.00	6711.64	0.01
Balmain 1	1043.80	0.17	37.10	222.57	100.00	1.50	66.67	9.00	400.00	0.02	0.44	0.05	90.00	7071.19	0.01
Balmain 1	1050.00	0.17	109.10	641.79	141.00	1.69	83.43	9.94	490.78	0.03	0.42	0.07	70.00	6591.79	0.01
Balmain 1	1050.71	0.17	34.91	209.48	100.00	1.50	66.67	9.00	400.00	0.03	0.42	0.06	90.00	6651.72	0.01

**Table 27. Trace metal data of the Velkerri Formation.**

Rock ID	Depth (m)	TOC (wt %)	P (ppm)	P/TOC (ppm/wt%)	V (ppm)	Mo (ppm)	V/Mo	Mo/TOC (ppm/wt%)	V/Mo /TOC (per wt %)	Fe (molar)	Al (molar)	Fe/Al	Cr (ppm)	Ti (ppm)	Cr/Ti
Altree 2	394.10	0.33	76.37	231.43	90.10	0.71	126.90	2.15	384.55	0.03	0.36	0.08	113.00	4794.03	0.02
Altree 2	396.48	0.38	65.46	172.27	96.00	0.80	120.00	2.11	315.79	0.04	0.38	0.10	80.00	4794.03	0.02
Altree 2	401.20	0.36	65.46	181.84	99.60	1.13	88.14	3.14	244.84	0.04	0.39	0.11	77.00	4794.03	0.02
Altree 2	405.90	0.30	54.55	181.84	79.90	1.62	49.32	5.40	164.40	0.05	0.32	0.16	69.00	4794.03	0.01
Altree 2	410.55	0.68	87.28	128.36	117.00	0.44	265.91	0.65	391.04	0.36	0.22	1.61	67.00	2996.27	0.02
Altree 2	415.15	0.40	65.46	163.66	97.10	0.71	136.76	1.78	341.90	0.09	0.38	0.23	82.00	5393.28	0.02
Altree 2	419.86	0.45	65.46	145.47	105.00	1.43	73.43	3.18	163.17	0.06	0.42	0.15	86.00	5393.28	0.02
Altree 2	424.61	0.34	65.46	192.54	98.50	0.70	140.71	2.06	413.87	0.11	0.37	0.31	80.00	4794.03	0.02
Altree 2	429.27	0.43	65.46	152.24	103.00	1.02	100.98	2.37	234.84	0.06	0.40	0.14	90.00	5393.28	0.02
Altree 2	433.88	0.45	54.55	121.23	95.50	0.87	109.77	1.93	243.93	0.09	0.36	0.24	77.00	4794.03	0.02
Altree 2	438.53	0.48	65.46	136.38	113.00	0.80	141.25	1.67	294.27	0.15	0.37	0.39	87.00	4794.03	0.02
Altree 2	443.27	0.48	65.46	136.38	111.00	0.55	201.82	1.15	420.45	0.07	0.40	0.18	86.00	5393.28	0.02
Altree 2	447.95	0.41	54.55	133.05	97.30	0.85	114.47	2.07	279.20	0.07	0.38	0.20	82.00	5393.28	0.02
Altree 2	452.64	0.68	87.28	128.36	124.00	1.12	110.71	1.65	162.82	0.09	0.43	0.21	106.00	5992.54	0.02
Altree 2	457.06	0.38	65.46	172.27	91.00	0.84	108.33	2.21	285.09	0.07	0.37	0.19	85.00	5393.28	0.02
Altree 2	469.00	0.70	65.46	93.52	124.00	0.97	127.84	1.39	182.62	0.09	0.38	0.23	87.00	5992.54	0.01
Altree 2	471.24	1.13	54.55	48.28	61.70	0.37	166.76	0.33	147.57	0.07	0.26	0.25	46.00	4194.78	0.01
Altree 2	475.91	0.85	54.55	64.18	81.10	0.67	121.04	0.79	142.41	0.07	0.31	0.22	62.00	4794.03	0.01
Altree 2	480.65	0.39	76.37	195.83	91.90	0.91	100.99	2.33	258.95	0.42	0.18	2.35	51.00	1797.76	0.03
Altree 2	485.45	0.48	54.55	113.65	101.00	1.50	67.33	3.13	140.28	0.08	0.35	0.22	66.00	4794.03	0.01
Altree 2	490.14	0.46	54.55	118.59	123.00	0.92	133.70	2.00	290.64	0.08	0.36	0.23	80.00	4794.03	0.02
Altree 2	494.77	0.58	65.46	112.87	90.10	0.82	109.88	1.41	189.44	0.06	0.36	0.17	77.00	4794.03	0.02
Altree 2	499.49	0.49	76.37	155.86	127.00	1.31	96.95	2.67	197.85	0.07	0.44	0.16	96.00	5992.54	0.02
Altree 2	504.35	0.40	76.37	190.93	123.00	1.13	108.85	2.83	272.12	0.05	0.43	0.12	94.00	5992.54	0.02
Altree 2	509.16	0.56	87.28	155.86	122.00	1.08	112.96	1.93	201.72	0.08	0.41	0.19	92.00	5393.28	0.02
Altree 2	518.05	0.46	65.46	142.31	116.00	1.14	101.75	2.48	221.21	0.07	0.40	0.18	84.00	5393.28	0.02
Altree 2	522.75	0.56	65.46	116.90	114.00	0.72	158.33	1.29	282.74	0.06	0.41	0.15	92.00	5992.54	0.02
Altree 2	527.37	0.61	65.46	107.32	110.00	0.83	132.53	1.36	217.26	0.07	0.39	0.19	93.00	5393.28	0.02
Altree 2	532.01	0.52	76.37	146.87	121.00	0.89	135.96	1.71	261.45	0.09	0.42	0.20	99.00	5992.54	0.02
Altree 2	536.75	0.64	65.46	102.28	112.00	0.79	141.77	1.23	221.52	0.07	0.39	0.18	94.00	5393.28	0.02
Altree 2	541.46	0.64	54.55	85.24	117.00	1.16	100.86	1.81	157.60	0.07	0.40	0.18	88.00	5393.28	0.02
Altree 2	545.98	0.76	76.37	100.49	131.00	2.38	55.04	3.13	72.42	0.10	0.40	0.24	92.00	5393.28	0.02
Altree 2	550.72	0.53	76.37	144.10	121.00	1.02	118.63	1.92	223.83	0.09	0.40	0.22	98.00	5992.54	0.02
Altree 2	555.24	0.62	76.37	123.18	105.00	0.67	156.72	1.08	252.77	0.13	0.37	0.34	90.00	5393.28	0.02
Altree 2	559.99	0.58	65.46	112.87	117.00	1.21	96.69	2.09	166.71	0.09	0.40	0.23	92.00	5711.05	0.02
Altree 2	564.75	0.86	98.19	114.18	153.00	2.29	66.81	2.66	77.69	0.07	0.40	0.18	89.00	5393.28	0.02
Altree 2	569.51	0.58	65.46	112.87	103.00	0.93	110.75	1.60	190.95	0.09	0.37	0.23	83.00	5393.28	0.02
Altree 2	574.40	0.73	76.37	104.62	118.00	0.97	121.65	1.33	166.64	0.11	0.40	0.27	100.00	6591.79	0.02
Altree 2	579.02	0.64	76.37	119.33	121.00	1.25	96.80	1.95	151.25	0.14	0.38	0.36	94.00	5393.28	0.02
Altree 2	583.49	0.56	76.37	136.38	122.00	0.76	160.53	1.36	286.65	0.10	0.40	0.24	97.00	5992.54	0.02
Altree 2	588.25	0.75	76.37	101.83	127.00	1.08	117.59	1.44	156.79	0.06	0.40	0.16	101.00	6591.79	0.02
Altree 2	593.09	0.59	76.37	129.45	121.00	1.40	86.43	2.37	146.49	0.17	0.36	0.49	84.00	5393.28	0.02
Altree 2	597.91	0.59	65.46	110.95	125.00	1.44	86.81	2.44	147.13	0.06	0.40	0.15	76.00	4794.03	0.02
Altree 2	602.77	0.54	76.37	141.43	116.00	1.00	116.00	1.85	214.81	0.13	0.38	0.34	89.00	5393.28	0.02
Altree 2	607.60	0.77	76.37	99.19	129.00	2.03	63.55	2.64	82.53	0.10	0.38	0.27	83.00	5393.28	0.02
Altree 2	612.34	0.55	87.28	158.70	103.00	1.81	56.91	3.29	103.47	0.19	0.34	0.55	82.00	4794.03	0.02
Altree 2	617.12	0.67	65.46	97.70	131.00	2.18	60.09	3.25	89.69	0.10	0.38	0.25	95.00	5393.28	0.02
Altree 2	621.84	3.54	458.24	129.45	362.00	17.10	21.17	4.83	5.98	0.06	0.27	0.24	31.00	3595.52	0.01
Altree 2	626.56	2.11	469.15	222.34	157.00	4.81	32.64	2.28	15.47	0.05	0.27	0.19	50.00	3595.52	0.01
Altree 2	631.30	1.24	163.66	131.98	179.00	4.40	40.68	3.55	32.81	0.07	0.36	0.19	72.00	5393.28	0.01
Altree 2	636.12	1.56	152.75	97.91	138.00	4.36	31.65	2.79	20.29	0.08	0.32	0.26	79.00	4794.03	0.02
Altree 2	640.98	2.57	381.86	148.58	273.00	10.37	26.33	4.04	10.24	0.07	0.32	0.21	54.00	4194.78	0.01
Altree 2	645.75	2.52	305.49	121.23	246.00	9.68	25.41	3.84	10.08	0.06	0.26	0.24	46.00	3595.52	0.01
Altree 2	650.50	3.07	490.97	159.92	222.00	6.91	32.13	2.25	10.46	0.05	0.25	0.19	47.00	3595.52	0.01
Altree 2	655.27	2.34	469.15	200.49	180.00	7.24	24.86	3.09	10.62	0.07	0.25	0.26	51.00	3595.52	0.01
Altree 2	661.98	4.44	600.07	135.15	409.00	12.34	33.14	2.78	7.46	0.04	0.24	0.18	30.00	2996.27	0.01
Altree 2	664.69	2.64	480.06	181.84	361.00	14.44	25.00	5.47	9.47	0.08	0.18	0.48	18.00	2397.02	0.01
Altree 2	669.51	4.13	676.44	163.79	574.00	42.48	13.51	10.29	3.27	0.08	0.18	0.42	<10	2397.02	

**Table 28. Trace metal data of the Velkerri Formation continued.**

Rock ID	Depth (m)	TOC (wt %)	P (ppm)	P/TOC (ppm/ wt%)	V (ppm)	Mo (ppm)	V/Mo	Mo/TOC (ppm/ wt%)	V/Mo /TOC (per wt %)	Fe (molar)	Al (molar)	Fe/Al	Cr (ppm)	Ti (ppm)	Cr/Ti
Altree 2	674.32	5.24	600.07	114.52	740.00	49.36	14.99	9.42	2.86	0.05	0.23	0.21	<10	2996.27	
Altree 2	679.11	3.47	720.08	207.52	338.00	19.81	17.06	5.71	4.92	0.04	0.21	0.20	34.00	2996.27	0.01
Altree 2	688.61	7.43	621.89	83.70	671.00	102.00	6.58	13.73	0.89	0.07	0.21	0.35	<10	2996.27	
Altree 2	697.90	6.05	621.89	102.79	574.00	101.00	5.68	16.69	0.94	0.07	0.19	0.40	<10	2397.02	
Altree 2	707.31	6.85	458.24	66.90	631.00	94.43	6.68	13.79	0.98	0.07	0.22	0.33	<10	2996.27	
Altree 2	722.05	6.18	523.70	84.74	475.00	79.11	6.00	12.80	0.97	0.07	0.25	0.30	16.00	2996.27	0.01
Altree 2	731.54	1.83	141.83	77.51	221.00	12.29	17.98	6.72	9.83	0.05	0.36	0.13	61.00	4794.03	0.01
Altree 2	736.33	8.07	796.46	98.69	307.00	66.96	4.58	8.30	0.57	0.11	0.27	0.39	45.00	3595.52	0.01
Altree 2	746.02	5.07	545.52	107.60	435.00	53.52	8.13	10.56	1.60	0.08	0.29	0.26	26.00	3595.52	0.01
Altree 2	750.28	0.84	109.10	129.89	117.00	4.32	27.08	5.14	32.24	0.12	0.31	0.37	71.00	4194.78	0.02
Altree 2	754.96	0.48	65.46	136.38	97.30	1.30	74.85	2.71	155.93	0.06	0.35	0.17	71.00	4794.03	0.01
Altree 2	760.33	5.20	490.97	94.42	410.00	70.23	5.84	13.51	1.12	0.08	0.31	0.25	32.00	3595.52	0.01
Altree 2	765.29	4.93	436.41	88.52	405.00	63.65	6.36	12.91	1.29	0.08	0.31	0.25	31.00	4194.78	0.01
Altree 2	769.64	5.67	578.25	101.98	473.00	91.85	5.15	16.20	0.91	0.09	0.29	0.30	15.00	3595.52	0.00
Altree 2	783.81	5.93	905.56	152.71	429.00	68.88	6.23	11.62	1.05	0.06	0.30	0.21	28.00	3595.52	0.01
Altree 2	793.37	7.63	1069.22	140.13	349.00	91.39	3.82	11.98	0.50	0.07	0.25	0.28	2020.00	2996.27	0.67
Altree 2	802.74	6.24	938.29	150.37	418.00	70.46	5.93	11.29	0.95	0.04	0.19	0.21	<10	2397.02	
Altree 2	812.11	5.95	851.01	143.03	364.00	39.13	9.30	6.58	1.56	0.03	0.21	0.15	<10	2397.02	
Altree 2	821.78	5.72	1003.75	175.48	244.00	14.99	16.28	2.62	2.85	0.03	0.21	0.14	16.00	2397.02	0.01
Altree 2	831.21	3.81	840.10	220.50	212.00	32.89	6.45	8.63	1.69	0.04	0.19	0.19	13.00	1797.76	0.01
Altree 2	845.48	3.54	960.11	271.22	137.00	8.92	15.36	2.52	4.34	0.03	0.16	0.21	26.00	1797.76	0.01
Altree 2	854.93	4.16	971.02	233.42	285.00	13.03	21.87	3.13	5.26	0.04	0.18	0.22	12.00	2397.02	0.01
Altree 2	864.50	4.25	1254.69	295.22	306.00	23.73	12.90	5.58	3.03	0.04	0.21	0.18	26.00	2397.02	0.01
Altree 2	873.77	1.95	971.02	497.96	245.00	4.94	49.60	2.53	25.43	0.04	0.25	0.18	18.00	2996.27	0.01
Altree 2	883.63	3.21	872.83	271.91	250.00	18.38	13.60	5.73	4.24	0.05	0.24	0.20	20.00	2996.27	0.01
Altree 2	898.25	1.74	949.20	545.52	201.00	5.75	34.96	3.30	20.09	0.07	0.15	0.43	18.00	2397.02	0.01
Altree 2	912.37	2.41	1014.66	421.02	108.00	2.06	52.43	0.85	21.75	0.07	0.16	0.42	24.00	1797.76	0.01
Altree 2	922.05	5.54	687.35	124.07	387.00	22.01	17.58	3.97	3.17	0.08	0.22	0.35	19.00	2996.27	0.01
Altree 2	926.59	4.02	687.35	170.98	385.00	23.56	16.34	5.86	4.06	0.08	0.22	0.38	20.00	2996.27	0.01
Altree 2	931.53	5.86	1265.60	215.97	432.00	61.55	7.02	10.50	1.20	0.07	0.20	0.36	13.00	2996.27	0.00
Altree 2	940.69	4.40	709.17	161.18	265.00	5.95	44.54	1.35	10.12	0.07	0.22	0.33	29.00	2996.27	0.01
Altree 2	950.64	0.12	54.55	454.60	60.40	0.40	151.00	3.33	1258.33	0.05	0.29	0.16	27.00	2996.27	0.01
Altree 2	957.65	0.07	141.83	2026.21	67.70	0.20	338.50	2.86	4835.71	0.08	0.30	0.27	22.00	4194.78	0.01
Altree 2	983.38	0.07	32.73	467.59	53.80	0.87	61.84	12.43	883.42	0.05	0.31	0.16	23.00	4194.78	0.01
Altree 2	1002.46	0.10	32.73	327.31	74.10	0.71	104.37	7.10	1043.66	0.06	0.34	0.16	18.00	4794.03	0.00
Altree 2	1019.75	0.07	43.64	623.45	61.30	1.02	60.10	14.57	858.54	0.06	0.39	0.16	22.00	4794.03	0.00
Altree 2	1040.86	0.05	294.58	5891.60	50.00	0.33	151.52	6.60	3030.30	0.07	0.25	0.29	24.00	2996.27	0.01
Altree 2	1055.15	3.80	43.64	11.48	75.30	5.38	14.00	1.42	3.68	0.06	0.31	0.21	53.00	2996.27	0.02
Altree 2	1088.21	0.15	76.37	509.15	116.00	7.06	16.43	47.07	109.54	0.07	0.42	0.16	93.00	6591.79	0.01
Altree 2	1117.48	0.31	65.46	211.17	125.00	0.86	145.35	2.77	468.87	0.07	0.46	0.16	85.00	6591.79	0.01
Altree 2	1122.40	0.09	43.64	484.91	86.70	0.48	180.63	5.33	2006.94	0.07	0.38	0.19	25.00	5393.28	0.00
Altree 2	1127.10	3.12	43.64	13.99	70.20	2.09	33.59	0.67	10.77	0.06	0.31	0.18	55.00	3915.36	0.01
Altree 2	1131.74	3.35	43.64	13.03	90.90	5.95	15.28	1.78	4.56	0.08	0.35	0.23	65.00	4194.78	0.02
Altree 2	1141.42	0.11	76.37	694.30	115.00	0.43	267.44	3.91	2431.29	0.06	0.43	0.14	90.00	6591.79	0.01
Altree 2	1150.63	0.04	76.37	1909.31	66.10	0.48	137.71	12.00	3442.71	0.09	0.37	0.24	31.00	4794.03	0.01
Altree 2	1155.43	0.18	65.46	363.68	124.00	0.58	213.79	3.22	1187.74	0.09	0.45	0.19	84.00	5992.54	0.01
Altree 2	1164.90	0.05	32.73	654.62	84.70	0.28	302.50	5.60	6050.00	0.08	0.37	0.21	64.00	4194.78	0.02
Altree 2	1174.62	0.12	54.55	454.60	101.00	0.20	505.00	1.67	4208.33	0.10	0.39	0.26	78.00	5393.28	0.01
Altree 2	1193.68	0.12	54.55	454.60	109.00	0.59	184.75	4.92	1539.55	0.09	0.42	0.20	68.00	5393.28	0.01
Altree 2	1203.28	3.53	109.10	30.91	173.00	12.70	13.62	3.60	3.86	0.06	0.34	0.17	59.00	4194.78	0.01
Altree 2	1208.10	0.13	65.46	503.56	59.30	0.52	114.04	4.00	877.22	0.08	0.30	0.26	55.00	3595.52	0.02
Altree 2	1220.65	0.16	43.64	272.76	69.10	0.37	186.76	2.31	1167.23	0.09	0.34	0.27	52.00	3595.52	0.01

**Table 29. Trace metal data of the Lower Roper Group: Jalboi, Crawford and Mainoru formations.**

Rock ID	Depth (m)	TOC (wt %)	P (ppm)	P/TOC (ppm/ wt%)	V (ppm)	Mo (ppm)	V/Mo	Mo/TOC (ppm/ wt%)	V/Mo /TOC (per wt %)	Fe (molar)	Al (molar)	Fe/Al	Cr (ppm)	Ti (ppm)	Cr/Ti
Urapunga 5	118.5	0.20	250.00	1250.00	80.00	<0.5				0.09	0.35	0.26	50.00	4194.78	0.01
Urapunga 5	119.3	0.25	220.00	880.00	80.00	<0.5				0.09	0.32	0.29	50.00	3955.07	0.01
Urapunga 5	120.2	0.39	230.00	589.74	100.00	<0.5				0.10	0.35	0.30	50.00	4194.78	0.01
Urapunga 5	120.55	0.25	230.00	920.00	80.00	<0.5				0.06	0.37	0.17	50.00	4374.55	0.01
Urapunga 5	123.55	0.29	280.00	965.52	110.00	<0.5				0.09	0.41	0.22	70.00	5153.58	0.01
Urapunga 5	130.6	0.24	80.00	333.33	90.00	<0.5				0.05	0.42	0.11	70.00	5513.13	0.01
Urapunga 5	139.9	0.31	660.00	2129.03	80.00	<0.5				0.03	0.39	0.07	50.00	4853.96	0.01
Urapunga 5	139.95	0.42	80.00	190.48	110.00	<0.5				0.04	0.43	0.09	70.00	5692.91	0.01
Urapunga 5	149.1	0.38	150.00	394.74	80.00	1.00	80.00	2.63	210.53	0.04	0.41	0.09	70.00	5273.43	0.01
Urapunga 5	149.5	0.33	120.00	363.64	120.00	<0.5				0.04	0.44	0.08	70.00	5213.51	0.01
Urapunga 5	150.5	0.24	460.00	1916.67	80.00	<0.5				0.04	0.37	0.10	50.00	4374.55	0.01
Urapunga 5	157.95	0.05	60.00	1200.00	80.00	<0.5				0.11	0.46	0.24	80.00	5453.21	0.01
Urapunga 5	160.5	0.08	150.00	1875.00	130.00	<0.5				0.13	0.54	0.24	100.00	6951.34	0.01
Urapunga 5	169.8	0.04	190.00	4750.00	100.00	<0.5				0.11	0.42	0.26	70.00	4434.48	0.02
Urapunga 5	229.6		160.00		90.00	<0.5				0.11	0.39	0.28	70.00	5333.36	0.01
Urapunga 5	326.2	0.51	220.00	431.37	110.00	<0.5				0.08	0.40	0.20	70.00	5093.66	0.01
Urapunga 5	334.5	0.69	270.00	391.30	160.00	1.00	160.00	1.45	231.88	0.09	0.52	0.17	100.00	7610.52	0.01
Urapunga 5	341.3	0.63	220.00	349.21	150.00	1.00	150.00	1.59	238.10	0.09	0.51	0.18	100.00	7250.97	0.01
Urapunga 5	347.8	0.51	190.00	372.55	90.00	<0.5				0.08	0.42	0.19	100.00	6471.94	0.02
Urapunga 5	348	0.51	180.00	352.94	120.00	<0.5				0.08	0.43	0.19	80.00	6232.24	0.01
Urapunga 5	354.7	0.45	230.00	511.11	110.00	<0.5				0.07	0.40	0.17	70.00	5872.69	0.01
Urapunga 5	356.9	0.51	190.00	372.55	140.00	<0.5				0.08	0.43	0.19	100.00	6651.72	0.02
Urapunga 5	361.9	0.54	280.00	518.52	140.00	1.00	140.00	1.85	259.26	0.09	0.39	0.24	100.00	8329.63	0.01
Urapunga 5	369.5	0.42	410.00	976.19	140.00	1.00	140.00	2.38	333.33	0.09	0.50	0.18	100.00	6831.49	0.01
Urapunga 5	375.2	0.51	380.00	745.10	130.00	1.00	130.00	1.96	254.90	0.09	0.42	0.20	80.00	5632.99	0.01
Urapunga 5	380.1	0.57	360.00	631.58	140.00	1.50	93.33	2.63	163.74	0.09	0.53	0.16	130.00	8209.78	0.02
Urapunga 5	381.3	0.71	450.00	633.80	190.00	1.50	126.67	2.11	178.40	0.08	0.53	0.15	110.00	8089.93	0.01
Urapunga 5	382.4	0.77	420.00	545.45	190.00	1.50	126.67	1.95	164.50	0.08	0.53	0.14	120.00	8269.70	0.01
Urapunga 5	387.3	0.50	420.00	840.00	160.00	1.50	106.67	3.00	213.33	0.08	0.44	0.17	70.00	6471.94	0.01
Urapunga 5	391.7	0.38	250.00	657.89	100.00	<0.5				0.09	0.37	0.24	50.00	4194.78	0.01
Urapunga 5	392.5	0.31	250.00	806.45	110.00	<0.5				0.07	0.34	0.20	70.00	4194.78	0.02
Urapunga 5	393.1	0.26	250.00	961.54	90.00	<0.5				0.08	0.31	0.26	50.00	4074.93	0.01
Urapunga 5	393.6	0.31	260.00	838.71	110.00	<0.5				0.08	0.35	0.21	70.00	4374.55	0.02
Urapunga 5	396.8	0.31	240.00	774.19	80.00	<0.5				0.09	0.35	0.25	70.00	4194.78	0.02
Urapunga 5	399.3	0.37	240.00	648.65	110.00	1.50	73.33	4.05	198.20	0.10	0.37	0.26	80.00	4973.81	0.02
Urapunga 5	399.9	0.27	220.00	814.81	90.00	<0.5				0.08	0.37	0.22	70.00	4314.63	0.02
Urapunga 5	401.5	0.21	250.00	1190.48	100.00	<0.5				0.07	0.37	0.20	70.00	4134.85	0.02
Urapunga 5	403	0.28	280.00	1000.00	100.00	<0.5				0.07	0.38	0.19	50.00	4254.70	0.01
Urapunga 5	403.5	0.24	240.00	1000.00	90.00	<0.5				0.09	0.39	0.23	50.00	4494.40	0.01
Urapunga 5	405.7	0.44	350.00	795.45	90.00	1.00	90.00	2.27	204.55	0.09	0.35	0.25	70.00	5153.58	0.01
Urapunga 5	412.45	0.37	340.00	918.92	110.00	<0.5				0.08	0.37	0.22	70.00	5213.51	0.01
Urapunga 5	416.05	0.22	290.00	1318.18	110.00	<0.5				0.08	0.36	0.23	50.00	4254.70	0.01
Urapunga 5	421.51	0.16	250.00	1562.50	100.00	<0.5				0.10	0.36	0.29	50.00	4134.85	0.01
Urapunga 5	428	0.05	280.00	5600.00	90.00	<0.5				0.13	0.34	0.37	50.00	4314.63	0.01
Urapunga 5	431.1	0.18	300.00	1666.67	100.00	<0.5				0.07	0.32	0.22	50.00	4254.70	0.01
Urapunga 5	435.7	0.21	290.00	1380.95	100.00	<0.5				0.07	0.34	0.19	50.00	3895.15	0.01
Urapunga 5	439.65	0.13	260.00	2000.00	110.00	<0.5				0.07	0.32	0.21	70.00	3835.22	0.02
Urapunga 5	442.75	0.32	300.00	937.50	100.00	<0.5				0.08	0.33	0.25	30.00	4554.33	0.01
Urapunga 5	448.5	0.29	300.00	1034.48	100.00	<0.5				0.08	0.32	0.24	50.00	4194.78	0.01
Urapunga 5	449.5	0.42	300.00	714.29	90.00	1.00	90.00	2.38	214.29	0.08	0.34	0.22	50.00	4374.55	0.01
Urapunga 5	453.5	0.40	340.00	850.00	90.00	1.00	90.00	2.50	225.00	0.10	0.30	0.33	50.00	3955.07	0.01
Urapunga 5	459.5	0.42	330.00	785.71	110.00	1.00	110.00	2.38	261.90	0.09	0.36	0.24	70.00	4554.33	0.02
Urapunga 5	464.5	0.29	380.00	1310.34	100.00	<0.5				0.10	0.33	0.32	50.00	3895.15	0.01
Urapunga 5	479.1	0.32	270.00	843.75	70.00	<0.5				0.10	0.34	0.28	50.00	4015.00	0.01
Urapunga 5	486.15	0.20	280.00	1400.00	110.00	<0.5				0.09	0.35	0.27	50.00	3955.07	0.01
Urapunga 5	487.5	0.11	320.00	2909.09	100.00	<0.5				0.10	0.32	0.31	50.00	3535.60	0.01
Urapunga 5	498.6	0.16	420.00	2625.00	100.00	<0.5				0.14	0.29	0.48	50.00	3355.82	0.01
Urapunga 5	505.1	0.34	290.00	852.94	90.00	<0.5				0.12	0.28	0.44	50.00	3116.12	0.02
Urapunga 5	507	0.41	430.00	1048.78	60.00	1.00	60.00	2.44	146.34	0.14	0.25	0.55	80.00	2756.57	0.03
Urapunga 5	516.1	0.24	320.00	1333.33	100.00	1.00	100.00	4.17	416.67	0.06	0.32	0.19	50.00	4015.00	0.01
Urapunga 5	535	0.34	320.00	941.18	100.00	<0.5				0.09	0.33	0.26	70.00	4314.63	0.02
Urapunga 5	535.6	0.31	320.00	1032.26	90.00	<0.5				0.09	0.34	0.25	70.00	4074.93	0.02
Urapunga 5	540.6	0.33	350.00	1060.61	90.00	<0.5				0.06	0.36	0.18	50.00	4074.93	0.01
Urapunga 5	541.2	0.29	320.00	1103.45	90.00	<0.5				0.08	0.35	0.22	70.00	4015.00	0.02
Urapunga 5	544.8	0.75	390.00	520.00	130.00	0.50	260.00	0.67	346.67	0.06	0.37	0.17	80.00	4374.55	0.02
Urapunga 5	547.8	0.89	400.00	449.44	140.00	<0.5				0.08	0.42	0.18	80.00	5153.58	0.02
Urapunga 5	563.1	0.61	510.00	836.07	100.00	1.00	100.00	1.64	163.93	0.06	0.35	0.16	70.00	4134.85	0.02
Urapunga 5	567	0.53	260.00	490.57	80.00	1.00	80.00	1.89	150.94	0.08	0.32	0.24	70.00	3835.22	0.02
Urapunga 5	571.2	0.61	210.00	344.26	90.00	1.50	60.00	2.46	98.36	0.07	0.31	0.24	50.00	3835.22	0.01
Urapunga 5	574	0.57	330.00	578.95	90.00	2.00	45.00	3.51	7						

**Table 30. Trace metal data of the Fraynes Formation.**

Rock ID	Depth (m)	TOC (wt %)	P (ppm)	P/TOC (ppm/wt%)	V (ppm)	Mo (ppm)	V/Mo	Mo/TOC (ppm/wt%)	V/Mo /TOC (per wt %)	Fe (molar)	Al (molar)	Fe/Al	Cr (ppm)	Ti (ppm)	Cr/Ti
MBSI	721.49	8.39	470.00	56.02	60.00	101.00	0.59	12.04	0.07	0.02	0.26	0.06	40.00	2517.27	0.02
MBSI	722.07	6.42	690.00	107.48	60.00	10.00	6.00	1.56	0.93	0.07	0.21	0.33	40.00	2637.14	0.02
MBSI	722.79	2.17	550.00	253.46	40.00	7.00	5.71	3.23	2.63	0.02	0.18	0.12	20.00	1857.98	0.01
MBSI	723.36	2.92	1360.00	465.75	120.00	13.50	8.89	4.62	3.04	0.03	0.26	0.13	40.00	3296.42	0.01
MBSI	782.58	1.56	1200.00	769.23	210.00	5.00	42.00	3.21	26.92	0.04	0.23	0.17	40.00	3596.09	0.01
MBSI	783.54	1.75	1330.00	760.00	190.00	11.50	16.52	6.57	9.44	0.05	0.29	0.16	90.00	3715.96	0.02
MBSI	784.65	3.43	1940.00	565.60	120.00	14.50	8.28	4.23	2.41	0.04	0.26	0.17	60.00	3356.35	0.02
MBSI	785.46	5.03	1180.00	234.59	150.00	41.00	3.66	8.15	0.73	0.08	0.27	0.31	80.00	3056.68	0.03
MBSI	786.54	4.97	2050.00	412.47	210.00	28.00	7.50	5.63	1.51	0.05	0.24	0.23	70.00	3416.29	0.02
MBSI	787.31	4.31	1580.00	366.59	240.00	27.00	8.89	6.26	2.06	0.07	0.27	0.25	40.00	3116.61	0.01
MBSI	788.31	1.83	2110.00	1153.01	170.00	8.00	21.25	4.37	11.61	0.05	0.25	0.19	60.00	3416.29	0.02
MBSI	789.12	2.09	2690.00	1287.08	210.00	12.50	16.80	5.98	8.04	0.04	0.25	0.18	70.00	3116.61	0.02
MBSI	864.70	0.84	50.00	59.52	—	2.50	—	2.98	—	0.04	0.04	1.13	10.00	479.48	0.02
MBSI	865.80	1.61	300.00	186.34	60.00	1.00	60.00	0.62	37.27	0.03	0.37	0.09	80.00	3955.70	0.02
MBSI	867.20	1.05	270.00	257.14	50.00	2.00	25.00	1.90	23.81	0.03	0.38	0.09	70.00	3596.09	0.02
MBSI	868.15	2.45	260.00	106.12	60.00	1.00	60.00	0.41	24.49	0.03	0.35	0.09	60.00	3656.03	0.02
MBSI	868.75	1.85	270.00	145.95	70.00	1.00	70.00	0.54	37.84	0.03	0.36	0.09	60.00	3895.77	0.02
MBSI	869.58	1.90	270.00	142.11	50.00	1.00	50.00	0.53	26.32	0.03	0.26	0.11	50.00	3116.61	0.02
MBSI	870.53	0.84	110.00	130.95	10.00	7.00	1.43	8.33	1.70	0.03	0.12	0.29	30.00	1378.50	0.02
MBSI	871.48	2.36	250.00	105.93	70.00	3.50	20.00	1.48	8.47	0.03	0.30	0.11	60.00	3296.42	0.02
MBSI	721.36	3.49	650.00	186.25	90.00	14.00	6.43	4.01	1.84	0.02	0.24	0.10	30.00	1678.18	0.02
MBSI	721.69	4.41	950.00	215.42	95.00	6.00	15.83	1.36	3.59	0.03	0.29	0.09	30.00	1768.08	0.02
MBSI	721.93	0.00	750.00	—	85.00	11.00	7.73	—	—	0.05	0.23	0.22	50.00	1768.08	0.03
MBSI	722.18	6.14	1050.00	171.01	70.00	6.00	11.67	0.98	1.90	0.09	0.21	0.42	50.00	1498.37	0.03
MBSI	722.37	5.93	7600.00	1281.62	55.00	9.50	5.79	1.60	0.98	0.09	0.20	0.45	30.00	1378.50	0.02
MBSI	722.55	3.06	250.00	81.70	30.00	1.00	30.00	0.33	9.80	0.03	0.11	0.24	20.00	749.19	0.03
MBSI	722.99	2.93	900.00	307.17	75.00	8.50	8.82	2.90	3.01	0.02	0.13	0.18	30.00	988.93	0.03
MBSI	723.15	3.46	2000.00	578.03	150.00	17.00	8.82	4.91	2.55	0.04	0.26	0.14	50.00	1947.88	0.03
MBSI	723.57	1.85	1200.00	648.65	90.00	13.00	6.92	7.03	3.74	0.03	0.32	0.10	20.00	1768.08	0.01
MBSI	780.77	1.19	1000.00	840.34	165.00	2.50	66.00	2.10	55.46	0.04	0.16	0.23	30.00	2067.75	0.01
MBSI	781.70	1.53	850.00	555.56	130.00	7.00	18.57	4.58	12.14	0.04	0.18	0.25	50.00	2127.69	0.02
MBSI	785.07	5.09	1600.00	314.34	210.00	29.50	7.12	5.80	1.40	0.06	0.24	0.24	60.00	1977.85	0.03
MBSI	785.24	6.25	2000.00	320.00	240.00	51.00	4.71	8.16	0.75	0.06	0.25	0.25	60.00	2157.66	0.03
MBSI	786.05	5.06	2400.00	474.31	250.00	30.00	8.33	5.93	1.65	0.07	0.26	0.25	50.00	2007.82	0.02
MBSI	786.26	2.59	1300.00	501.93	125.00	19.50	6.41	7.53	2.48	0.41	0.14	2.89	50.00	1288.60	0.04
MBSI	786.91	5.00	2800.00	560.00	235.00	31.50	7.46	6.30	1.49	0.06	0.25	0.24	60.00	1947.88	0.03
MBSI	787.81	2.84	1200.00	422.54	225.00	15.50	14.52	5.46	5.11	0.05	0.22	0.24	50.00	1768.08	0.03
MBSI	788.71	2.07	3000.00	1449.28	215.00	13.00	16.54	6.28	7.99	0.05	0.27	0.17	60.00	2157.66	0.03
MBSI	789.46	1.79	1900.00	1061.45	190.00	9.50	20.00	5.31	11.17	0.05	0.25	0.19	60.00	1887.95	0.03
MBSI	867.50	2.20	250.00	113.64	90.00	0.50	180.00	0.23	81.82	0.04	0.35	0.12	60.00	2337.46	0.03
MBSI	868.66	2.01	250.00	124.38	90.00	<0.5	—	—	—	0.03	0.34	0.09	60.00	2247.56	0.03
MBSI	868.90	1.89	250.00	132.28	90.00	0.50	180.00	0.26	95.24	0.04	0.34	0.11	60.00	2367.43	0.03
MBSI	867.90	2.33	300.00	128.76	90.00	0.50	180.00	0.21	77.25	0.04	0.35	0.10	60.00	2427.36	0.02
MBSI	868.49	1.66	200.00	120.48	90.00	0.50	180.00	0.30	108.43	0.04	0.35	0.11	80.00	2517.27	0.03
MBSI	869.30	1.78	300.00	168.54	90.00	2.50	36.00	1.40	20.22	0.04	0.34	0.12	50.00	2307.49	0.02
MBSI	869.77	1.56	250.00	160.26	90.00	0.50	180.00	0.32	115.38	0.03	0.35	0.08	50.00	2367.43	0.02
MBSI	870.10	1.79	250.00	139.66	80.00	0.50	160.00	0.28	89.39	0.03	0.34	0.10	50.00	2157.66	0.02
MBSI	871.22	1.95	300.00	153.85	70.00	2.00	35.00	1.03	17.95	0.03	0.34	0.09	50.00	1917.92	0.03
MBSI	872.93	1.65	250.00	151.52	90.00	2.00	45.00	1.21	27.27	0.03	0.33	0.08	60.00	2517.27	0.02

**Table 31. Trace metal data of the Barney Creek Formation.**

Rock ID	Depth (m)	TOC (wt %)	P (ppm)	P/TOC (ppm/ wt%)	V (ppm)	Mo (ppm)	V/Mo	Mo/TOC (ppm/ wt%)	V/Mo /TOC (per wt %)	Fe (molar)	Al (molar)	Fe/Al	Cr (ppm)	Ti (ppm)	Cr/Ti
Bing Bong 5	34.00	0.00			22.50	<0.9				0.03	0.19	0.17	30.30	2397.02	0.01
Bing Bong 5	70.35	1.52			24.60	<0.9				0.03	0.18	0.15	32.10	2397.02	0.01
Bing Bong 5	73.00	1.15			39.60	1.30	30.46	1.13	26.49	0.04	0.16	0.25	37.70	2397.02	0.02
Bing Bong 5	76.30	1.66			29.30	1.30	22.54	0.78	13.58	0.03	0.16	0.16	36.00	1797.76	0.02
Bing Bong 5	81.00	1.06			31.50	0.90	35.00	0.85	33.02	0.03	0.14	0.18	22.00	1797.76	0.01
Bing Bong 5	96.00	0.69			46.00	<0.9				0.04	0.20	0.22	45.10	2397.02	0.02
Bing Bong 5	100.50	0.90			34.60	<0.9				0.06	0.17	0.32	48.80	2397.02	0.02
Bing Bong 5	107.00	0.56	218.21	389.66	43.00	<0.9				0.04	0.21	0.21	44.90	2397.02	0.02
Bing Bong 5	111.60	0.66			28.10	<0.9				0.05	0.16	0.29	40.30	1797.76	0.02
Bing Bong 5	114.00	0.57			43.20	0.90	48.00	1.58	84.21	0.05	0.19	0.27	42.30	2397.02	0.02
Bing Bong 5	117.00	0.47			46.40	<0.9				0.05	0.19	0.26	39.00	2397.02	0.02
Bing Bong 5	118.20	0.78			41.30	1.00	41.30	1.28	52.95	0.05	0.20	0.25	42.20	2397.02	0.02
Bing Bong 5	123.70	1.04			42.50	1.80	23.61	1.73	22.70	0.07	0.20	0.33	46.30	2397.02	0.02
Bing Bong 5	125.60	7.57	109.10	14.41	66.90	7.00	9.56	0.92	1.26	0.06	0.21	0.27	49.90	2996.27	0.02
Bing Bong 5	127.00	1.13			35.10	2.80	12.54	2.48	11.09	0.05	0.18	0.29	40.70	2397.02	0.02
Bing Bong 5	128.00	0.92	436.41	474.36	32.40	1.70	19.06	1.85	20.72	0.04	0.18	0.23	44.70	2397.02	0.02
Bing Bong 5	138.00	0.75			38.60	2.50	15.44	3.33	20.59	0.04	0.20	0.22	46.10	2397.02	0.02
Bing Bong 5	144.00	1.34			32.40	4.40	7.36	3.28	5.50	0.06	0.20	0.32	39.80	2397.02	0.02
Bing Bong 5	154.00	1.38			37.90	6.50	5.83	4.71	4.23	0.07	0.15	0.49	26.20	1797.76	0.01
Bing Bong 5	156.30	1.06			46.90	3.20	14.66	3.02	13.83	0.05	0.21	0.22	34.70	1797.76	0.02
Bing Bong 5	162.00	0.48			20.30	<0.9				0.02	0.21	0.10	29.00	1797.76	0.02
Bing Bong 5	168.00	0.81			33.40	2.90	11.52	3.58	14.22	0.03	0.15	0.19	22.90	1797.76	0.01
Bing Bong 5	170.00	1.74	436.41	250.81	47.70	3.90	12.23	2.24	7.03	0.05	0.17	0.27	36.50	1797.76	0.02
Bing Bong 5	171.00	1.84			35.50	2.30	15.43	1.25	8.39	0.04	0.17	0.24	35.50	1797.76	0.02
Bing Bong 5	174.00	1.74			37.60	15.70	2.39	9.02	1.38	0.06	0.15	0.40	30.30	1797.76	0.02
Bing Bong 5	176.00	1.32			76.40	10.90	7.01	8.26	5.31	0.04	0.19	0.22	34.50	2397.02	0.01
Bing Bong 5	177.00	1.15	109.10	94.87	60.00	6.40	9.38	5.57	8.15	0.04	0.20	0.18	33.70	2397.02	0.01
Bing Bong 5	178.00	0.99	109.10	110.21	54.80	5.80	9.45	5.86	9.54	0.10	0.19	0.52	36.20	2397.02	0.02
Bing Bong 5	183.00	0.51			55.00	<0.9				0.03	0.23	0.15	56.90	2397.02	0.02
Bing Bong 5	213.00	0.01			50.60	<0.9				0.14	0.18	0.78	24.30	2397.02	0.01
Bing Bong 5	214.80	2.15	327.31	152.24	77.90	5.10	15.27	2.37	7.10	0.09	0.20	0.42	39.40	2397.02	0.02
Bing Bong 5	215.80	2.23	327.31	146.78	58.60	6.20	9.45	2.78	4.24	0.08	0.20	0.38	37.90	2397.02	0.02
Bing Bong 5	216.80	1.60			50.50	4.00	12.63	2.50	7.89	0.06	0.21	0.30	41.70	2397.02	0.02
Bing Bong 5	217.80	1.59			41.40	4.40	9.41	2.77	5.92	0.11	0.17	0.68	34.70	2397.02	0.01
Bing Bong 5	218.00	2.13			36.20	3.60	10.06	1.69	4.72	0.05	0.16	0.28	26.00	1797.76	0.01
Bing Bong 5	220.00	3.02	218.21	72.25	60.60	13.80	4.39	4.57	1.45	0.09	0.19	0.45	34.70	1797.76	0.02
Bing Bong 5	221.00	3.24	218.21	67.35	72.60	5.80	12.52	1.79	3.86	0.04	0.18	0.23	38.30	2397.02	0.02
Bing Bong 5	222.20	3.62	218.21	60.28	77.80	11.30	6.88	3.12	1.90	0.05	0.18	0.27	36.00	2397.02	0.02
Bing Bong 5	223.00	1.25			29.50	2.40	12.29	1.92	9.83	0.04	0.08	0.53	22.50	1198.51	0.02
Bing Bong 5	224.00	1.70	109.10	64.18	44.00	4.30	10.23	2.53	6.02	0.07	0.12	0.54	22.00	1198.51	0.02
Bing Bong 5	224.60	1.19			<20	1.70		1.43		0.04	0.06	0.74	<20	599.25	
Bing Bong 5	225.50	0.98			20.60	1.60	12.88	1.63	13.14	0.03	0.06	0.52	<20	599.25	
Bing Bong 5	226.50	1.00	109.10	109.10	35.70	2.50	14.28	2.50	14.28	0.03	0.09	0.35	21.40	1198.51	0.02
Bing Bong 5	227.70	0.94	109.10	116.07	22.50	3.00	7.50	3.19	7.98	0.04	0.11	0.41	<20	1198.51	
Bing Bong 5	228.20	1.24	327.31	263.96	80.60	5.70	14.14	4.60	11.40	0.06	0.17	0.33	39.50	2397.02	0.02
Bing Bong 5	229.00	1.25	218.21	174.57	51.60	6.70	7.70	5.36	6.16	0.06	0.11	0.58	23.20	1198.51	0.02
Bing Bong 5	231.90	1.87	327.31	175.03	91.70	12.40	7.40	6.63	3.95	0.05	0.17	0.30	32.20	1797.76	0.02
Bing Bong 5	250.60	0.56	109.10	194.83	50.30	3.90	12.90	6.96	23.03	0.03	0.15	0.22	28.30	1797.76	0.02
Bing Bong 5	255.00	0.54			44.90	3.10	14.48	5.74	26.82	0.04	0.13	0.27	25.30	1797.76	0.01
Bing Bong 5	267.00	0.65	109.10	167.85	112.00	23.30	4.81	35.85	7.40	0.09	0.24	0.36	45.20	2996.27	0.02
Bing Bong 5	276.00	0.62	109.10	175.97	67.00	3.90	17.18	6.29	27.71	0.04	0.18	0.22	41.70	2397.02	0.02
Bing Bong 5	289.00	0.99	218.21	220.41	104.00	6.30	16.51	6.36	16.67	0.05	0.22	0.21	50.60	2996.27	0.02
Bing Bong 5	296.50	1.08	218.21	202.04	118.00	8.60	13.72	7.96	12.70	0.05	0.20	0.23	54.60	2996.27	0.02
Bing Bong 5	303.60	1.16	218.21	188.11	151.00	7.00	21.57	6.03	18.60	0.05	0.21	0.26	49.80	2996.27	0.02
Bing Bong 5	305.00	1.54	327.31	212.54	159.00	13.90	11.44	9.03	7.43	0.06	0.22	0.29	58.50	3595.52	0.02
Bing Bong 5	307.00	4.40	218.21	49.59	118.00	18.20	6.48	4.14	1.47	0.08	0.23	0.33	57.00	2996.27	0.02
Bing Bong 5	308.00	3.43	109.10	31.81	108.00	13.50	8.00	3.94	2.33	0.06	0.23	0.28	47.50	2996.27	0.02
Bing Bong 5	309.15	1.53	327.31	213.93	162.00	10.80	15.00	7.06	9.80	0.05	0.20	0.26	54.60	2397.02	0.02
Bing Bong 5	315.00	3.38	218.21	64.56	208.00	5.40	38.52	1.60	11.40	0.04	0.24	0.17	66.80	2996.27	0.02
Bing Bong 5	327.00	0.82	218.21	266.11	212.00	7.80	27.18	9.51	33.15	0.05	0.25	0.18	66.80	2996.27	0.02
Bing Bong 5	335.75	0.75	218.21	290.94	190.00	4.20	45.24	5.60	60.32	0.04	0.28	0.15	88.90	2996.27	0.03

**Table 33. Trace metal data of the Barney Creek Formation continued.**

Rock ID	Depth (m)	TOC (wt %)	P (ppm)	P/TOC (ppm/ wt%)	V (ppm)	Mo (ppm)	V/Mo	Mo/TOC (ppm/ wt%)	V/Mo /TOC (per wt %)	Fe (molar)	Al (molar)	Fe/Al	Cr (ppm)	Ti (ppm)	Cr/Ti
GR4 95.3	95.30	0.41	187.66	457.70	73.00	0.20		0.49	890.24	0.04	0.24	0.15	46.00	3056.19	0.02
GR4 105.6	105.60	1.40	145.11	103.65	81.00	4.30	18.84	3.07	13.46	0.05	0.20	0.24	58.00	2516.87	0.02
GR4 111.0	111.00	1.21	137.47	113.61	59.00	3.40	17.35	2.81	14.34	0.04	0.19	0.23	33.00	2456.94	0.01
GR4 118.0	118.00	1.50	216.03	144.02	124.00	2.20	56.36	1.47	37.58	0.04	0.20	0.21	45.00	2576.79	0.02
GR4 125.7	125.70	1.30	213.84	164.49	113.00	4.00	28.25	3.08	21.73	0.05	0.23	0.21	46.00	2756.57	0.02
GR4 128.8	128.80	1.33	200.75	150.94	138.00	1.70	81.18	1.28	61.03	0.05	0.22	0.22	47.00	3715.37	0.01
GR4 140.6	140.60	1.92	363.32	189.23	142.00	9.60	14.79	5.00	7.70	0.06	0.24	0.24	59.00	3116.12	0.02
GR4 148.5	148.50	1.46	332.77	227.92	154.00	10.70	14.39	7.33	9.86	0.05	0.27	0.20	59.00	3295.90	0.02
GR4 153.4	153.40	0.88	196.39	223.17	123.00	2.10	58.57	2.39	66.56	0.05	0.21	0.23	58.00	2576.79	0.02
GR7 599.5	599.50	1.44	164.75	114.41	58.00	4.90	11.84	3.40	8.22	0.04	0.18	0.24	38.00	2397.02	0.02
GR7 605.8	605.80	1.34	157.11	117.25	54.00	5.90	9.15	4.40	6.83	0.04	0.20	0.22	33.00	2277.16	0.01
GR7 616.9	616.90	1.35	151.65	112.34	64.00	4.90	13.06	3.63	9.67	0.04	0.18	0.23	34.00	2337.09	0.01
GR7 628.5	628.50	1.41	161.47	114.52	66.00	6.00	11.00	4.26	7.80	0.04	0.18	0.23	41.00	2456.94	0.02
GR7 638.0	638.00	1.38	195.30	141.52	65.00	4.50	14.44	3.26	10.47	0.04	0.17	0.23	39.00	2277.16	0.02
GR7 647.1	647.10	1.25	150.56	120.45	67.00	3.50	19.14	2.80	15.31	0.04	0.22	0.20	40.00	2756.57	0.01
GR7 657.6	657.60	1.44	166.93	115.92	80.00	4.40	18.18	3.06	12.63	0.04	0.16	0.24	41.00	2097.39	0.02
GR7 668.4	668.40	1.21	156.02	128.94	74.00	3.30	22.42	2.73	18.53	0.05	0.19	0.24	48.00	2516.87	0.02
GR7 678.0	678.00	1.27	134.20	105.67	72.00	5.50	13.09	4.33	10.31	0.04	0.15	0.26	40.00	2037.46	0.02
GR7 771.2	771.20	1.47	241.12	164.03	103.00	3.60	28.61	2.45	19.46	0.05	0.24	0.20	52.00	3595.52	0.01
GR7 792.0	792.00	1.30	248.76	191.35	96.00	1.70	56.47	1.31	43.44	0.05	0.22	0.21	54.00	3235.97	0.02
GR7 802.0	802.00	1.15	176.75	153.69	88.00	1.30	67.69	1.13	58.86	0.04	0.19	0.22	40.00	2636.72	0.02
GR7 812.6	812.60	1.14	201.84	177.05	103.00	2.80	36.79	2.46	32.27	0.05	0.21	0.24	43.00	2636.72	0.02
GR7 824.0	824.00	0.88	138.56	157.46	74.00	1.30	56.92	1.48	64.69	0.05	0.20	0.23	46.00	2696.64	0.02
GR7 840.0	840.00	1.23	271.67	220.87	122.00	5.00	24.40	4.07	19.84	0.05	0.24	0.23	54.00	3116.12	0.02
GR7 850.0	850.00	1.16	185.48	159.89	117.00	3.10	37.74	2.67	32.54	0.04	0.20	0.21	45.00	3116.12	0.01
GR7 860.0	860.00	2.64	718.99	272.35	175.00	13.20	13.26	5.00	5.02	0.05	0.24	0.22	68.00	3176.04	0.02
GR7 870.1	870.10	2.78	842.28	302.98	143.00	13.90	10.29	5.00	3.70	0.06	0.24	0.24	34.00	3116.12	0.01
GR7 881.0	881.00	0.80	240.03	300.04	110.00	2.90	37.93	3.63	47.41	0.08	0.32	0.23	79.00	3535.60	0.02
GR7 891.0	891.00	0.99	282.58	285.43	171.00	1.20	142.50	1.21	143.94	0.07	0.26	0.28	88.00	3235.97	0.03
GR7 901.0	901.00	0.95	270.58	284.82	197.00	3.10	63.55	3.26	66.89	0.06	0.28	0.21	87.00	3235.97	0.03

**Table 32. Trace metal data of the Wollogorang Formation.**

Rock ID	Depth (m)	TOC (wt %)	P (ppm)	P/TOC (ppm/ wt%)	V (ppm)	Mo (ppm)	V/Mo	Mo/TOC (ppm/ wt%)	V/Mo /TOC (per wt %)	Fe (molar)	Al (molar)	Fe/Al	Cr (ppm)	Ti (ppm)	Cr/Ti
Mt Young 2	52.40	0.30	520.00	1733.33	60.00	<0.5				0.03	0.13	0.22	40.00	1797.76	0.02
Mt Young 2	57.20	0.66	260.00	393.94	130.00	2.50	52.00	3.79	78.79	0.04	0.10	0.41	20.00	1078.66	0.02
Mt Young 2	58.00	0.46	250.00	543.48	170.00	4.00	42.50	8.70	92.39	0.03	0.14	0.25	40.00	1617.99	0.02
Mt Young 2	59.40	0.29	150.00	517.24	60.00	2.00	30.00	6.90	103.45	0.04	0.15	0.25	40.00	2337.09	0.02
Mt Young 2	60.40	0.35	170.00	485.71	140.00	2.00	70.00	5.71	200.00	0.04	0.14	0.27	20.00	1498.13	0.01
Mt Young 2	62.40	0.98	220.00	224.49	210.00	29.00	7.24	29.59	7.39	0.03	0.17	0.21	40.00	1737.84	0.02
Mt Young 2	63.80	2.16	260.00	120.37	90.00	2.75	3.27	12.73	1.52	0.05	0.13	0.35	40.00	1797.76	0.02
Mt Young 2	65.80	0.86	160.00	186.05	50.00	9.50	5.26	11.05	6.12	0.04	0.06	0.65	20.00	659.18	0.03
Mt Young 2	66.80	1.96	360.00	183.67	70.00	24.50	2.86	12.50	1.46	0.04	0.11	0.35	20.00	1258.43	0.02
Mt Young 2	67.90	2.84	730.00	257.04	120.00	36.50	3.29	12.85	1.16	0.06	0.21	0.30	50.00	2397.02	0.02
Mt Young 2	70.20	0.89	260.00	292.13	170.00	2.50	68.00	2.81	76.40	0.02	0.17	0.11	20.00	2397.02	0.01
Mt Young 2	71.40	0.69	230.00	333.33	30.00	1.00	30.00	1.45	43.48	0.03	0.06	0.45	<10	838.96	
Mt Young 2	72.00	1.73	240.00	138.73	40.00	20.50	1.95	11.85	1.13	0.04	0.10	0.44	20.00	1138.58	0.02
Mt Young 2	74.30	5.07	1260.00	248.52	90.00	59.50	1.51	11.74	0.30	0.03	0.16	0.21	40.00	2217.24	0.02
Mt Young 2	76.30	7.23	1650.00	228.22	150.00	53.50	2.80	7.40	0.39	0.04	0.26	0.17	50.00	3535.60	0.01
Mt Young 2	77.05	8.49	1320.00	155.48	190.00	54.50	3.49	6.42	0.41	0.03	0.25	0.13	90.00	3355.82	0.03
Mt Young 2	79.40	3.01	710.00	235.88	180.00	62.50	2.88	20.76	0.96	0.06	0.33	0.17	50.00	4134.85	0.01
Mt Young 2	80.20	1.79	410.00	229.05	310.00	34.00	9.12	18.99	5.09	0.03	0.21	0.12	40.00	2756.57	0.01
Mt Young 2	82.00	0.56	250.00	446.43	40.00	13.50	2.96	24.11	5.29	0.03	0.05	0.59	<10	599.25	
Mt Young 2	84.00	0.34	610.00	1794.12	20.00	2.50	8.00	7.35	23.53	0.03	0.03	0.77	<10	539.33	
Mt Young 2	84.50	0.41	430.00	1048.78	100.00	1.00	100.00	2.44	243.90	0.03	0.33	0.08	40.00	4254.70	0.01
Mt Young 2	85.90	0.27	520.00	1925.93	50.00	1.00	50.00	3.70	185.19	0.04	0.15	0.23	20.00	1617.99	0.01
Mt Young 2	88.30	0.27	620.00	2296.30	70.00	<0.5				0.05	0.23	0.21	40.00	2277.16	0.02
Mt Young 2	89.00	0.28	700.00	2500.00	100.00	<0.5				0.05	0.29	0.16	50.00	3415.75	0.01
Mt Young 2	90.20	1.37	680.00	496.35	160.00	8.50	18.82	6.20	13.74	0.05	0.27	0.18	40.00	2996.27	0.01
Mt Young 2	92.20	0.61	510.00	836.07	90.00	2.50	36.00	4.10	59.02	0.05	0.15	0.35	40.00	1917.61	0.02
Mt Young 2	94.00	0.31	200.00	645.16	40.00	1.00	40.00	3.23	129.03	0.05	0.06	0.74	20.00	958.81	0.02
Mt Young 2	96.00	0.30	390.00	1300.00	40.00	1.00	40.00	3.33	133.33	0.06	0.10	0.61	20.00	1378.28	0.01

### Source Rock Analyser data

Table 34. ‘Rock Eval’ data of the Tent Hill Formation.

Rock ID	Depth (m)	S1 (mg HC / g)	S2 (mg HC / g)	S3 (mg HC / g)	Tmax (°C)	TOC (%)	Production Index [S1/(S1+S2)]	HI	OI
MSDP02	24.00	0.05	0.18	0.08	572.00	0.22	0.22	82.00	36.00
MSDP02	37.30	0.05	0.17	0.04	511.00	0.14	0.23	121.00	29.00
MSDP02	44.30	0.05	0.16	0.03	409.00	0.22	0.24	73.00	14.00
MSDP02	58.00	0.03	0.11	0.04	558.00	0.10	0.21	110.00	40.00
MSDP02	71.00	0.02	0.08	0.06	560.00	0.09	0.20	89.00	67.00
MSDP02	82.00	0.03	0.09	0.03	564.00	0.06	0.25	150.00	50.00
MSDP02	93.00	0.03	0.09	0.03	571.00	0.04	0.25	225.00	75.00
MSDP02	105.00	0.03	0.10	0.02	575.00	0.11	0.23	91.00	18.00
MSDP02	112.30	0.05	0.15	0.03	539.00	0.20	0.25	75.00	15.00
MSDP02	118.00	0.03	0.03	0.02	575.00	0.02	0.23	500.00	100.00
MSDP02	125.20	0.03	0.09	0.02	357.00	0.06	0.25	150.00	33.00
MSDP02	132.00	0.03	0.10	0.12	345.00	0.10	0.23	100.00	120.00
MSDP02	133.10	0.03	0.10	0.06	574.00	0.10	0.23	100.00	60.00
MSDP02	136.40	0.03	0.10	0.02	572.00	0.06	0.23	167.00	33.00
MSDP02	137.38	0.03	0.10	0.04	567.00	0.06	0.23	167.00	67.00
MSDP02	143.40	0.04	0.11	0.20	569.00	0.07	0.27	157.00	286.00
MSDP02	146.30	0.03	0.09	0.09	568.00	0.01	0.25	900.00	900.00
MSDP02	147.80	0.05	0.16	0.02	549.00	0.15	0.24	107.00	13.00
MSDP02	153.60	0.00		0.25	386.00	0.23			109.00
MSDP02	158.00	0.00	0.01	0.28	420.00	0.15		7.00	187.00
MSDP02	162.20	0.05	0.16	0.32	465.00	0.23	0.24	70.00	139.00
MSDP02	187.00	0.00	0.01	0.26	564.00	0.13		8.00	200.00
MSDP02	199.90	0.01	0.01	0.36	395.00	0.21	0.50	5.00	171.00
MSDP03	215.25	0.00		0.18	567.00	0.16			113.00

**Table 35. ‘Rock Eval’ data of the Tapley Hill Formation.**

Rock ID	Depth (m)	S1	S2	S3	Tmax	TOC	Production Index	HI	OI
		(mg HC / g)	(mg HC / g)	(mg HC / g)	(°C)	(%)	[S1/(S1+S2)]		
MSDP02	238.80	0.00	N/A	0.22	563.00	0.54	N/A	N/A	41.00
MSDP02	246.70	0.03	0.09	0.17	581.00	0.28	0.25	32.00	61.00
MSDP02	252.50	0.05	0.16	0.18	406.00	0.49	0.24	33.00	37.00
MSDP02	254.60	0.04	0.11	0.17	562.00	0.43	0.27	26.00	40.00
MSDP02	259.40	0.00	0.01	0.21	576.00	0.43	N/A	2.00	49.00
MSDP02	265.50	0.03	0.09	0.23	572.00	0.51	0.25	18.00	45.00
MSDP02	267.70	0.04	0.09	0.32	569.00	0.60	0.31	15.00	53.00
MSDP02	270.85	0.00	0.01	0.23	510.00	0.62	N/A	2.00	37.00
MSDP02	276.15	0.05	0.12	0.22	571.00	0.68	0.29	18.00	32.00
MSDP02	283.00	0.04	0.09	0.25	567.00	0.74	0.31	12.00	34.00
MSDP02	284.88	0.00	N/A	0.18	565.00	0.60	N/A	N/A	30.00
MSDP02	288.90	0.00	N/A	0.18	599.00	0.60	N/A	N/A	30.00
MSDP02	296.30	0.04	0.10	0.17	N/A	0.70	0.29	14.00	24.00
MSDP02	297.10	0.03	0.09	0.21	565.00	0.74	0.25	12.00	28.00
MSDP02	300.80	0.02	0.07	0.15	564.00	0.64	0.22	11.00	23.00
MSDP02	306.50	0.02	0.07	0.22	555.00	0.66	0.22	11.00	33.00
MSDP02	309.10	0.02	0.06	0.17	568.00	0.71	0.25	8.00	24.00
MSDP02	315.85	0.02	0.07	0.15	570.00	0.76	0.22	9.00	20.00
MSDP02	319.95	0.03	0.08	0.25	572.00	0.80	0.27	10.00	31.00
MSDP02	324.15	0.02	0.05	0.14	573.00	0.76	0.29	7.00	18.00
MSDP02	324.20	0.01	0.07	0.15	553.00	0.73	0.13	10.00	21.00
MSDP02	335.70	0.06	0.18	0.15	592.00	0.82	0.25	22.00	18.00

**Table 36. ‘Rock Eval’ data of the Gillen Formation.**

Rock ID	Depth (m)	S1	S2	S3	Tmax	TOC	Production Index	HI	OI
		(mg HC / g)	(mg HC / g)	(mg HC / g)	(°C)	(%)	[S1/(S1+S2)]		
BL002	60.30	0.10	0.08	0.27	360.00	1.81	0.56	4.00	15.00
BL002	62.00	0.07	0.11	0.26	599.00	1.38	0.39	8.00	19.00
BL002	62.50	0.04	0.07	0.21	409.00	0.46	0.36	15.00	46.00
BL002	65.00	0.04	0.07	0.09	420.00	0.93	0.36	8.00	10.00
BL002	67.00	0.10	0.08	0.43	399.00	2.24	0.56	4.00	19.00
BL002	68.50	0.05	0.09	0.25	344.00	1.08	0.36	8.00	23.00
BL002	72.00	0.03	0.08	0.24	330.00	0.95	0.27	8.00	25.00
BL002	74.00	0.07	0.09	0.32	329.00	2.10	0.44	4.00	15.00
BL002	75.00	0.06	0.13	0.35	322.00	3.16	0.32	4.00	11.00
BL002	77.00	0.06	0.09	0.09	402.00	1.39	0.40	6.00	6.00
BL002	77.50	0.13	0.11	0.23	381.00	1.34	0.54	8.00	17.00
BL002	80.10	0.05	0.07	0.19	407.00	0.97	0.42	7.00	20.00
BL002	84.40	0.07	0.07	0.17	425.00	1.34	0.50	5.00	13.00
BL002	86.00	0.09	0.09	0.28	432.00	1.84	0.50	5.00	15.00
BL002	87.40	0.04	0.08	0.28	576.00	1.60	0.33	5.00	18.00
BL002	90.00	0.13	0.07	0.40	358.00	2.48	0.65	3.00	16.00
BL002	92.10	0.07	0.12	0.22	391.00	1.57	0.37	8.00	14.00
BL002	93.10	0.05	0.08	0.40	N/A	2.22	0.38	4.00	18.00
BL002	95.50	0.04	0.08	0.25	315.00	2.38	0.33	3.00	11.00
BL002	96.70	0.05	0.09	0.47	320.00	2.90	0.36	3.00	16.00
BL002	97.50	0.05	0.07	0.46	349.00	3.86	0.42	2.00	12.00
BL002	99.00	0.06	0.11	0.62	397.00	4.98	0.35	2.00	12.00
BL002	102.00	0.04	0.09	0.55	390.00	7.36	0.31	1.00	7.00
BL002	105.00	0.04	0.05	0.17	432.00	0.82	0.44	6.00	21.00
BL002	108.30	0.04	0.05	0.12	525.00	0.26	0.44	19.00	46.00
BL002	108.50	0.03	0.05	0.02	610.00	0.39	0.38	13.00	5.00
BL002	110.00	0.03	0.06	0.15	508.00	0.98	0.33	6.00	15.00
BL002	113.70	0.05	0.07	0.16	404.00	0.56	0.42	13.00	29.00
BL002	122.00	0.06	0.10	0.11	400.00	0.56	0.38	18.00	20.00
BL002	123.10	0.04	0.05	0.05	596.00	0.36	0.44	14.00	14.00
BL002	128.30	0.09	0.08	0.15	317.00	1.20	0.53	25.00	21.00
BL002	150.10	0.07	0.09	0.02	355.00	1.05	0.44	9.00	2.00
BL002	155.15	0.04	0.05	0.13	418.00	0.58	0.44	9.00	22.00

Table 37. ‘Rock Eval’ data of the Kyalla Formation.

Rock ID	Depth (m)	S1	S2	S3	Tmax	TOC	Production Index [S1/(S1+S2)]	HI	OI
		(mg HC / g)	(mg HC / g)	(mg HC / g)	(°C)	(%)			
Elliot 1	672.00	0.06	0.41	0.75	433.20	0.66	0.13	62.00	114.00
Elliot 1	681.00	0.06	0.24	3.15	435.28	0.53	0.20	45.00	594.00
Elliot 1	691.00	0.03	0.39	2.11	437.83	0.53	0.07	74.00	398.00
Elliot 1	696.40	0.11	0.46	0.13	433.64	0.54	0.19	85.00	24.00
Elliot 1	709.33	0.03	0.26	5.19	433.64	0.52	0.10	50.00	998.00
Elliot 1	717.00	0.05	0.33	1.63	437.16	0.72	0.13	46.00	226.00
Elliot 1	721.00	0.04	0.54	0.43	437.84	0.81	0.07	67.00	53.00
Elliot 1	758.00	0.03	0.27	1.68	433.51	0.67	0.10	40.00	251.00
Elliot 1	766.00	0.04	0.29	0.58	439.56	0.61	0.12	48.00	95.00
Elliot 1	780.00	0.05	0.32	0.18	434.45	0.63	0.14	51.00	29.00
Elliot 1	797.00	0.05	0.32	0.30	435.60	0.66	0.14	48.00	45.00
Elliot 1	805.00	0.06	0.78	0.09	441.53	0.86	0.07	91.00	10.00
Elliot 1	820.56	0.03	0.39	0.12	437.71	0.72	0.07	54.00	17.00
Elliot 1	849.36	0.03	0.22	0.14	444.21	0.54	0.12	41.00	26.00
Elliot 1	857.10	0.03	0.32	0.07	445.41	0.64	0.09	50.00	11.00
Elliot 1	876.40	0.10	0.87	0.06	441.81	0.95	0.10	92.00	6.00
Elliot 1	891.60	0.06	0.37	0.07	433.43	0.70	0.14	53.00	10.00
Elliot 1	899.13	0.03	0.21	0.03	440.81	0.55	0.13	38.00	5.00
Elliot 1	907.84	0.03	0.26	0.06	442.92	0.58	0.10	45.00	10.00
Elliot 1	918.70	0.05	0.18	0.02	442.78	0.52	0.22	35.00	4.00
Elliot 1	929.70	0.07	0.65	0.11	444.92	1.14	0.10	57.00	10.00
Elliot 1	936.50	0.13	0.43	0.15	447.47	0.84	0.23	51.00	18.00
Elliot 1	944.35	0.06	0.46	0.07	445.05	0.80	0.12	58.00	9.00
Elliot 1	962.42	0.05	0.33	0.11	448.70	0.70	0.13	47.00	16.00
Balmain 1	976.11	0.95	10.99	0.17	437.00	2.66	0.08	413.16	6.39
Balmain 1	985.37	1.00	11.73	0.14	436.00	2.68	0.08	437.69	5.22
Balmain 1	990.01	1.11	12.20	0.17	434.00	3.02	0.08	403.97	5.63
Balmain 1	994.52	0.55	4.81	0.13	434.00	1.49	0.10	322.82	8.72
Balmain 1	1013.37	0.45	3.78	0.10	435.01	1.87	0.11	202.00	5.00
Balmain 1	1018.90	0.26	2.16	0.08	436.07	1.38	0.11	157.00	6.00
Balmain 1	1040.10	0.03	0.20	0.01	450.02	0.51	0.13	39.00	2.00
Balmain 1	1043.80	0.04	0.20	0.05	445.16	0.53	0.17	38.00	9.00

**Table 38. ‘Rock Eval’ data of the Vulkarri Formation.**

Rock ID	Depth	S1	S2	S3	Tmax	TOC	Production Index	HI	OI
		(m)	(mg HC / g)	(mg HC / g)	(mg HC / g)	(°C)	(%)	[S1/(S1+S2)]	
Altree 2	617.12	0.18	0.58	0.24	427.00	0.67	0.23	86.00	36.00
Altree 2	621.84	1.45	10.26	0.24	428.00	3.54	0.12	290.00	7.00
Altree 2	640.98	0.66	4.75	0.31	428.00	2.57	0.12	185.00	12.00
Altree 2	650.50	2.43	9.60	0.22	433.00	3.07	0.20	313.00	7.00
Altree 2	655.27	0.71	3.33	0.35	426.00	2.34	0.18	142.00	15.00
Altree 2	661.98	2.50	15.44	0.22	433.00	4.44	0.14	348.00	5.00
Altree 2	664.69	1.67	8.43	0.39	428.00	2.64	0.17	319.00	15.00
Altree 2	669.51	1.92	15.29	0.35	430.00	4.13	0.11	370.00	9.00
Altree 2	674.32	2.54	18.02	0.21	431.00	5.24	0.12	344.00	4.00
Altree 2	679.11	1.99	12.83	0.23	432.00	3.47	0.13	370.00	7.00
Altree 2	688.61	3.03	27.16	0.18	433.00	7.43	0.10	365.00	2.00
Altree 2	697.90	2.42	20.62	0.29	434.00	6.05	0.11	341.00	5.00
Altree 2	707.31	2.01	20.96	0.25	430.00	6.85	0.09	306.00	4.00
Altree 2	722.05	1.90	17.34	0.24	429.00	6.18	0.10	280.00	4.00
Altree 2	736.33	2.28	21.35	0.32	433.00	8.07	0.10	265.00	4.00
Altree 2	746.02	1.30	9.67	0.28	427.00	5.07	0.12	191.00	6.00
Altree 2	760.33	1.61	10.01	0.32	430.00	5.20	0.14	192.00	6.00
Altree 2	769.64	1.77	9.57	0.27	429.00	5.67	0.16	169.00	5.00
Altree 2	783.81	1.91	12.13	0.21	430.00	5.93	0.14	204.00	4.00
Altree 2	793.37	2.17	15.68	0.32	432.00	7.63	0.12	206.00	4.00
Altree 2	802.74	2.44	16.43	0.27	432.00	6.24	0.13	263.00	4.00
Altree 2	812.11	2.33	17.52	0.25	437.00	5.95	0.12	295.00	4.00
Altree 2	821.78	2.21	15.95	0.33	438.00	5.72	0.12	279.00	6.00
Altree 2	831.21	2.08	10.06	0.34	436.00	3.81	0.17	264.00	9.00
Altree 2	845.48	3.42	9.97	0.18	433.00	3.54	0.26	281.00	5.00
Altree 2	854.93	3.31	9.13	0.20	433.00	4.16	0.27	220.00	5.00
Altree 2	873.77	1.60	3.60	0.18	435.00	1.95	0.31	184.00	9.00
Altree 2	883.63	1.82	6.00	0.18	429.00	3.21	0.23	187.00	6.00
Altree 2	898.25	1.31	4.04	0.71	429.00	1.74	0.24	232.00	41.00
Altree 2	912.37	3.49	7.34	0.20	407.00	2.41	0.32	305.00	8.00
Altree 2	922.05	2.66	10.92	0.26	437.00	5.54	0.20	197.00	5.00
Altree 2	926.59	1.40	3.80	0.29	422.00	4.02	0.27	95.00	7.00
Altree 2	931.53	2.55	11.28	0.29	434.00	5.86	0.18	193.00	5.00
Altree 2	940.69	2.80	8.02	0.21	436.00	4.40	0.26	182.00	5.00
Marmbulligan 1	129.00	0.12	4.11	0.06	432.00	1.79	0.03	230.00	3.00
Marmbulligan 1	135.50	0.29	9.94	0.18	433.00	2.61	0.03	381.00	7.00
Marmbulligan 1	139.65	0.46	24.43	0.19	435.00	4.74	0.02	515.00	4.00
Marmbulligan 1	144.20	0.48	27.95	0.31	435.00	5.38	0.02	520.00	6.00
Marmbulligan 1	149+B6	0.79	35.60	0.20	434.00	6.46	0.02	551.00	3.00
Marmbulligan 1	157.00	0.58	32.80	0.17	435.00	6.16	0.02	532.00	3.00
Marmbulligan 1	173.50	0.66	36.41	0.19	431.00	7.33	0.02	497.00	3.00
Marmbulligan 1	206.00	0.45	8.81	0.16	433.00	2.97	0.05	297.00	5.00
Marmbulligan 1	214.30	0.41	5.77	0.08	434.00	2.32	0.07	249.00	3.00
Marmbulligan 1	314.00	0.98	8.29	0.57	433.00	3.66	0.11	227.00	16.00
Marmbulligan 1	316.00	0.30	3.49	0.30	428.00	1.60	0.08	218.00	19.00
Marmbulligan 1	324.50	1.00	30.64	0.13	436.00	8.49	0.03	361.00	2.00
Marmbulligan 1	341.60	1.17	25.84	0.14	438.00	7.48	0.04	345.00	2.00
Marmbulligan 1	347.00	0.61	19.43	0.18	438.00	6.18	0.03	314.00	3.00
Marmbulligan 1	350.00	0.93	27.27	0.20	440.00	8.64	0.03	316.00	2.00
Marmbulligan 1	355.00	0.85	26.18	0.30	439.00	7.60	0.03	344.00	4.00
Marmbulligan 1	364.00	0.58	14.35	0.21	442.00	5.97	0.04	240.00	4.00
Marmbulligan 1	374.50	1.00	14.16	0.10	437.00	4.89	0.07	290.00	2.00
Marmbulligan 1	384.00	0.74	9.43	0.14	434.00	3.31	0.07	285.00	4.00
Marmbulligan 1	514.00	0.51	5.71	0.26	438.00	3.97	0.08	144.00	7.00
Marmbulligan 1	589.00	0.54	7.79	0.20	439.00	3.40	0.06	229.00	6.00

**Table 39. ‘Rock Eval’ data of the Velkerri Formation continued.**

Rock ID	Depth (m)	S1 (mg HC / g)	S2 (mg HC / g)	S3 (mg HC / g)	Tmax (°C)	TOC (%)	Production Index [S1/(S1+S2)]	HI	OI
Amungee NW1	2239.00	0.14	0.23	0.14	N/A	4.22	0.38	5.00	3.00
Amungee NW1	2241.12	0.18	0.27	0.12	309.00	4.47	0.40	6.00	3.00
Amungee NW1	2243.19	0.17	0.24	0.26	317.00	4.19	0.41	6.00	6.00
Amungee NW1	2245.25	0.19	0.23	0.10	337.00	4.47	0.45	5.00	2.00
Amungee NW1	2247.32	0.19	0.26	0.33	323.00	4.22	0.42	6.00	8.00
Amungee NW1	2249.38	0.19	0.24	0.20	309.00	4.42	0.44	5.00	5.00
Amungee NW1	2251.44	0.26	0.29	0.15	321.00	4.56	0.47	6.00	3.00
Amungee NW1	2253.58	0.26	0.30	0.33	327.00	4.78	0.46	6.00	7.00
Amungee NW1	2255.62	0.18	0.24	0.25	314.00	4.31	0.43	6.00	6.00
Amungee NW1	2259.76	0.20	0.25	0.11	335.00	5.10	0.44	5.00	2.00
Amungee NW1	2261.80	0.21	0.28	0.28	323.00	4.45	0.43	6.00	6.00
Amungee NW1	2263.86	0.22	0.29	0.22	336.00	5.31	0.43	5.00	4.00
Amungee NW1	2265.94	0.24	0.28	0.29	322.00	3.97	0.46	7.00	7.00
Amungee NW1	2268.00	0.19	0.26	0.30	338.00	4.17	0.42	6.00	7.00
Amungee NW1	2270.13	0.22	0.31	0.53	314.00	4.90	0.42	6.00	11.00
Amungee NW1	2272.24	0.20	0.28	0.21	323.00	5.04	0.42	6.00	4.00
Amungee NW1	2274.30	0.17	0.25	0.29	307.00	4.62	0.40	5.00	6.00
Amungee NW1	2275.58	0.21	0.26	0.18	309.00	5.15	0.45	5.00	3.00
Tanumbirini 1	3198.00	0.07	0.17		360.00	0.57	0.29	30.00	
Tanumbirini 1	3199.00	0.09	0.21	0.07	426.00	1.71	0.30	12.00	4.00
Tanumbirini 1	3200.00	0.09	0.19	0.13	305.00	1.21	0.32	16.00	11.00
Tanumbirini 1	3202.00	0.12	0.20	0.08		2.36	0.38	8.00	3.00
Tanumbirini 1	3205.00	0.12	0.22	0.12	323.00	2.45	0.35	9.00	5.00
Tanumbirini 1	3209.00	0.10	0.21	0.07	313.00	2.33	0.32	9.00	3.00
Tanumbirini 1	3220.45	0.11	0.22	0.07	329.00	3.65	0.33	6.00	2.00
Tanumbirini 1	3220.68	0.15	0.27	0.20	319.00	3.41	0.36	8.00	6.00
Tanumbirini 1	3220.90	0.14	0.25	0.34	332.00	4.04	0.36	6.00	8.00
Tanumbirini 1	3220.95	0.11	0.19	0.14	304.00	3.14	0.37	6.00	4.00
Tanumbirini 1	3223.00	0.12	0.23	0.11		3.50	0.34	7.00	3.00
Tanumbirini 1	3226.00	0.15	0.24	0.14	330.00	4.37	0.38	5.00	3.00
Tanumbirini 1	3227.00	0.11	0.18	0.13	381.00	3.22	0.38	6.00	4.00
Tanumbirini 1	3240.00	0.13	0.21	0.13		5.16	0.38	4.00	3.00
Tanumbirini 1	3249.00	0.13	0.20	0.22		4.97	0.39	4.00	4.00
Tanumbirini 1	3252.00	0.12	0.17	0.25	318.00	5.33	0.41	3.00	5.00
Tanumbirini 1	3255.00	0.14	0.24	0.20	305.00	5.50	0.37	4.00	4.00
Tanumbirini 1	3261.00	0.12	0.21	0.09	301.00	3.68	0.36	6.00	2.00
Tanumbirini 1	3267.00	0.10	0.19	0.13	350.00	3.65	0.34	5.00	4.00
Tanumbirini 1	3270.00	0.11	0.22	0.16	307.00	3.81	0.33	6.00	4.00
Tanumbirini 1	3272.14	0.09	0.19	0.08	501.00	3.01	0.32	6.00	3.00
Tanumbirini 1	3272.30	0.12	0.21	0.13	314.00	4.76	0.36	4.00	3.00
Tanumbirini 1	3272.40	0.07	0.17	0.09	577.00	2.50	0.29	7.00	4.00
Tanumbirini 1	3272.56	0.07	0.17	0.03	426.00	1.79	0.29	9.00	2.00
Tanumbirini 1	3272.68	0.12	0.23	0.10		3.61	0.34	6.00	3.00
Tanumbirini 1	3273.00	0.09	0.19	0.05	489.00	2.62	0.32	7.00	2.00
Tanumbirini 1	3279.00	0.08	0.19	0.06	350.00	2.01	0.30	9.00	3.00
Tanumbirini 1	3285.00	0.08	0.20	0.11	447.00	2.77	0.29	7.00	4.00
Tanumbirini 1	3288.00	0.08	0.18	0.27	324.00	1.49	0.31	12.00	18.00

**Table 40. ‘Rock Eval’ data of the Lower Roper Group: Jalboi, Crawford and Mainoru formations.**

Rock ID	Depth (m)	S1	S2	S3	Tmax	TOC	Production Index [S1/(S1+S2)]	HI	OI
		(mg HC / g)	(mg HC / g)	(mg HC / g)	(°C)	(%)			
Urapunga 5	118.50	0.05	0.12	0.11	578.00	0.20	0.29	60.00	55.00
Urapunga 5	119.30	0.04	0.16	0.05	575.00	0.25	0.20	64.00	20.00
Urapunga 5	120.20	0.03	0.10	0.08	559.00	0.39	0.23	26.00	21.00
Urapunga 5	120.55	0.04	0.15	0.06	570.00	0.25	0.21	60.00	24.00
Urapunga 5	123.55	0.04	0.14	0.09	559.00	0.29	0.22	48.00	31.00
Urapunga 5	130.60	0.05	0.15	0.05	572.00	0.24	0.25	63.00	21.00
Urapunga 5	139.90	0.07	0.21	0.04	361.00	0.31	0.25	68.00	13.00
Urapunga 5	139.95	0.13	0.24	0.05	360.00	0.42	0.35	57.00	12.00
Urapunga 5	149.10	0.14	0.46	0.01	363.00	0.38	0.23	121.00	3.00
Urapunga 5	149.50	0.06	0.14	0.06	324.00	0.33	0.30	42.00	18.00
Urapunga 5	150.50	0.04	0.12	0.08	565.00	0.24	0.25	50.00	33.00
Urapunga 5	157.95	0.08	0.19	0.11	356.00	0.05	0.30	380.00	220.00
Urapunga 5	160.50	0.05	0.14	0.14	325.00	0.08	0.26	175.00	175.00
Urapunga 5	169.80	0.05	0.18	0.09	578.00	0.04	0.22	450.00	225.00
Urapunga 5	326.20	0.05	0.15	0.08	562.00	0.51	0.25	29.00	16.00
Urapunga 5	334.50	0.05	0.23	0.06	440.00	0.69	0.18	33.00	9.00
Urapunga 5	341.30	0.05	0.18	0.09	346.00	0.63	0.22	29.00	14.00
Urapunga 5	347.80	0.08	0.17	0.10	435.00	0.51	0.32	33.00	20.00
Urapunga 5	348.00	0.05	0.17	0.09	499.00	0.51	0.23	33.00	18.00
Urapunga 5	354.70	0.05	0.16	0.07	434.00	0.45	0.24	36.00	16.00
Urapunga 5	356.90	0.04	0.13	0.06	562.00	0.51	0.24	25.00	12.00
Urapunga 5	361.90	0.06	0.13	0.04	576.00	0.54	0.32	24.00	7.00
Urapunga 5	369.50	0.05	0.18	0.08	455.00	0.42	0.22	43.00	19.00
Urapunga 5	375.20	0.06	0.16	0.09	555.00	0.51	0.27	31.00	18.00
Urapunga 5	380.10	0.04	0.16	0.05	537.00	0.57	0.20	28.00	9.00
Urapunga 5	381.30	0.05	0.20	0.07	451.00	0.71	0.20	28.00	10.00
Urapunga 5	382.40	0.05	0.20	0.10	451.00	0.77	0.20	26.00	13.00
Urapunga 5	387.30	0.04	0.17	0.07	498.00	0.50	0.19	34.00	14.00
Urapunga 5	391.70	0.05	0.20	0.08	447.00	0.38	0.20	53.00	21.00
Urapunga 5	392.50	0.05	0.15	0.07	504.00	0.31	0.25	48.00	23.00
Urapunga 5	393.10	0.05	0.15	0.06	572.00	0.26	0.25	58.00	23.00
Urapunga 5	393.60	0.05	0.14	0.08	482.00	0.31	0.26	45.00	26.00
Urapunga 5	396.80	0.04	0.14	0.04	514.00	0.31	0.22	45.00	13.00
Urapunga 5	399.30	0.05	0.17	0.08	518.00	0.37	0.23	46.00	22.00
Urapunga 5	399.90	0.05	0.18	0.10	499.00	0.27	0.22	67.00	37.00
Urapunga 5	401.50	0.04	0.16	0.05	509.00	0.21	0.20	76.00	24.00
Urapunga 5	403.00	0.06	0.20	0.09	494.00	0.28	0.23	71.00	32.00
Urapunga 5	403.50	0.05	0.16	0.10	498.00	0.24	0.24	67.00	42.00
Urapunga 5	405.70	0.05	0.15	0.04	309.00	0.44	0.25	34.00	9.00
Urapunga 5	412.45	0.05	0.15	0.14	502.00	0.37	0.25	41.00	38.00
Urapunga 5	416.05	0.05	0.25	0.01	440.00	0.22	0.17	114.00	5.00
Urapunga 5	421.51	0.04	0.14	0.05	508.00	0.16	0.22	88.00	31.00
Urapunga 5	428.00	0.04	0.17	0.04	507.00	0.05	0.19	340.00	80.00
Urapunga 5	431.10	0.04	0.13	0.10	567.00	0.18	0.24	72.00	56.00
Urapunga 5	435.70	0.05	0.19	0.07	483.00	0.21	0.21	90.00	33.00
Urapunga 5	439.65	0.04	0.15	0.14	438.00	0.13	0.21	115.00	108.00
Urapunga 5	442.75	0.05	0.17	0.10	538.00	0.32	0.23	53.00	31.00
Urapunga 5	448.50	0.05	0.16	0.07	500.00	0.29	0.24	55.00	24.00
Urapunga 5	449.50	0.04	0.20	0.11	452.00	0.42	0.17	48.00	26.00
Urapunga 5	453.50	0.05	0.22	0.49	415.00	0.40	0.19	55.00	123.00
Urapunga 5	459.50	0.06	0.22	0.16	481.00	0.42	0.21	52.00	38.00
Urapunga 5	464.50	0.06	0.15	0.87	416.00	0.29	0.29	52.00	300.00

**Table 41. ‘Rock Eval’ data of the Mainoru Formation continued.**

Rock ID	Depth (m)	S1	S2	S3	Tmax	TOC	Production Index [S1/(S1+S2)]	HI	OI
		(mg HC / g)	(mg HC / g)	(mg HC / g)	(°C)	(%)			
Urapunga 5	479.10	0.05	0.15	0.17	517.00	0.32	0.25	47.00	53.00
Urapunga 5	486.15	0.05	0.18	0.08	497.00	0.20	0.22	90.00	40.00
Urapunga 5	487.50	0.04	0.13	0.17	500.00	0.11	0.24	118.00	155.00
Urapunga 5	498.60	0.05	0.15	0.40	516.00	0.16	0.25	94.00	250.00
Urapunga 5	505.10	0.04	0.13	0.81	434.00	0.34	0.24	38.00	238.00
Urapunga 5	507.00	0.04	0.11	0.60	571.00	0.41	0.27	27.00	146.00
Urapunga 5	516.10	0.05	0.14	0.30	445.00	0.24	0.26	58.00	125.00
Urapunga 5	535.00	0.05	0.13	0.13	456.00	0.34	0.28	38.00	38.00
Urapunga 5	535.60	0.05	0.15	0.08	484.00	0.31	0.25	48.00	26.00
Urapunga 5	540.60	0.05	0.15	0.03	450.00	0.33	0.25	45.00	9.00
Urapunga 5	541.20	0.04	0.12	0.05	437.00	0.29	0.25	41.00	17.00
Urapunga 5	544.80	0.09	0.18	0.06	440.00	0.75	0.33	24.00	8.00
Urapunga 5	547.80	0.09	0.18	0.05	437.00	0.89	0.33	20.00	6.00
Urapunga 5	563.10	0.09	0.21	0.03	442.00	0.61	0.30	34.00	5.00
Urapunga 5	567.00	0.08	0.17	0.02	444.00	0.53	0.32	32.00	4.00
Urapunga 5	571.20	0.09	0.18	0.06	439.00	0.61	0.33	30.00	10.00
Urapunga 5	574.00	0.09	0.17	0.04	434.00	0.57	0.35	30.00	7.00
Urapunga 5	578.90	0.06	0.14	0.05	446.00	0.37	0.30	38.00	14.00
Urapunga 5	583.90	0.10	0.20	0.03	443.00	0.63	0.33	32.00	5.00
Urapunga 5	587.70	0.08	0.16	0.04	431.00	0.47	0.33	34.00	9.00
Urapunga 5	591.40	0.10	0.18	0.05	436.00	0.55	0.36	33.00	9.00
Urapunga 5	597.80	0.11	0.17	0.04	445.00	0.46	0.39	37.00	9.00
Urapunga 6	78.70	0.07	0.20	0.10	563.00	0.27	0.26	74.00	37.00
Urapunga 6	232.90	0.05	0.21	1.40	398.00	0.37	0.19	57.00	378.00
Urapunga 6	234.20	0.04	0.15	0.09	337.00	0.39	0.21	38.00	23.00
Urapunga 6	234.70	0.04	0.18	0.76	404.00	0.29	0.18	62.00	262.00
Urapunga 6	235.50	0.04	0.16	0.04	466.00	0.44	0.20	36.00	9.00
Urapunga 6	237.40	0.04	0.17	0.25	499.00	0.31	0.19	55.00	81.00
Urapunga 6	239.60	0.04	0.17	0.07	354.00	0.51	0.19	33.00	14.00
Urapunga 6	243.90	0.03	0.15	1.53	398.00	0.34	0.17	44.00	450.00
Urapunga 6	245.60	0.05	0.20	0.08	445.00	0.44	0.20	45.00	18.00
Urapunga 6	247.05	0.04	0.18	1.50	385.00	0.29	0.18	62.00	517.00
Urapunga 6	248.35	0.04	0.14	0.01	312.00	0.28	0.22	50.00	4.00
Urapunga 6	249.60	0.04	0.17	0.05	472.00	0.34	0.19	50.00	15.00
Urapunga 6	250.80	0.04	0.16	0.03	467.00	0.43	0.20	37.00	7.00
Urapunga 6	251.40	0.04	0.16	3.98	432.00	0.30	0.20	53.00	1327.00
Urapunga 6	256.00	0.04	0.17	3.63	562.00	0.26	0.19	65.00	1396.00
Urapunga 6	267.60	0.05	0.20	3.13	410.00	0.25	0.20	80.00	1252.00
Urapunga 6	269.30	0.04	0.18	3.67	337.00	0.30	0.18	60.00	1223.00
Urapunga 6	420.10	0.05	0.19	0.11	553.00	0.14	0.21	136.00	79.00
Urapunga 6	422.10	0.05	0.17	0.07	573.00	0.27	0.23	63.00	26.00

**Table 42. ‘Rock Eval’ data of the Fraynes Formation.**

Rock ID	Depth (m)	S1	S2	S3	Tmax	TOC	Production Index [S1/(S1+S2)]	HI	OI
		(mg HC / g)	(mg HC / g)	(mg HC / g)	(°C)	(%)			
MBSI	721.36	0.28	2.03	0.21	451.00	3.49	0.12	58.00	6.00
MBSI	721.49	0.46	7.23	0.22	446.00	8.39	0.06	86.00	3.00
MBSI	721.69	0.27	3.23	0.02	448.77	4.41	0.08	73.24	0.45
MBSI	721.93	0.42	2.38	0.07	479.00	0.00	0.15	1.46	0.00
MBSI	722.07	0.59	2.30	0.04	473.00	6.42	0.20	36.00	1.00
MBSI	722.18	0.51	1.85	0.00	467.42	6.14	0.22	30.13	0.00
MBSI	722.37	0.60	1.41	0.31	458.36	5.93	0.30	23.78	5.23
MBSI	722.55	0.44	1.08	0.34	466.00	3.06	0.29	35.00	11.00
MBSI	722.79	0.28	0.90	0.46	458.00	2.17	0.24	41.00	21.00
MBSI	722.99	0.37	1.19	0.30	468.00	2.93	0.24	41.00	10.00
MBSI	723.15	0.40	1.31	0.16	453.00	3.46	0.23	38.00	5.00
MBSI	723.36	0.35	0.98	0.24	444.00	2.92	0.26	34.00	8.00
MBSI	723.57	0.24	0.60	0.07	445.57	1.85	0.29	32.43	3.78
MBSI	780.77	0.25	0.64	0.28	430.78	1.19	0.28	53.78	23.53
MBSI	781.70	0.43	0.87	0.38	436.20	1.53	0.33	56.86	24.84
MBSI	782.58	0.30	0.81	0.39	432.00	1.56	0.27	52.00	25.00
MBSI	783.54	0.26	0.76	0.12	427.00	1.75	0.25	43.00	7.00
MBSI	784.65	0.40	1.11	0.12	440.00	3.43	0.26	32.00	3.00
MBSI	785.07	0.73	1.60	0.03	454.06	5.09	0.31	31.43	0.59
MBSI	785.24	0.80	2.20	0.12	451.00	6.25	0.27	35.00	2.00
MBSI	785.46	0.54	1.55	0.13	450.00	5.03	0.26	31.00	3.00
MBSI	786.05	0.64	1.52	0.03	466.68	5.06	0.30	30.04	0.59
MBSI	786.26	0.33	0.48	0.04	451.56	2.59	0.41	18.53	1.54
MBSI	786.54	0.56	1.42	0.12	444.00	4.97	0.28	29.00	2.00
MBSI	786.91	0.62	1.32	0.06	452.11	5.00	0.32	26.40	1.20
MBSI	787.31	0.51	1.48	0.14	460.00	4.31	0.26	34.00	3.00
MBSI	787.81	0.36	0.95	0.19	435.00	2.84	0.27	33.00	7.00
MBSI	788.31	0.23	0.64	0.16	424.00	1.83	0.26	35.00	9.00
MBSI	788.71	0.23	0.73	0.11	432.00	2.07	0.24	35.00	5.00
MBSI	789.12	0.23	0.62	0.17	434.00	2.09	0.27	30.00	8.00
MBSI	789.46	0.19	0.65	0.13	420.00	1.79	0.23	36.00	7.00
MBSI	864.70	0.12	0.23	0.29	414.00	0.84	0.34	27.00	35.00
MBSI	865.80	0.08	0.35	0.01	481.00	1.61	0.19	22.00	1.00
MBSI	867.20	0.07	0.41	0.03	433.00	1.05	0.15	39.00	3.00
MBSI	867.50	0.11	0.43	0.00	506.95	2.20	0.20	19.55	0.00
MBSI	867.90	0.10	0.37	0.00	470.83	2.33	0.21	15.88	0.00
MBSI	868.15	0.11	0.58	0.02	436.00	2.45	0.16	24.00	1.00
MBSI	868.49	0.13	0.26	0.00	471.72	1.66	0.33	15.66	0.00
MBSI	868.66	0.13	0.37	0.00	463.04	2.01	0.26	18.41	0.00
MBSI	868.75	0.09	0.43	0.02	482.00	1.85	0.17	23.00	1.00
MBSI	868.90	0.09	0.31	0.00	492.19	1.89	0.23	16.40	0.00
MBSI	869.30	0.10	0.40	0.02	475.00	1.78	0.20	22.00	1.00
MBSI	869.58	0.10	0.45	0.05	501.00	1.90	0.18	24.00	3.00
MBSI	869.77	0.07	0.28	0.00	501.80	1.56	0.20	17.95	0.00
MBSI	870.10	0.11	0.46	0.02	372.00	1.79	0.19	26.00	1.00
MBSI	870.53	0.08	0.23	0.34	423.00	0.84	0.26	27.00	40.00
MBSI	871.22	0.12	0.53	0.07	428.00	1.95	0.18	27.00	4.00
MBSI	871.48	0.14	0.56	0.02	461.00	2.36	0.20	24.00	1.00
MBSI	872.93	0.07	0.39	0.00	508.82	1.65	0.15	23.64	0.00

**Table 43. ‘Rock Eval’ data of the Barney Creek Formation.**

Rock ID	Depth (m)	S1 (mg HC / g)	S2 (mg HC / g)	S3 (mg HC / g)	Tmax (°C)	TOC (%)	Production Index [S1/(S1+S2)]	HI	OI
Bing Bong 5	214.80	0.18	0.41	0.34	439	2.15	0.31	19	16
Bing Bong 5	215.80	0.2	0.41	0.28	442	2.23	0.33	18	12
Bing Bong 5	216.80					1.6			
Bing Bong 5	217.80					1.59			
Bing Bong 5	218.00	0.17	0.43	0.35	444	2.13	0.28	20	16
Bing Bong 5	220.00	0.19	0.54	0.33	442	3.02	0.26	18	11
Bing Bong 5	221.00	0.33	0.92	0.37	448	3.24	0.26	28	11
Bing Bong 5	222.20	0.27	0.97	0.33	449	3.62	0.22	27	9
Bing Bong 5	223.00					1.25			
Bing Bong 5	224.00					1.7			
Bing Bong 5	224.60					1.19			
Bing Bong 5	225.50					0.98			
Bing Bong 5	226.50					1			
Bing Bong 5	227.70					0.94			
Bing Bong 5	228.20	0.11	0.29	0.32	430	1.24	0.28	23	25
Bing Bong 5	229.00	0.12	0.21	0.43	433	1.25	0.37	16	34
Bing Bong 5	231.90	0.15	0.42	0.32	439	1.87	0.26	22	17
Bing Bong 5	250.60					0.56			
Bing Bong 5	255.00					0.54			
Bing Bong 5	267.00					0.65			
Bing Bong 5	276.00					0.62			
Bing Bong 5	289.00					0.99			
Bing Bong 5	296.50	0.13	0.36	0.22	436	1.08	0.26	34	20
Bing Bong 5	303.60	0.15	0.27	0.19	432	1.16	0.36	24	16
Bing Bong 5	305.00	0.18	0.3	0.25	436	1.54	0.38	20	16
Bing Bong 5	307.00	0.3	1.15	0.33	444	4.4	0.21	26	8
Bing Bong 5	308.00	0.31	0.74	0.31	441	3.43	0.29	21	9
Bing Bong 5	309.15	0.23	0.47	0.2	436	1.53	0.33	31	13
Bing Bong 5	315.00	0.22	0.7	0.33	441	3.38	0.24	21	10
Bing Bong 5	327.00	0.08	0.21	0.16	431	0.82	0.28	25	19
Bing Bong 5	335.75					0.75			

Table 44. ‘Rock Eval’ data of the Barney Creek Formation continued.

Rock ID	Depth (m)	S1	S2	S3	Tmax	TOC	Production Index [S1/(S1+S2)]	HI	OI
		(mg HC / g)	(mg HC / g)	(mg HC / g)	(°C)	(%)			
GR4	95.30	0.15	0.70	0.31	388.00	0.41	0.18	171.00	76.00
GR4	105.60	0.15	1.55	0.48	433.00	1.40	0.09	111.00	34.00
GR4	111.00	0.15	1.22	0.31	433.00	1.21	0.11	101.00	26.00
GR4	118.00	0.23	2.39	0.30	435.00	1.50	0.09	159.00	20.00
GR4	125.70	0.18	1.84	0.29	434.00	1.30	0.09	142.00	22.00
GR4	128.80	0.19	1.80	0.24	432.00	1.33	0.10	135.00	18.00
GR4	140.60	0.43	4.02	0.41	430.00	1.92	0.10	209.00	21.00
GR4	148.50	0.25	1.95	0.34	431.00	1.46	0.11	134.00	23.00
GR4	153.40	0.16	0.83	0.28	439.00	0.88	0.16	94.00	32.00
GR7	599.50	0.31	2.09	0.38	435.00	1.44	0.13	145.00	26.00
GR7	605.80	0.25	1.99	0.33	433.00	1.34	0.11	149.00	25.00
GR7	616.90	0.27	1.50	0.41	434.00	1.35	0.15	111.00	30.00
GR7	628.50	0.34	2.08	0.44	433.00	1.41	0.14	148.00	31.00
GR7	638.00	0.30	1.91	0.41	434.00	1.38	0.14	138.00	30.00
GR7	647.10	0.26	1.56	0.40	431.00	1.25	0.14	125.00	32.00
GR7	657.60	0.38	2.24	0.47	431.00	1.44	0.15	156.00	33.00
GR7	668.40	0.26	1.30	0.37	434.00	1.21	0.17	107.00	31.00
GR7	678.00	0.27	1.31	0.53	436.00	1.27	0.17	103.00	42.00
GR7	771.20	0.31	1.59	0.34	438.00	1.47	0.16	108.00	23.00
GR7	792.00	0.26	1.26	0.37	438.00	1.30	0.17	97.00	28.00
GR7	802.00	0.25	1.29	0.43	430.00	1.15	0.16	112.00	37.00
GR7	812.60	0.25	1.11	0.34	432.00	1.14	0.18	97.00	30.00
GR7	824.00	0.08	0.39	0.40	426.00	0.88	0.17	44.00	45.00
GR7	840.00	0.21	1.15	0.28	436.00	1.23	0.15	93.00	23.00
GR7	850.00	0.20	1.05	0.35	431.00	1.16	0.16	91.00	30.00
GR7	860.00	0.57	3.34	0.36	436.00	2.64	0.15	127.00	14.00
GR7	870.10	0.76	3.85	0.33	438.00	2.78	0.16	138.00	12.00
GR7	881.00	0.14	0.52	0.17	411.00	0.80	0.21	65.00	21.00
GR7	891.00	0.18	0.70	0.19	432.00	0.99	0.20	71.00	19.00
GR7	901.00	0.15	0.57	0.22	437.00	0.95	0.21	60.00	23.00

**Table 45. ‘Rock Eval’ data of the Wollogorang Formation.**

Rock ID	Depth (m)	S1	S2	S3	Tmax	TOC	Production Index [S1/(S1+S2)]	HI	OI
		(mg HC / g)	(mg HC / g)	(mg HC / g)	(°C)	(%)			
Mt Young 2	52.40	0.04	0.16	0.55	480.00	0.30	0.20	53.00	183.00
Mt Young 2	57.20	0.05	0.18	0.27	607.00	0.66	0.22	27.00	41.00
Mt Young 2	58.00	0.05	0.17	0.39	575.00	0.46	0.23	37.00	85.00
Mt Young 2	59.40	0.05	0.16	0.37	419.00	0.29	0.24	55.00	128.00
Mt Young 2	60.40	0.05	0.18	0.46	570.00	0.35	0.22	51.00	131.00
Mt Young 2	62.40	0.06	0.18	0.48	408.00	0.98	0.25	18.00	49.00
Mt Young 2	63.80	0.05	0.16	0.23	N/A	2.16	0.24	7.00	11.00
Mt Young 2	65.80	0.06	0.16	0.18	306.00	0.86	0.27	19.00	21.00
Mt Young 2	66.80	0.06	0.16	0.25	391.00	1.96	0.27	8.00	13.00
Mt Young 2	67.90	0.07	0.20	0.16	385.00	2.84	0.26	7.00	6.00
Mt Young 2	70.20	0.07	0.19	0.23	403.00	0.89	0.27	21.00	26.00
Mt Young 2	71.40	0.05	0.16	0.27	419.00	0.69	0.24	23.00	39.00
Mt Young 2	72.00	0.07	0.20	0.20	385.00	1.73	0.26	12.00	12.00
Mt Young 2	74.30	0.10	0.21	0.28	344.00	5.07	0.32	4.00	6.00
Mt Young 2	76.30	0.07	0.18	0.47	358.00	7.23	0.28	2.00	7.00
Mt Young 2	77.05	0.09	0.24	0.27	330.00	8.49	0.27	3.00	3.00
Mt Young 2	79.40	0.08	0.19	0.24	405.00	3.01	0.30	6.00	8.00
Mt Young 2	80.20	0.06	0.15	0.24	426.00	1.79	0.29	8.00	13.00
Mt Young 2	82.00	0.05	0.16	0.65	318.00	0.56	0.24	29.00	116.00
Mt Young 2	84.00	0.04	0.15	0.92	430.00	0.34	0.21	44.00	271.00
Mt Young 2	84.50	0.06	0.17	0.45	411.00	0.41	0.26	41.00	110.00
Mt Young 2	85.90	0.06	0.15	0.44	429.00	0.27	0.29	56.00	163.00
Mt Young 2	88.30	0.05	0.16	0.50	359.00	0.27	0.24	59.00	185.00
Mt Young 2	89.00	0.06	0.18	0.41	415.00	0.28	0.25	64.00	146.00
Mt Young 2	90.20	0.09	0.23	0.48	342.00	1.37	0.28	17.00	35.00
Mt Young 2	92.20	0.08	0.20	0.75	397.00	0.61	0.29	33.00	123.00
Mt Young 2	94.00	0.05	0.14	0.72	491.00	0.31	0.26	45.00	232.00
Mt Young 2	96.00	0.06	0.14	0.64	500.00	0.30	0.30	47.00	213.00

**Table 46. ‘Rock Eval’ data of the standards used: Green River Shale, the SRA standard and an Adelaide standard.**

ID	SRA TOC	S1	S2	S3	Tmax (°C)	HI	OI	S2/S3	S1/TOC *100	PI
Green River Shale Std 1	26.12	9.48	216.84	5.19	439	830	20	41.8	36	0.04
Green River Shale Std 1	25.72	9.41	212.27	5.26	440	825	20	40.4	37	0.04
Green River Shale Std 1	21.90	8.21	161.85	5.62	440	739	26	28.8	37	0.05
Green River Shale Std 1	23.72	8.74	192.47	5.19	439	811	22	37.1	37	0.04
Green River Shale Std 1	23.63	8.60	190.07	5.03	439	804	21	37.8	36	0.04
Green River Shale Std 1	23.94	8.68	193.97	5.01	440	810	21	38.7	36	0.04
Green River Shale Std 1	25.71	9.55	212.42	5.21	440	826	20	40.8	37	0.04
Green River Shale Std 1	23.72	8.74	192.47	5.19	439	811	22	37.1	37	0.04
Green River Shale Std 2	25.11	9.29	205.39	5.05	440	818	20	40.7	37	0.04
SRA Std 1	4.05	0.59	12.09	1.39	418	299	34	8.7	15	0.05
SRA Std 1	3.95	0.57	11.69	1.35	419	296	34	8.7	14	0.05
SRA Std 1	3.93	0.59	12.21	1.38	419	311	35	8.8	15	0.05
SRA Std 1	3.99	0.57	11.71	1.37	419	293	34	8.5	14	0.05
SRA std 1	3.89	0.57	11.45	1.30	419	294	33	8.8	15	0.05
SRA std 1	3.75	0.53	10.83	1.36	419	289	36	8.0	14	0.05
SRA Std 1	3.86	0.69	11.80	1.35	419	306	35	8.7	18	0.06
SRA Std 1	4.07	0.59	12.00	1.39	418	295	34	8.6	14	0.05
SRA Std 1	3.98	0.54	11.31	1.40	419	284	35	8.1	14	0.05
Adelaide Std 1	3.43	0.43	10.72	0.33	423	313	10	32.5	13	0.04
Adelaide Std 1	3.41	0.42	10.75	0.31	423	315	9	34.7	12	0.04
Adelaide Std 1	3.43	0.41	10.06	0.32	422	293	9	31.4	12	0.04
Adelaide Std 1	3.22	0.38	9.67	0.31	422	300	10	31.2	12	0.04
Adelaide Std 1	3.41	0.41	10.34	0.33	423	303	10	31.3	12	0.04
Adelaide Std 1	3.30	0.37	9.29	0.34	423	282	10	27.3	11	0.04
Adelaide Std 1	3.44	0.40	10.24	0.36	423	298	10	28.4	12	0.04
Adelaide Std 1	3.39	0.41	10.21	0.35	423	301	10	29.2	12	0.04
Adelaide Std 1	3.39	0.40	10.17	0.35	423	300	10	29.1	12	0.04
Adelaide Std 1	3.99	0.57	11.76	1.47	419	295	37	8.0	14	0.05
Adelaide Std 1	3.43	0.42	10.82	0.38	423	315	11	28.5	12	0.04
Adelaide Std 1	3.30	0.39	9.84	0.33	423	298	10	29.8	12	0.04
Adelaide Std 2	3.34	0.38	9.97	0.32	423	299	10	31.2	11	0.04
Adelaide Std 2	3.37	0.42	10.35	0.32	423	307	9	32.3	12	0.04
Adelaide Std 2	3.37	0.42	10.35	0.32	423	307	9	32.3	12	0.04
Adelaide Std 2	3.37	0.37	10.45	0.34	423	310	10	30.7	11	0.03
Adelaide Std 3	3.35	0.40	9.97	0.34	423	298	10	29.3	12	0.04